From characters to words

The effect of training and expertise on the development of neural print tuning in children

Thesis (cumulative thesis)
Presented to the Faculty of Arts and Social Sciences
of the University of Zurich
for the degree of Doctor of Philosophy

by Georgette Pleisch

Accepted in the autumn term 2017
on the recommendation of the doctoral committee:

Prof. Dr. Moritz Daum (main supervisor)
and
Prof. Dr. Silvia Brem (principal scientific supervisor)

Zurich, 2019

Content

Summary

Learning to read is associated with a neural specialization for the visual processing of orthographic information. This visual specialization is associated with the development of the print-sensitive N1 event related potential (ERP) and the emergence of print-sensitive activations in the left ventral occipitotemporal (vOT) cortex. However, some children are impaired in reading acquisition and their neural specialization to print weaker than that of their normal-reading peers. Strongly impaired children are diagnosed with developmental dyslexia.

A group of children at-risk for developmental dyslexia was tested behaviorally and with multimodal neuroimaging measures shortly before the start of reading acquisition (kindergarten) and afterwards (middle of first grade). This PhD project aimed to investigate the specialization for the visual processing of print during learning and to clarify how print sensitivity is reflected in neural activation as measured with electroencephalography (EEG) and functional magnetic resonance imaging (fMRI).

In the first study of this thesis, prereading children underwent a computerized grapheme-phoneme training to learn the associations between letters, written in an artificial script, and known natural speech sounds. During simultaneous EEG-fMRI recordings in kindergarten, the children solved an implicit audiovisual target detection task, in which they were presented with various visual stimulus types. The short training induced visual print-sensitive activation to characters in both the visual N1 and in the left vOT, which was driven by learning phonological associations. The training performance and the level of expertise modulated the neural activation to visual stimuli as measured with both EEG and fMRI.

The second study investigated the further development of visual print processing by testing the same children in the middle of first grade. In a simultaneous EEG-fMRI session, first graders solved a visual one-back task including words, nonwords and false-font strings. The neuroimaging data showed coarse print sensitivity in the N1 ERP amplitude, but not in the hemodynamic response of the vOT, in both normal and poor-reading children. Attenuation in print-sensitive activation of the vOT in poor-reading

children could be demonstrated by using single-trial ERP-informed fMRI analysis, which emphasized how neural activation in the vOT is directly related to the N1 ERP.

Taken together, the findings of this thesis emphasize the importance of neural tuning to print in reading. Visual print-sensitive activation can be induced by training grapheme-phoneme correspondences in prereading children. Fine differences between normal and poor reading development in print tuning start during initial reading acquisition. This finding emphasizes the importance of early identification of poor reading outcome and adequate intervention for struggling beginning readers.

Zusammenfassung

Das Lesen Lernen geht mit einer neuronalen Spezialisierung für die Verarbeitung von Schrift einher. Diese visuelle Spezialisierung zeigt sich in der Entwicklung einer für die Schriftverarbeitung typischen funktionellen Aktivierung im Gehirn, die mit bildgebenden Methoden gemessen werden kann. Einerseits im ereigniskorrelierten Potential (EKP) etwa 150-200ms (N1) nach der Stimuluspräsentation und andererseits in einer starken Aktivierung in linken ventralen okzipitotemporalen (vOT) Hirnregionen. Eine ungenügende Entwicklung der neuronalen Spezialisierung konnte bei Kindern mit Problemen beim Lesen Lernen, wie zum Beispiel Kindern mit Dylsexie festgestellt werden.

Eine Gruppe von Kindern mit einem Risiko für eine Dyslexie wurde im Kindergarten und in der Mitte der ersten Klasse mit Verhaltenstests und multimodalen bildgebenden Verfahren untersucht. Ziel dieses PhD Projektes war es die Entwicklung der neuronalen Spezialisierung für Schrift während dem Lernprozess und in Abhängigkeit der Lesefertigkeiten bei Kindern zu charakterisieren.

Für die erste Studie trainierten Kindergartenkinder während ca. 20 Minuten Pseudobuchstaben mit einer Lernsoftware am Computer. Dabei lernten sie die Verknüpfung zwischen unbekannten (Pseudo-) Schriftzeichen und deutschen Sprachlauten. Während der simultanen Aufnahme von EEG und MRT lösten die Kinder anschliessend eine implizite Zielreiz-Aufgabe, bei der ihnen die gelernten sowie neue, unbekannte Schriftzeichen, Buchstaben und Zahlen präsentiert wurden. Beim Vergleich von gelernten und neuen Zeichen zeigte sich ein Trainingseffekt sowohl in der N1 als auch im linken vOT Kortex. Zudem modulierten der Trainingserfolg und die Expertise in der Zeichenverarbeitung die neuronale Aktivierung, was sowohl in den EEG als auch in den fMRT Daten ersichtlich war.

Die zweite Studie untersuchte die weitere Entwicklung der Schriftverarbeitung indem die gleichen Kinder in der Mitte der ersten Klasse erneut gemessen wurden. In der simultanen EEG-MRT Messung lösten die Kinder eine implizite Leseaufgabe mit richtigen Wörtern, Fantasiewörtern und Wörtern geschrieben in einer Pseudoschrift. Die Daten weisen auf eine verstärkte und spezifische Verarbeitung von Schrift im N1 EKP hin, diese Spezialisierung war aber in der Aktivität des linken vOT weder für

normale noch für schwache Leser zu sehen. Eine beginnende Spezialisierung für Schrift im linken vOT konnte hingegen in einer single-trial EKP-informierten fMRT Analyse gezeigt werden. Dabei trat eine verminderte Modulation des linken vOT durch die N1 bei den schwachen Lesern hervor, was den direkten Zusammenhang zwischen der N1 und dem linken vOT verdeutlicht.

Zusammengefasst lässt sich aus den Resultate schliessen, dass der visuellen Spezialisierung beim Lesen Lernen ein hoher Stellenwert beigemessen werden muss. Visuelle Spezialisierung für Schrift kann durch gezieltes Training bereits bei Kindern ohne Leseerfahrung induziert werden. Aus den Resultaten lässt sich ableiten, dass sich die feinen neuronalen Unterschiede zwischen einer normalen und einer schwachen Leseentwicklung bereits kurz nach dem intensiven Lesestart auszubilden beginnen. Dieses Resultat zeigt die Wichtigkeit der Früherkennung einer schwachen Leseentwicklung und somit der passenden Förderung schon bei Schulbeginn.

1 General Introduction

Every year in August, thousands of children start their school carrier with their first day in school. In Switzerland, children start structured and tutored learning by the age of six to seven years. According to Piaget (1965), children at this age reach a new stage in their development in which the use of logical thinking prevails. Entering school promotes this process, especially for language and mathematics. Most children look forward to the start of first grade; they are curious about the new situation and genuinely motivated to learn. Many of the new students are eager to learn to read. In their everyday life, they encounter written language in various ways; digital technologies in particular have increased the amount of written communication in recent years (West & Chew, 2014). The children start with some basic letter knowledge and some rudimentary reading skills, and for 90-97% percent of the children, learning to read is a smooth and joyful process. For these children, reading is both a pleasure and a skill crucial for their educational success.

For 3-10% of the children, however, learning to read presents difficulties that cannot be explained by inadequate schooling or low intelligence and they are diagnosed with developmental dyslexia (Snowling, 2013). For them, it is difficult to segment words into syllables or single letters and to combine single letters to form meaningful words (B. A. Shaywitz et al., 2002). Many studies have been conducted to understand the special needs of such children and to refine the diagnosis and interventions (Schulte-Korne, 2010). Although the predominant view at the beginning of the 20th century assumed insufficient educational and didactical professionalism (Schulte-Korne, 2010), laziness, or diminished intelligence as major causes for developmental dyslexia, this view has fortunately been revised. Neuroimaging studies clearly support today's view of a neurobiological origin for the highly inefficient reading process of struggling readers (Norton, Beach, & Gabrieli, 2015; S. E. Shaywitz & Shaywitz, 2008). In addition, it has been shown that genetic factors and environmental aspects influence the development of functional brain networks (Galaburda, Sherman, Rosen, Aboitiz, & Geschwind, 1985). Studies in brain plasticity found differences in more than a dozen genes between

normal readers and readers diagnosed with developmental dyslexia (Carrion-Castillo, Franke, & Fisher, 2013; Galaburda et al., 1985).

Because developmental dyslexia may partly be explained by genetic influences, if developmental dyslexia runs in a family, the prevalence rises dramatically, to 30-65% (Pennington & Lefly, 2001). In addition, preschool language impairments (Gooch, Hulme, Nash, & Snowling, 2014) form another source of increased risk for developmental dyslexia.

Learning to read starts in the middle of childhood and recruits brain areas typically associated with speech processing and visual processing of objects, faces, and print (Dehaene & Cohen, 2011; Epstein & Kanwisher, 1998; Hannagan, Amedi, Cohen, Dehaene-Lambertz, & Dehaene, 2015; Hasson, Harel, Levy, & Malach, 2003; Kanwisher, McDermott, & Chun, 1997; Malach, Levy, & Hasson, 2002). Several studies have investigated visual processing of words, letter strings, and letters in comparison to false-font characters, symbol strings, and numbers. Stronger activations for print (words, letters) than symbols (false-font strings) are evident both in specific electrophysiological components (Araújo, Bramão, Faísca, Petersson, & Reis, 2012; Araújo, Faísca, Bramão, Reis, & Petersson, 2015; Bentin, Mouchetant-Rostaing, Giard, Echallier, & Pernier, 1999; Brem et al., 2005; Eberhard-Moscicka, Jost, Raith, & Maurer, 2015; Hasko, Groth, Bruder, Bartling, & Schulte-Korne, 2013; Maurer, Brem, Bucher, & Brandeis, 2005; Park, Chiang, Brannon, & Woldorff, 2014; Schendan, Ganis, & Kutas, 1998) and in functional magnetic resonance imaging responses (fMRI; Bach et al., 2010; Ben-Shachar, Dougherty, Deutsch, & Wandell, 2011; Brem et al., 2010; Carreiras, Quiñones, Hernández-Cabrera, & Duñabeitia, 2014; Cohen et al., 2003; Dehaene & Cohen, 2011; Price & Devlin, 2011). This superiority in the activation patterns for print over those for non-linguistic control conditions is referred to as print tuning or print sensitivity (Centanni, King, Eddy, Whitfield-Gabrieli, & Gabrieli, 2017; Maurer et al., 2011). Despite growing insights into alterations in specific brain networks in children and adults, it remains largely unclear how sensitivity to print develops with reading acquisition and how sources of risk for dyslexia affect the development of the functional reading network and the establishment of print-sensitive processing in children.

1.1 Print sensitivity and its relevance in reading

The human visual system is highly specialized to recognize visually presented stimuli accurately and rapidly (Thorpe, Fize, & Marlot, 1996). The specialization of the left ventral occipitotemporal (vOT) cortex for face recognition was investigated, and it was found that one part of the ventral fusiform gyrus, the fusiform face area, is specialized for processing human faces (Kanwisher & Yovel, 2006). In addition, perceptual learning of a specific object category, for example in bird-experts or dog-experts, has been shown to lead to stronger neural activations in the vOT (Gauthier et al., 2000; Tanaka & Curran, 2001). Reading is also an acquired skill that is based on intensive training, so it is unsurprising that similar findings have been reported for visual specialization in the vOT to print (Ben-Shachar et al., 2011; Cohen & Dehaene, 2004; Szwed, Ventura, Querido, Cohen, & Dehaene, 2012). Further, supporting findings have described lesions in the left fusiform gyrus affecting the reading ability of patients (Damasio & Damasio, 1983; Foundas, Daniels, & Vasterling, 1998; Pflugshaupt et al., 2009). Therefore, visual print sensitivity, which mainly occurs in the vOT, is indispensable for successful reading and thus a crucial process in reading acquisition.

1.1.1 The role of the N1 ERP in visual print processing

Several event-related potential (ERP) studies describe an early ERP component showing print-sensitive activation, known as the print-sensitive N1 (Bentin et al., 1999; Brem et al., 2005; Eberhard-Moscicka et al., 2015; Helenius, Tarkiainen, Cornelissen, Hansen, & Salmelin, 1999; Maurer, Brandeis, & McCandliss, 2005). One characteristic of the print-sensitive N1 is its strong activation for written material (Bentin et al., 1999; Schendan et al., 1998; Tarkiainen, Helenius, Hansen, Cornelissen, & Salmelin, 1999), which is reflected in increased negative amplitudes over left occipitotemporal electrodes after 150-200ms. Therefore, it can be assumed that the print-sensitive N1 develops during reading acquisition, which typically starts with formal reading instruction at school.

The development of the print-sensitive N1 has been investigated in a range of age groups from prereading children to adolescents and proficient-reading adults. Before reading acquisition, children

show no print-sensitive activation (Maurer et al., 2006). However, training of grapheme-phoneme correspondences initiated print-sensitive N1 activation in prereading children (Brem et al., 2010). This is in line with findings on formal reading acquisition. In particular, print-sensitive N1 activation became apparent in first-grade children after one year of formal schooling (Eberhard-Moscicka et al., 2015) and in second-grade children (Maurer et al., 2006). Interestingly, the amplitude of the N1 was stronger for children than for adults, indicating that children recruit broader areas in the brain to process print (Maurer et al., 2006). Further, print-sensitive activation in adolescents did not show adult-like reduced print-sensitive activation even after several years of reading in school (Brem et al., 2005). Hence, it can be assumed that print sensitivity develops during childhood and adolescence and reaches its final stage in early adulthood (Brem et al., 2005; Maurer, Brem, et al., 2005).

The development of the visual N1 print sensitivity is impaired in poor readers and dyslexic readers. A series of studies found lower print sensitivity in dyslexic children (Fraga González et al., 2014; Hasko et al., 2013) and in dyslexic adults (Mahé, Bonnefond, Gavens, Dufour, & Doignon-Camus, 2012) than in age-matched controls. In their longitudinal study, Maurer et al. (2007) found that dyslexic children showed atypical developmental patterns, as reflected in a lower print sensitivity, than that of normal-reading children. Interestingly, this effect disappeared by fifth grade (Maurer et al., 2011). In another study with adults, dyslexic readers showed stronger N1 amplitudes than normal readers during the processing of symbol strings compared to letter strings (Araújo et al., 2015). This finding seems to contradict studies reporting no print sensitivity in dyslexic readers and might be explained by the string length, which was longer than those used in comparable studies were.

In addition to the investigations of the print-sensitive N1 generated by word processing, numbers have been used as a sample of print (Park et al., 2014; Park, Hebrank, Polk, & Park, 2012). It was shown that digits lead to a print-sensitive activation in the vOT cortex of adults (Park et al., 2012). Numbers also evoked greater N1 amplitude than letters over the right hemisphere (Park et al., 2014), thus demonstrating the double dissociation in the processing of letters and numbers regarding their

lateralization. Hence, N1 print sensitivity can be measured reliably with various culturally defined characters representing spoken language.

In summary, measurements on the scalp capture the electrical activity of a large number of neurons during the processing of print and thus indicate print-sensitive activation. However, the brain areas responsible for the signal remain unclear. For a considerable time, print-sensitive activation in the vOT has been proposed as the generator of the visual N1 activation (Araújo et al., 2012; Brem et al., 2010; Cohen et al., 2000; Eberhard-Moscicka et al., 2015; Fraga González et al., 2014; Hasko et al., 2013; Mahé et al., 2012; Pammer et al., 2004; Pegado et al., 2014). In 1994, Nobre et al. reported that print sensitivity is generated in the vOT, specifically in the fusiform gyrus. In their intracranial EEG study, electrodes were placed in the fusiform gyrus of adult patients, and ERPs were recorded during the presentation of words and word-like stimuli. They reported that the fusiform gyrus showed a higher activation for letter-strings than for control stimuli (Nobre et al., 1994). Other studies have used non-invasive localization techniques and have shown that the print-sensitive N1 is located in the left vOT (Braun, Hutzler, Ziegler, Dambacher, & Jacobs, 2009; Brem et al., 2006; Brem et al., 2009; Kast, Bezzola, Jancke, & Meyer, 2011; Maurer et al., 2011). Nevertheless, it remains unclear, how development and reading acquisition at the start of formal reading instruction influence the neural function in the left vOT and hence, the putative relation between the N1 and the left vOT.

1.1.2 The role of the vOT in visual print processing

The activation of specific regions in the left vOT cortex, including the fusiform gyrus, has been associated with visual print processing (Booth et al., 2001; Brunswick, McCrory, Price, Frith, & Frith, 1999; Cohen et al., 2002; Price & Devlin, 2003; B. A. Shaywitz et al., 2001). Dehaene, Cohen, Sigman, and Vinckier (2005) suggest a functional system located in the left occipitotemporal cortex. They term this the visual word form system (VWFS), and they associate it with the specialization for reading-specific processes which depends on reading experience (Booth et al., 2001; Norton et al., 2015; B. A. Shaywitz et al., 2002). Although the studies and reviews mentioned above agree with the involvement of the left vOT in reading, opinions differ on the functional and structural predispositions. It has been

proposed that the left vOT contains a small, highly specialized area for word processing termed the visual word form area (VWFA; Cohen et al. 2000; Cohen et al. 2002). However, other researchers question the existence of a word-selective region and argue that the proposed VWFA is also activated during picture processing and repeating words auditorily (Price & Devlin, 2003; Vogel, Petersen, & Schlaggar, 2014). In addition, recent studies have shown that the VWFA was only found when individual differences in the exact location of the specialized area were taken into account (Centanni et al., 2017; Glezer, Jiang, & Riesenhuber, 2009).

Several models have been suggested in recent years to explain the function of the left VWFS. The *interactive account model* (Price & Devlin, 2011) provides a sound explanation for experience-dependent and literacy-dependent activation patterns to print in the vOT evident from numerous neuroimaging experiments (Ben-Shachar et al., 2011; Dehaene & Cohen, 2007; Devlin, Jamison, Gonnerman, & Matthews, 2006; Xue, Chen, Jin, & Dong, 2006). This concept is based on the *free energy principle* (Friston, 2010) and arises from the assumption of a hierarchically organized brain in which bottom-up and top-down interactions form the basis of sensory processing. Based on this concept, vOT print sensitivity results from the integration and matching of visual sensory input and its predictions from phonological areas (Dehaene et al., 2010; Devlin et al., 2006).

Cantlon, Pinel, Dehaene, and Pelphrey (2011)'s model propose a more selectionist view. They found that activation in visual areas changes in the course of development due to the selection of preferred stimuli over nonpreferred information. Hence, expertise is reflected in a decreasing activation for nonpreferred stimuli during the development of visual processing (Cantlon et al., 2011). The decrease in activation is explained by pruning mechanisms, which eliminate seldom-used neurons (Cantlon et al., 2011).

The *neuronal recycling hypothesis* (Dehaene & Cohen, 2011) proposes that literacy acquisition leads to local competition within the VWFA, originally dedicated to processing other visual object categories, such as faces (Dehaene et al., 2010). Such competition during reading acquisition in children and in

illiterate adults may cause enhanced activation to words and reduced activation to faces or checkerboards (Dehaene et al., 2010). In addition, literacy acquisition also enhanced phonological activation in the planum temporale providing top-down information to orthographic processing (Dehaene et al., 2010).

Concurrently with the dispute over the underlying processes, the VWFS has been investigated regarding other aspects of visual processing. Several studies report more fine-tuned specialization within the left vOT (Baker et al., 2007; Brem et al., 2009; Glezer, Kim, Rule, Jiang, & Riesenhuber, 2015; Thesen et al., 2012; Vinckier et al., 2007). Depending on the readability of letter strings, the activation in the left vOT has been shown to change from posterior areas for all printed strings to anterior areas for real words, indicating an internal structure of the vOT sensitive to the complexity of written strings (Brem et al., 2009; Vinckier et al., 2007). In addition, formal reading acquisition at school and grapheme-phoneme training in prereading children changed activation patterns in the vOT towards print-sensitive responses (Ben-Shachar et al., 2011; Brem et al., 2010; Brem et al., 2006; Brem et al., 2009; Turkeltaub, Gareau, Flowers, Zeffiro, & Eden, 2003). Thesen et al. (2012) proposed the existence of a letter form area (LFA) for processing letters; this was identified by comparing consonant strings and real words (Thesen et al., 2012) and was located posterior to the VWFA in the vOT. Specialized areas have been described for digits. Abboud, Maidenbaum, Dehaene, and Amedi (2015) reported a number-specific area in the right inferior temporal gyrus, which did not overlap with the number area in the right fusiform gyrus reported in a study by Shum et al. (2013). It remains to be clarified whether a specific visual region becomes specialized for numbers with development.

Further, studies comparing good readers to poor readers have shown that poor readers have reduced print-sensitive activation in the vOT (Maurer et al., 2011; Richlan, Kronbichler, & Wimmer, 2009; van der Mark et al., 2009). This finding might indicate that poor readers recruit less specialized parts of the left vOT than good readers do when processing printed material. However, it remains unclear exactly how poor reading skills and familial risk are related to deviations in print tuning. In addition, the early development of the VWFS and the specialization of specific areas to different types of print (words,

letters, and digits) within this system is still largely unknown. Therefore, insights into the activation patterns of letters and numbers in prereading children shortly before reading acquisition might shed light on the early recruitment of these areas.

As mentioned before, genetic factors and language impairments increase the risk of developing impaired reading skills. Various risk factors have been investigated regarding their influence on functional and structural neural aspects. Prereading children at familial risk for developmental dyslexia showed reduced grey-matter volume in the left vOT including the fusiform gyrus (Raschle, Chang, & Gaab, 2011). This result is in line with previous findings that showed reduced gray matter for dyslexic children and adults (Richlan, Kronbichler, & Wimmer, 2013) and leads to the conclusion that relevant cortical tissue is reduced even before reading acquisition starts (Raschle et al., 2011). In addition, functional processing during a phonological task was diminished in at-risk prereading children in the vOT and in temporoparietal regions, indicating that reading-related tasks are processed in an insufficient way (Raschle, Zuk, & Gaab, 2012). Further, children later diagnosed with dyslexia were shown to exibit reduced cortical thickness in temporoparietal areas, in the fusiform gyrus and in inferior frontal regions (Clark et al., 2014). Similarly, children who would later be diagnosed with dyslexia showed lower print sensitivity than children who would not be diagnosed even before the start of formal reading acquisition (Brem et al., 2013; Maurer et al., 2007). These results indicate that important brain functions and structures for reading are not formed and automatized in the same way during early childhood in dyslexic children as in healthy children.

1.1.3 Learning and training in reading acquisition

To investigate the neural mechanisms underlying the establishment of visual expertise, the process of learning to respond to print-like stimuli has been simulated in various studies (Brem et al., 2017; Hashimoto & Sakai, 2004; Maurer, Blau, Yoncheva, & McCandliss, 2010; Song, Hu, Li, Li, & Liu, 2010; Yoncheva, Blau, Maurer, & McCandliss, 2010; Yoncheva, Wise, & McCandliss, 2015). Yoncheva et al. (2015) confirmed that training artificial grapheme-phoneme correspondences resulted in a more pronounced left-lateralized N1 activation than the training of whole word reading of an artificial script.

Similar, Song et al. (2010) found activation differences in the VWFA after the participants learned to associate unknown symbols with real English sounds. When presented with words, pseudowords, letter strings, and novel stimuli built from the learned script, the activation was significantly greater for words in the VWFA than for untrained stimuli (Hashimoto & Sakai, 2004; Song et al., 2010). Taken together, these findings indicate that visual expertise for artificial print-like stimuli emerges after a short training period in adults.

Training real grapheme-phoneme correspondences is a common intervention for dyslexic readers (Galuschka, Ise, Krick, & Schulte-Körne, 2014). It is assumed that insufficient integration of letter-speech sound associations leads to dysfluent reading in dyslexia (Blomert, 2011; Ehri, 2005). When dyslexic children trained the associations of graphemes and their corresponding phonemes, dyslexic readers were shown to improve their reading fluency more strongly with the additional training than without it, and also more strongly than a non-impaired control group (Fraga González et al., 2015). Furthermore, training of real grapheme-phoneme correspondences initiated print sensitivity in the posterior VWFS and in the N1 ERP in prereading children (Brem et al., 2010). Hence, simulating the process of letter acquisition using artificial letters can shed light on the developmental process of visual expertise.

1.2 Non-invasive neuroimaging methods to study reading in children

As demonstrated so far, EEG and fMRI are both suitable methods for measuring functional brain responses, such as visual processing. This section briefly presents the two modalities and their application. Moreover, it discusses the advantages and disadvantages of each modality and finally elucidates the challenges and the benefits of acquiring EEG and fMRI simultaneously.

The measurement of electrophysiological brain responses on the scalp was first described in the 1920s (Berger, 1929). In an EEG, electrodes positioned on the scalp record voltage fluctuations relative to a reference electrode. Electrical activity measured on the scalp has been shown to be associated with

postsynaptic potentials of pyramidal neurons, however, a large number of neurons with the same spatial orientation need to be active at the same time (Luck, 2014).

Later, ERP were discovered (Dawson, 1951). An ERP is an EEG signal that is time-locked to the presentation of an external event. Because the amplitude of an ERP is much smaller than spontaneous EEG, a considerable number of instances of the same external event has to be repeated (20-1000 times) and averaged to extract a meaningful ERP (Luck, 2014). Traditionally, the time course of an ERP average is illustrated as a waveform with positive and negative peaks, which are referred to as ERP components. In addition, topographic maps are often used to visualize the electrical distribution of ERP components over the scalp. Usually, the ERP components are labelled according to their polarity (P=positive, N=negative) and their latency. Roughly, ERPs are divided into early (before 250 ms) exogenous components, representing physical properties of an event, and later (after 250 ms) endogenous components, representing cognitive processes (Luck, 2014).

EEG has a very high temporal resolution, and measurements are possible in the range of milliseconds. Hence, this method is used to shed light on the time course of neural processes. So far, it has not been possible to determine exactly where in the brain a typical EEG activation pattern is generated. This inverse problem describes the phenomenon that a specific signal measured on the scalp cannot be attributed to one sole dipole, only to multiple neural generators (Luck, 2014). To overcome this problem, localization techniques have been developed, such as distributed source modeling. With this approach, the range of possible sources is restricted to the smoothest three-dimensional current source distribution (Pascual-Marqui, 1999). However, even such elaborate source localization techniques cannot solve the inverse problem and the solutions remain estimations with low spatial resolution.

Another method for measuring brain function is fMRI, which measures changes in cerebral blood flow using a strong magnetic field. Neural activity fluctuates constantly which leads to varying metabolic needs for oxygen and subsequently to changes in cerebral blood flow. Oxygen is transported by blood,

which is either oxygenated (diamagnetic) or deoxygenated (paramagnetic). Concentration fluctuations between oxygenated and deoxygenated blood result in a blood-oxygen-level dependent response (BOLD; Ogawa, Lee, Kay, and Tank, 1990). The course of the BOLD response is depicted in the hemodynamic response function (Huettel, Song, & McCarthy, 2009) and lasts approximately 15 to 20 seconds. The BOLD responses in fMRI recordings are localized with a spatial resolution in the range of millimeters. This allows inferences to be made about where in the brain specific perceptual and cognitive processes take place. However, the temporal resolution provided by fMRI is in the range of seconds, so the time course of neural processes cannot be measured as precisely as in EEG.

The disadvantages of each modality can be overcome by combining the two in simultaneous EEG-fMRI recordings. In a remarkable study, Logothetis, Pauls, Augath, Trinath, and Oeltermann (2001) showed that changes in the BOLD response to specific stimuli are based on local field potentials (LFP). LFPs are characterized as electrical charge differences in the dendrites of neurons (Logothetis et al., 2001). Hence, we can assume that the BOLD response is based on the same electrical generators in neurons as the EEG signal measured on the scalp.

Traditionally, EEG and fMRI are measured in two separate sessions, and the data is combined in the analysis (Ullsperger & Debener, 2010). More elaborate measurement equipment also allows EEG to be recorded during fMRI scanning. Simultaneous recordings of EEG and fMRI are not biased by daily training or learning that might influence cognitive processes between sessions (Huster, Debener, Eichele, & Herrmann, 2012). In addition, simultaneous recording needs less time than sequentially recorded EEG and fMRI. This advantage is particularly important in pediatric studies, as motivation and attentional span are much lower in small children than in adults (Bookheimer, 2000).

However, several artefacts affect EEG recorded in the changing magnetic field. Gradient switching causes major amplitude changes to be superimposed the raw EEG; the swinging of electrodes within the magnetic field leads to disturbed signals on single EEG channels; and physiological changes, such as the pulse rate of the heart are amplified in the magnetic field. These artefacts cause multiple

challenges in the preprocessing of the EEG signal. Nevertheless, specific preparation arrangements and the use of elaborate preprocessing algorithms (Allen, Josephs, & Turner, 2000; Mandelkow, Halder, Boesiger, & Brandeis, 2006) can reduce or correct for these influences on the EEG signal, respectively.

Different approaches have been proposed to combine EEG and fMRI data in concurrent analyses. That of fMRI-informed EEG analysis aims to overcome the inverse problem of EEG by using individual statistical maps from standard fMRI analyses for source localization (Hauser et al., 2015; Huster et al., 2012). These statistical maps serve as constraints on possible source localization. This approach is used to investigate cognitive processes that are relatively stable within different recording sessions and settings, for example visual working memory (Bledowski et al., 2006), so it is possible to use EEG and fMRI data recorded in separate sessions (Huster et al., 2012).

The EEG-informed fMRI analysis takes into account the temporal information derived from EEG (Huster et al., 2012). This approach is based on the assumption of a direct link between the time fluctuation in the EEG signal and the fluctuation in the fMRI signal. Therefore, data from individual EEG trials are used to model the fMRI data (Huster et al., 2012). This technique uses the individual ERP properties of the processes elicited by an event of interest. This feature is extracted and convoluted exactly with the BOLD response elicited by the same event of interest (Huster et al., 2012). So far, this method has been used to investigate the impact of error-related negativity on the midcingulate cortex (Debener et al., 2005) and to test temporal influences on fMRI activations (Eichele et al., 2005; Hauser et al., 2014; Iannaccone et al., 2015).

Both modalities have major advantages that can be combined by using a simultaneous approach, which is also less time-consuming for the participants. Therefore, our sample of young children was measured with simultaneous EEG-fMRI to identify relations between the visual N1 and the activation of the left vOT during visual processing.

1.3 Aims and hypotheses

Learning to read has been examined in a large number of studies, either by investigating the natural course of reading acquisition at school or by training children or adults in the basics of reading. These studies have often focused on visual reading processing and reported print sensitivity patterns in the N1 ERP and in the VWFS BOLD response.

Despite the considerable research into visual print processing with both EEG and fMRI, the focus has mostly been on the processing of entire words or letter strings. Few studies have examined on single-letter processing, and no study to date has explored specialization for letters in children learning to read. However, because letters (graphemes) are the smallest units of a written word and because grapheme-phoneme learning is a core problem for children with developmental dyslexia (Blomert, 2011)., it is important to better understand how the brain processes single letters.

The present PhD thesis contributes i) to a better understanding of the specialization of visual processing for print during learning and ii) to clarifying the mutual relation of the print-sensitive N1 ERP and the print-specific vOT activation of the left VWFS.

In the first study, we investigated the emergence of functional specialization to specific stimulus categories in the human cortex. Cortical specialization represents a pivotal developmental process that sets the basis for targeted and efficient information processing. Using the example of reading, we investigated the emergence of functional specialization at a crucial initial learning stage in a group of preschool (6.5yrs) children at varying risk for developmental dyslexia. We specifically manipulated expertise with previously unfamiliar characters through training and compared the processing of unfamiliar characters with that of other categories of prevalent, culturally meaningful characters (letters, digits) varying in their levels of expertise in prereaders. We varied expertise by presenting numbers from one to six, real letters, a set of six trained false-font characters, and a set of novel false-font stimuli.

We hypothesized that the different types of visual characters require different levels of expertise and therefore elicit graded activation patterns in both the N1 ERP and the left vOT BOLD response. According to the interactive account model (Price & Devlin, 2011), more activation was expected for prereaders in stimuli requiring higher expertise such as numbers and trained false-font stimuli. Both for the novel, unknown false-font characters and for real letters, for which no or only very low levels of expertise was assumed in kindergarteners, no print-sensitive activation was expected in either the N1 ERP or the BOLD response in the vOT.

In the second study, we investigated the relation between the print-sensitive N1 to words and the print specific activation in the left VWFS during an important learning stage in first-grade children. After half a year of reading instruction at school, the processing of print was recorded simultaneously in EEG and fMRI during the processing of visually presented words, nonwords, and false-font strings. We aimed specifically to identify and quantify differences in visual print sensitivity arising between children with normal reading development and children with impaired reading development. In addition, by combining EEG data and fMRI data directly in an ERP informed fMRI analysis, we aimed to clarify on how the print sensitivity of the N1 ERP modulates the BOLD activation in the left vOT in beginning readers.

We expected that differences between normal readers and poor readers would be evident in both the N1 ERP and the vOT BOLD signal. Stronger print-sensitive activation was expected in the visual ERP N1 and in the left vOT for normal readers than for poor readers. These differences were expected to be confirmed in the single-trial analyses when considering the individual time course of the processing of print.

2 Study A: Emerging neural specialization of the ventral occipitotemporal cortex with literacy acquisition

Georgette Pleisch[1,2], Iliana I. Karipidis[1,2], Christian Brauchli[1], Martina Röthlisberger[1], Christoph Hofstetter[1], Philipp Stämpfli[3], Susanne Walitza[1,2], Silvia Brem[1,2,3]

[1]Department of Child and Adolescent Psychiatry and Psychotherapy, Psychiatric Hospital, University of Zurich, Switzerland

[2]Neuroscience Center Zurich, University of Zurich and ETH Zurich, Zurich, Switzerland

[3]MR-Center of the University Hospital for Psychiatry and the Department of Child and Adolescent Psychiatry and Psychotherapy, University of Zurich, Switzerland

A similar version of this article has been published as:

Pleisch, G., Karipidis, I.I., Brauchli, C., Röthlisberger, M., Hofstetter, C., Stämpfli, P., Walitza, S., Brem, S., 2019. Emerging neural specialization of the ventral occipitotemporal cortex to characters through phonological association learning in preschool children. NeuroImage 189, 813-831.

2.1 Summary

How is functional specialization in the human cortex initialized during child development? Using a multimodal approach we demonstrate on the example of the vOT cortex in prereading children, how varying expertise modulates the preferential response to single characters, representing the building blocks of print units. We directly manipulated the level of expertise, firstly, by training false-font-speech sound associations and, secondly, by presenting characters differing in category and expertise (false-fonts, letters and digits). Neural correlates of print processing were tracked with simultaneous high-density electroencephalography and functional magnetic resonance imaging. We found a training performance and expertise dependent modulation of the visual event-related potential around 220ms (N1) and the corresponding vOT activation. Our results emphasize the critical role of the rapidly emerging top-down input to the vOT during specialization and represent a fundamental step forward

regarding the understanding of the mechanisms initiating functional specialization in the developing brain.

2.2 Introduction

The development of functional specialization in specific cortical patches is critical for information processing in various domains (Houdé, Rossi, Lubin, & Joliot, 2010). The last 15 years of neuroimaging research have provided important insights into the functional specialization of the left vOT cortex to print during reading acquisition in children (Brem et al., 2010; James, 2010; Maurer et al., 2011; Saygin et al., 2016), adults (Dehaene et al., 2010), and regarding symbol training in primates (Srihasam, Mandeville, Morocz, Sullivan, & Livingstone, 2012). However, it remains unclear, which processes initiate the functional specialization and consequently the preferential cortical activations seen in the left vOT arising during child development. Progressive visual specialization for print is a pivotal process underlying reading acquisition (Pegado et al., 2014) and shape learning (Sigman et al., 2005). As the left vOT is implicated in processing a variety of visual categories (Dehaene & Cohen, 2007; Hasson et al., 2003; Kourtzi & Kanwisher, 2001; Yovel & Kanwisher, 2004), an increasing engagement of regions evolutionary intended for objects or faces (Dehaene & Cohen, 2007) may emerge for processing print during reading acquisition (Dehaene et al., 2010).

Regarding reading, learning drives the expertise seen in the neural responses of the left vOT (Ben-Shachar et al., 2011; Price & Devlin, 2011; Xue et al., 2006) and the corresponding characteristic occipitotemporal negativity in the ERP N1 after around 150-250ms (Brem et al., 2009; Maurer et al., 2011). The process of learning print, to characterize the neural correlates of visual specialization, has been simulated in adults (Hashimoto & Sakai, 2004; Maurer et al., 2010; Song et al., 2010) or directly tracked in the course of reading acquisition in children (Brem et al., 2010; James, 2010; Maurer, Brem, et al., 2005) and adults (Dehaene et al., 2010). fMRI studies have shown that training induces stronger activation in a subregion of the vOT referred to as the VWFS (Brem et al., 2010; Vinckier et al., 2007) for trained compared with untrained print-like stimuli in adults (Hashimoto & Sakai, 2004; Song et al., 2010; Xue et al., 2006) or real letter strings in children (Brem et al., 2010; James, 2010). Literacy

acquisition in illiterate adults induced a local competition of faces and print and resulted in an enhanced vOT response to print and a refinement of left vOT organization (Dehaene et al., 2010). ERP studies largely converge with fMRI results by showing more pronounced visual N1 amplitude over occipitotemporal regions for trained associations in adults (Maurer et al., 2010) and children (Brem et al., 2010; Maurer et al., 2011).

Especially in the case of reading acquisition, the functional reorganization of specific cortical regions and the emergence of cortical activation preference to print may be driven by increasingly interactive and integrative processing of information (Price & Devlin, 2011) within areas fulfilling the anatomical and connectional requirements to adopt a novel function (Abboud et al., 2015; Dehaene & Cohen, 2007). This integrative concept emanates from the assumption of a hierarchically organized brain in which bottom-up and top-down interactions form the basis of specialized neural processing (Friston, 2010; Johnson, 2011). In particular, sufficiently plastic cortical patches evolutionarily serving functionally similar processes may reorient neural resources to culturally novel functional processes through learning (Dehaene & Cohen, 2007): Bottom-up sensory input from visual areas and top-down information from higher order cognitive areas are integrated in vOT regions. Thus, the vOT specialization for print results from the integration and matching of visual sensory input, and predictions from phonological areas (Dehaene et al., 2010; Price & Devlin, 2011). Accordingly, neural activity representing visual specialization in the vOT increases in initial and early stages of learning and is reduced with gaining expertise or by impairments such as developmental dyslexia (Price & Devlin, 2011). This inversed U-shaped learning and expertise activation curve has been explained by the presence and strength of prediction errors and was found during normal reading acquisition (Maurer, Brem, et al., 2005). Prediction errors occur due to the mismatch of incoming bottom-up sensory and top-down cognitive information. Thus, activation in the left vOT is modulated by word reading skills in children (Ben-Shachar et al., 2011; Maurer et al., 2011) and adults (Dehaene et al., 2010; Pegado et al., 2014; Xue et al., 2006). In poor-reading children, however, this matching process may show a

protracted or impaired development resulting in reduced activation, especially in early learning stages (Brem et al., 2013; Clark et al., 2014; Dehaene et al., 2010).

Despite the growing number of neuroimaging studies examining reading in young children (Boros et al., 2016; Brem et al., 2010; Hoeft et al., 2007; James, 2010) and recent findings of early developing structural connectivity in prereaders dictating the functional fate of the left vOT (Saygin et al., 2016), there is a substantial lack of direct evidence on how neural reorganization, leading to specialized processing of print, is initialized in children. When assessing the natural course of reading development by following children longitudinally (Clark et al., 2014) or in cross-sectional studies (Brem et al., 2009; Dehaene et al., 2010; B. A. Shaywitz et al., 2007; Turkeltaub et al., 2003), learning-related reorganization processes are likely to be confounded by effects of age, general maturation, and emerging phonological and semantic associations that partly develop in concert. Thereby, such studies cannot fully answer the question to what extent enhanced visual familiarity or the feedback from phonological or semantic association areas drive the functional brain specialization to print. To address this question, we simulated the very first step in reading acquisition in prereaders through false-font-speech sound association learning. When it comes to learning a novel script, studying prereaders, who do not yet possess a functional reading network, allows for overcoming the undesirable interference with an existing reading system, an obstacle encountered in studies on literate adults (Hashimoto & Sakai, 2004; Maurer et al., 2010) or children (Saygin et al., 2016).

Here, prereading children at varying risk for developmental dyslexia were examined with simultaneous high-density 128-channel EEG-fMRI recordings and an extensive behavioral battery. Participants performed a short association training of false-font characters with natural speech sounds (grapheme-phoneme correspondence (GPC) training), simulating the crucial step of systematic letter-speech sound learning in alphabetic languages (Blomert, 2011). In the subsequent neuroimaging session, this approach allowed us to determine how vOT activation to trained false-fonts is modulated through arising phonological associations. In addition, we manipulated the impact of expertise and learning stage by comparing the processing of different types of visual characters, for which prereading children

show varying levels of visual familiarity and expertise to higher order phonological, semantic and/or magnitude associations. The level of expertise varied from highly familiar Arabic numbers with distinct phonological, semantic, and magnitude associations to visually familiar lower case Latin letters with partly known phonological associations and finally, matched false-font characters whose phonological association knowledge was experimentally manipulated.

According to the interactive account model of vOT specialization (Price & Devlin, 2011), we hypothesized that vOT activity and the corresponding visual N1 are modulated by children's expertise on the respective character type through establishing feedback circles with higher order language regions. Moreover, while increased visual familiarity, emerging from perceptual learning processes through the abundant visual exposure to a certain character type or specific visual training, may modulate activation in the left vOT and the corresponding visual N1 (Brem et al., 2005; Sigman et al., 2005), we did not expect that visual familiarity alone would drive major enhancement of cortical preference and consequently neural specialization (Abboud et al., 2015). Such enhancement is rather hypothesized to reflect specific association learning and hence consensual integration of the visual input and feedback predictions from higher order processing regions (Price & Devlin, 2011).

In line with our hypotheses, expertise modulated neural responses in the form of changes in activation preferences and functional connectivity. More specifically, activation to false-font characters after GPC training became more pronounced (left vOT and N1) and connectivity was initialized as compared with the matched false-font characters for which no associations had been trained. Importantly, these learning effects were modulated by children's performance during the training, excluding a sole effect of visual familiarity. The early visual N1 ERP activity after around 220ms demonstrated a pronounced sensitivity to higher order input, as strongest amplitudes were found for digits whereas letters and novel false-fonts hardly differed. Together, these findings importantly extend previous knowledge on training enhanced neural specialization for print (Brem et al., 2010; Maurer et al., 2010; Song et al., 2010) by directly showing newly established functional connectivity to higher order areas.

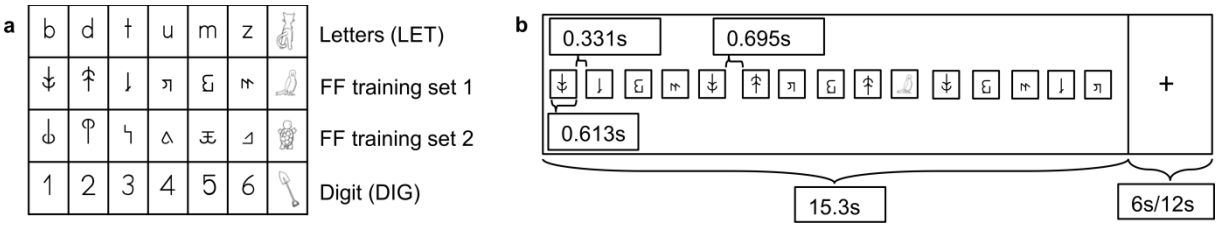

Figure 2.1 Character types, artificial GPC false-font training sets, and task design. (a) The implicit audiovisual target detection task was divided in four parts, each including one character type: Letters, digits, trained and novel false-fonts. Children had to press the response button whenever a visual, auditory or audiovisual target appeared (last column). During the GPC training, children learned to associate one set of six artificial graphemes to known phonemes: The stimulus sets (1/2) for TFF and NFF were counterbalanced across subjects. (b) Illustration of the sequence and timing of one visual stimulation block. Each part included four visual blocks among blocks of auditory and audiovisual stimulation.

2.3 Results

During simultaneous high-density EEG-fMRI recordings, 31 German speaking prereading children at varying familial risk for developmental dyslexia participated in an implicit audiovisual target detection experiment (Karipidis et al., 2017) comprising four parts. In each part, one character type was presented: Letters (LET), trained false-fonts (TFF), novel false-fonts (NFF) and digits (DIG; Figure 2.1a).

Data quality criteria for EEG or fMRI were met by 23 and 24 children respectively (Table S2.1). A core group of 18 children (8f, mean: 6.7+-.36y; Table 2.1) met criteria for both EEG and fMRI analyses and are described henceforth. Each child's individual risk score for developmental dyslexia (0.53±.2) was included in all analyses as a covariate to control for familial risk. The subjects' behavioral characterization and learning achievement were assessed in separate sessions preceding the simultaneous EEG/fMRI measurement and included intelligence scores (IQ $>$ 85, 108±13.3), reading skills (2.9±3.1 words), and letter and number knowledge (15.4±3.6 letters and 15.3±5.0 numbers). Weighted accuracy (81±9%) and training duration (19±3.7 min) were used to characterize the children's performance in the artificial GPC training (Karipidis et al., 2017; Lyytinen, Erskine, Kujala, Ojanen, & Richardson, 2009).

To examine how the varying levels of expertise influenced the activity in occipitotemporal brain areas, we focused on the early visual N1 ERP component (Bentin et al., 1999), and

Table 2.1 Subject characteristics and performance on behavioral measures

Variables	N	
Sex (male/female)	10/8	
Handedness (right/left)	16/2	
FF training set (1/2)	10/8	
	Mean ± SD	Range
Age (y)	6.7±.36	6.1-7.2
IQ estimation (nonverbal)[1)]	108±13.3	85-125
Familial risk for dyslexia[2)]	0.53±0.2	0.26-0.8
GPC training duration (in min)	19±3.7	12-26
GPC training accuracy (weighted in %)	81±9	62-91
Reading (20 one- or two-syllable words)[3)]	2.9±3.1	0-10
Letter speech-sound knowledge (52 upper and lower case)[3)]	15.4±3.6	2-35
Letter speech-sound knowledge experiment (b,d,t,u,m,z)[3)]	1.2±1.0	0-3
Number knowledge (21 one- to three-digit numbers) [3)]	15.3±5.0	7-21
Rapid naming RAN (objects/second)[4)]	27±17	1-50
Phonological awareness TEPHOBE[4)]	47±19	2-90

[1)] Block design test of the Wechsler Intelligence Scale for Children (HAWIK-IV)
[2)] Highest parental adult reading history questionnaire value (ARHQ)
[3)] Number of correctly named items
[4)] Age-matched percentile scores

BOLD brain responses in the vOT (Yovel & Kanwisher, 2004). Data acquired during each part of the implicit audiovisual target detection experiment was analyzed using linear mixed models (LMMs), including fixed and random effects, and general linear models (GLMs). P-values of post-hoc t-tests corrected for multiple comparisons using the Tukey-Kramer method are specifically marked by indexing the uncorrected p-value with asterisks, whereby $^{(*)}$ denotes a p_{corr} <0.1, * a p_{corr} <0.05, ** a p_{corr} <0.01, and *** a p_{corr} <0.001. Pearson correlations for normally distributed data and Spearman correlations for non-normally distributed data are reported to clarify the relationship between specific behavioral skills and brain activity.

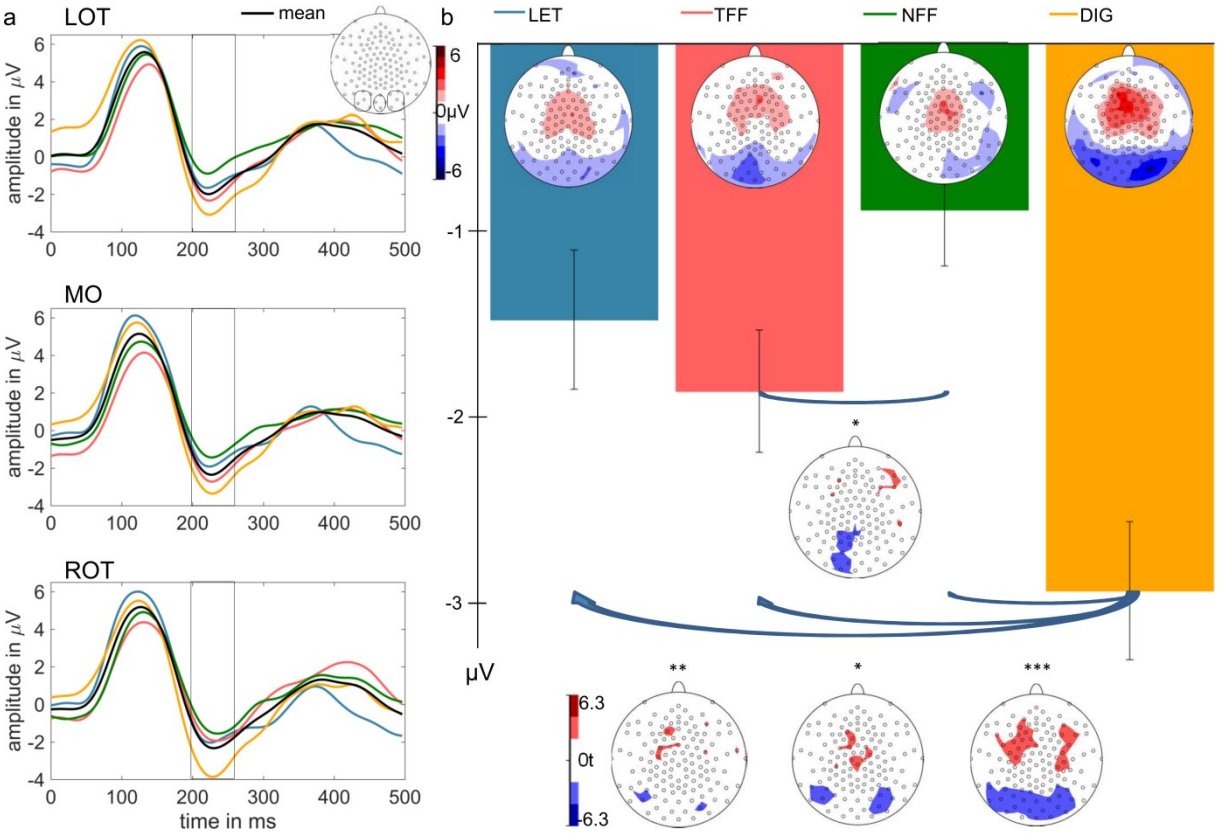

Figure 2.2 Visual expertise and training effect in the N1 ERP (n=18). (a) ERP waveforms for the four character types in the three defined electrode clusters (LOT, MO, and ROT, see encircled electrodes). The N1 interval (194-254ms) is framed in grey. (b) The color bars depict the mean amplitude values for each character type, pooled over the three clusters (LOT, MO, ROT) within the N1 interval. Error bars denote standard errors. Superimposed on the bars are the corresponding potential field maps. The two bottom rows show t-maps illustrating the statistical differences between the character types: Training induced pronounced N1 amplitude differences between TFF and NFF over middle and left occipital regions. DIG showed most pronounced negativity over (right) posterior regions as also reflected in the t-maps. *=p_{corr}<0.05, **=p_{corr}<0.01, ***= p_{corr}<0.001, LET= letter, TFF= trained false-font, NFF= novel false-font, DIG= digit, LOT=left occipitotemporal, MO=middle occipital, ROT=right occipitotemporal.

2.3.1 Modulation of the visual N1 ERP through expertise

We determined the interval for the N1 (194-254ms) based on the mean global field power (GFP) over all four character types. The mean amplitude values within this interval for left and right occipitotemporal electrode clusters (LOT, ROT) and a cluster of middle occipital electrodes (MO) were used for further analyses (Figure 2.2a).

For the N1 interval, the LMM of the GFP amplitude with fixed factor character type (LET, TFF, NFF, DIG) revealed no significant effects. The LMM for the predefined electrode clusters with fixed factor character type and cluster (LOT, MO, ROT) revealed a significant character type effect

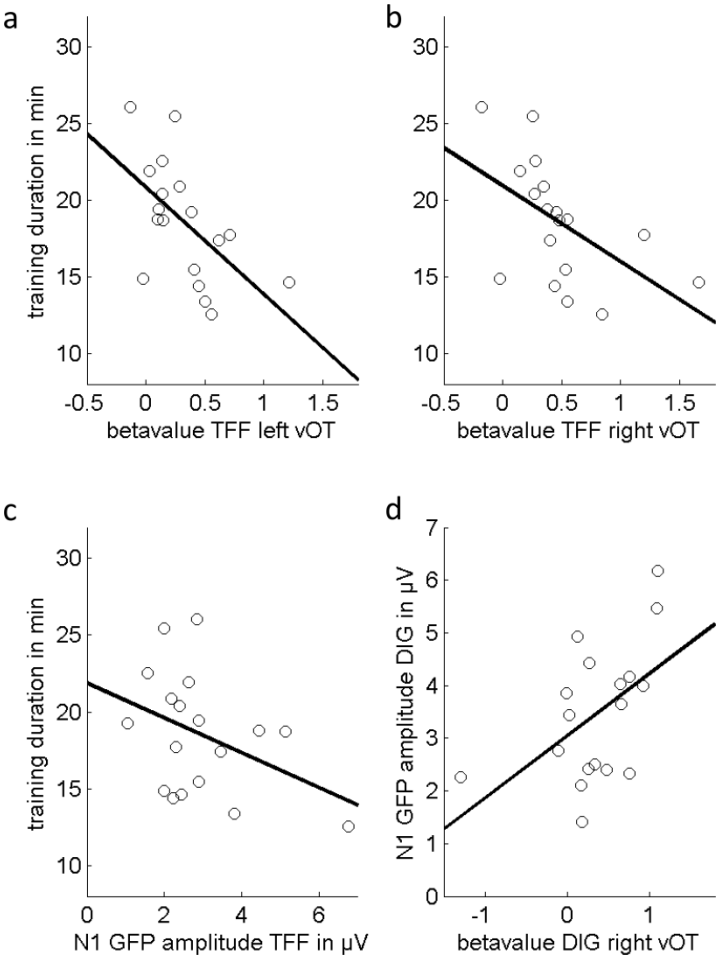

Figure 2.3 Effects of training on brain activity and link between ERP and BOLD activation (n=18). (a, b) The vOT activation for TFF correlated bilaterally with training duration showing that efficient learning enhances vOT preference to print (left: Pearson r=-0.55, p=0.022, right: Pearson r=-0.49, p=0.048). (c) Trend to a negative correlation of N1 GFP of TFF with training duration (Spearman r = -0.45, p = 0.071). (d) Correlation of N1 and fMRI vOT activation: The right vOT activation for DIG correlated positively with the right N1 (ROT) amplitude for DIG (Pearson r=0.52, p=0.034).

[F(3,187)=8.34, p<0.0001; Figure 2.2b]. This difference was driven by the significantly stronger N1 for DIG than for all the other types (DIG<LET: t=-3.35, p=0.0010**, DIG<TFF: t=-2.68, p=0.0080*, DIG<NFF: t=-4.87, p<0.0001***). Of particular importance, the N1 for TFF was significantly more negative than for NFF (TFF<NFF: t=-2.95, p=0.0036*; Figure 2.2b; Figure S2.1).

These results answer two important questions: 1) Association training induced specialization for characters after only 220ms even when controlling for visual familiarity and prior knowledge. This extends previous findings on visual specialization for words in prereading children (Brem et al., 2010) and, for the first time, shows fast emerging preferential activation through association learning for written characters. This effect was modulated by training performance reflected by a trend to a negative correlation between training duration and the N1 GFP for TFF (Spearman r = -0.45, p = 0.071;

Table 2.2 Results of fMRI whole brain and connectivity analyses

cluster	cluster size	peak voxel	MNI coordinates			Hemisphere	Brain region
$p(FWE_{corr})$	k	T	x	y	z		
LET>NFF							
0.00244	74	5.41	52	-18	6	r	STG
LET>DIG							
0.00001	186	6.21	-29	54	15	l	MFG
Correlation of training duration and TFF vs. baseline							
0.00901	63	-6.76	-35	-81	-9	l	IOG/LING
Correlation of N1 (ROT) amplitude and corresponding BOLD activation for DIG							
0.00001	193	-7.72	16	-45	69	r	PoCG/PCL
Functional connectivity TFF>NFF (using cluster-based false discovery rate correction (FDR_{corr}) of p<0.05 (CDT of p<0.01))							
0.00947	553	4.18	-40	-64	60	l	IPG

Listed are the MNI coordinates (x, y, z) using a cluster-based family-wise error corrected (FWE_{corr}) threshold of p<0.05 (on a cluster-defining threshold (CDT) of p<0.001, k=40). MNI=Montreal Neurological Insitute, LET= letter, TFF= trained false-font, NFF= novel false-font, DIG= digit, STG=superior temporal gyrus, MFG=middle frontal gyrus, IOG=inferior occipital gyrus, IPG=inferior parietal gyrus, PreCG=precentral gyrus, STP=superior temporal pole, LING=lingual gyrus, MTP=middle temporal pole, PoCG=postcentral gyrus, PCL=paracentral lobule, l=left, r=right

Figure 2.3c). 2) Processing numbers led to the strongest N1 response indicating the children's advanced level of expertise for numbers and their semantic, phonological and magnitude associations by the end of kindergarten, similar to the preferential activation to words after first reading instruction (Brem et al., 2013; Maurer et al., 2011).

2.3.2 Modulation of the vOT BOLD signal through expertise

Next, we report results of second-level voxel-wise random effect analyses to characterize activation differences evoked by visual processing of the four character types using a cluster-based family-wise error corrected (FWE_{corr}) threshold of p<0.05 (on a cluster-defining threshold (CDT) of p<0.001). As expected, all four character types showed pronounced occipitotemporal activation (Figure 2.4a&Table S2.2). This activation was bilateral for LET, TFF and NFF but only reached significance in the right hemisphere for DIG, pointing to beginning visual specialization for numbers in the right hemisphere (Abboud et al., 2015; Park et al., 2014; Shum et al., 2013). Direct character type contrasts revealed only minor differences in whole brain analyses, mostly driven by single letter processing: LET showed more

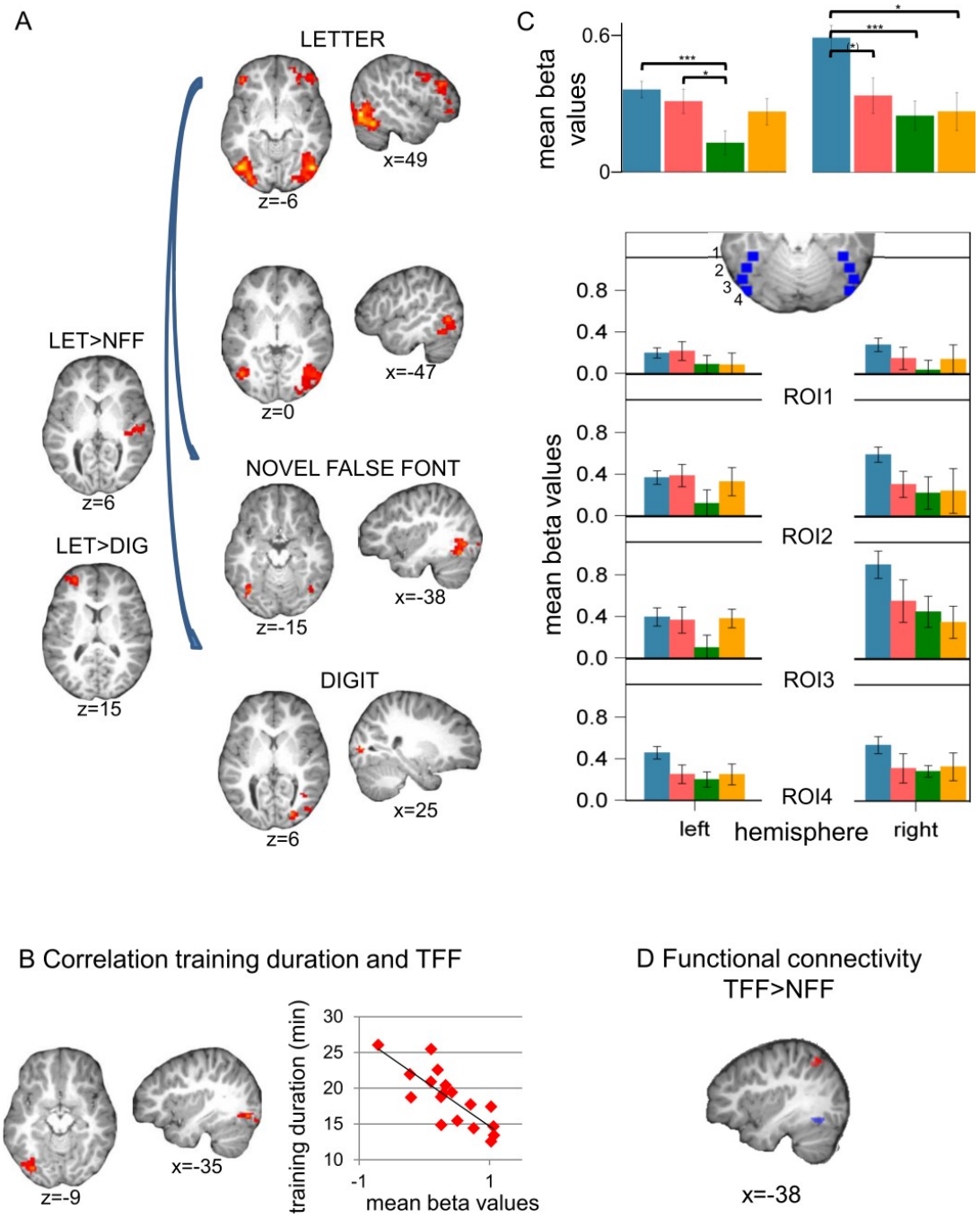

Figure 2.4 Modulation of the BOLD signal through training and expertise (n=18). (a) Left column: Whole brain activation by character type vs. baseline. Right column: Character type contrasts. LET showed stronger activation than NFF and DIG in the right superior temporal gyrus and the left middle frontal gyrus respectively (cluster-based $p(FWE_{corr})<0.05$). (b) Voxel-wise whole brain correlation of BOLD response to TFF with children's training duration in the GPC training session. Faster learning was correlated with significantly higher activation in the left vOT (cluster-based $p(FWE_{corr})<0.05$). The negative correlation of the vOT activation plotted against training duration is shown on the right hand side for illustration purposes. (c) ROI analyses in the vOT. Top: Mean beta values for each character type combined over the four left and right vOT ROIs (locations illustrated in the axial section) showing significant activation preference to letters in both hemispheres and a training effect over the left hemisphere as shown in post-hoc tests ($^{(*)}=p_{corr}<0.1$,$*=p_{corr}<0.05$, $**=p_{corr}<0.01$, $***=p_{corr}<0.001$, Figure 2.2&Figure 2.4 - Supplementary file 2). Bottom: Mean beta values for each ROI and character type in both hemispheres, for illustration purposes. (d) Functional connectivity. Correlation of the left FFG seed region (blue) connectivity to superior parietal regions (red) for TFF with decreasing training duration (cluster-based $p(FWE_{corr})<0.05$). Error bars denote standard errors. LET= letter, TFF= trained false-font, NFF= novel false-font, DIG= digit, FFG= fusiform gyrus.

activation than NFF in the right superior temporal gyrus and the left middle frontal gyrus extending to superior frontal areas when compared with DIG (Figure 2.4a, Table 2.2). Of note, TFF exhibited more pronounced activation in the bilateral middle temporal gyrus as compared with NFF, on an uncorrected threshold of p<0.001 (Figure S2.2&Table S2.3).

The training duration of the artificial GPC training correlated significantly with the TFF BOLD response in the left vOT, demonstrating that a higher activation was associated with faster learning (Figure 2.4b, Table 2.2). Importantly, this finding survived an even stronger correction ($p(FWE_{corr})<0.01$, using a CDT of p<0.001), is also confirmed by the supportive analyses of the enlarged fMRI-group (Figure S2.3) and thus can clearly be considered as a robust result, unaffected by potential inflated false-positive rates (Eklund, Nichols, & Knutsson, 2016).

The emergence of preferential activation to print in the vOT was further investigated by creating two summary region of interests (ROIs) covering the entire cortical activation within the vOT of all four character types in both hemispheres (ROI lvOT and ROI rvOT; blue mask in Figure 2.4d). The LMM analysis with fixed factors hemisphere (lvOT, rvOT) and character type revealed a significant effect for hemisphere [F(3,117)=11.46, p=0.0010], with more pronounced activation in the right compared with the left hemisphere (t=-3.38, p=0.0010**). A correlational analysis of both ROIs with training duration and accuracy revealed distinct relations: We found negative correlations for training duration and beta values for TFF in the left (r=-0.55, p=0.022) and right (r=-0.49, p=0.048) vOT ROIs (Figure 2.3a and b). In addition, training accuracy correlated positively with the rvOT ROI (r=0.50, p=0.040). These results strongly support the theory that poor learning performance in terms of duration (slow) or accuracy is associated with diminished BOLD activation in the vOT after training. Furthermore, the correlation of the bilateral ROIs with the mean amplitude of the N1 GFP revealed a significantly positive correlation between the rvOT BOLD and the N1 GFP (r=0.52, p=0.034) for DIG only (Figure 2.3d) indicating early lateralization effects for DIG.

In order to explore more local characteristics of character type specific processing along the vOT (Brem et al., 2009; Vinckier et al., 2007), we additionally defined four ROIs along an anterior to posterior axis with the centers of mass in the left and right vOT ROIs, described above (Figure 2.4c). The extracted beta values were analyzed in a LMM with fixed factors ROI (from anterior to posterior: R1, R2, R3, R4), hemisphere, and character type. This analysis revealed significant main effects of ROI [$F(3, 520)=10.54$, $p<0.0001$], hemisphere [$F(1,520)=5.58$, $p=0.0185$], character type [$F(3,520)=16.92$, $p<0.0001$] and a trend for an interaction of character type and hemisphere [$F(3,520)=2.24$, $p=0.0827$].

Post-hoc comparisons regarding the ROIs along the vOT pooled over both hemispheres revealed a significantly decreased overall activation for the most anterior ROI 1 compared with all other ROIs (ROI 2 ($t=-3.10$, $p=0.0020$*), ROI 3 ($t=-5.29$, $p<0.0001$***) and ROI 4 ($t=-3.87$, $p<0.0001$***)) and enhanced activation for ROI 3 compared with ROI 4 ($t=2.07$, $p=0.0388$). Comparing character types across ROIs and hemispheres (Figure 2.4c) revealed stronger activation for LET compared with TFF ($t=2.99$, $p=0.0029$*), NFF ($t=6.77$, $p<0.0001$***), and DIG ($t=3.73$, $p=0.0002$**). Importantly, TFF was stronger than NFF activation ($t=2.35$, $p=0.0191$ (*)). Further, the activation was significantly stronger in the right than in the left hemisphere ($t=2.36$, $p=0.0185$*).

The trend for the interaction of character type and hemisphere was driven by an overall stronger activation for LET in the right than in the left hemisphere ($t=4.61$, $p<0.0001$***). Post-hoc LMMs for each hemisphere separately revealed character type (left: [$F(3,255)=6.74$, $p=0.0002$]; right: [$F(3,252)=9.00$, $p<0.0001$]) and ROI effects (left: [$F(3,255)=3.36$, $p=0.0193$]; right: [$F(3,252)=7.06$, $p=0.0001$]) in both models. Subsequent post-hoc t-tests to clarify differences between character types revealed stronger activation for LET compared with NFF ($t=4.45$, $p<0.0001$***) and for TFF compared with NFF ($t=2.74$, $p=0.0066$*) for the left hemispheric ROIs and stronger activation for LET compared with the other character types (TFF: ($t=2.58$, $p=0.0103$(*)); NFF: ($t=4.53$, $p<0.0001$***); DIG: ($t=3.02$, $p=0.0028$*)) in the right hemisphere. The significant training effect in left vOT ROIs was verified by the enlarged fMRI-group (Figure S2.3).

2.3.3 *Enhanced functional connectivity to superior parietal/lateral occipital regions for trained false-fonts*

Second level random effect results ($FWE_{corr.}$ of $p<0.05$, using a CDT of $p<0.001$) of bilateral fusiform gyrus (FFG) seed-based functional connectivity analyses are summarized in the Supplemental Information Figure S2.4 and Table 2.3 for each character type and the corresponding contrasts.

There was no significant difference in the functional connectivity from the left or right FFG seed regions between TFF and NFF. The functional connectivity of the left FFG seed region for TFF showed a significant negative correlation with training duration to a cluster in the left superior parietal gyrus/lateral occipital cortex (LOC; Figure 2.4d, Table 2.2).

Table 2.3 Functional connectivity seed-voxel analyses

Functional connectivity							
Left FFG seed	$p(FWE_{corr})$	k	T	x	y	z	Brain region
TFF vs baseline	0.001	180	9.53	-46	-66	-16	ITG/FFG
CFF vs baseline	<0.001	429	7.84	-40	-64	-12	ITG/FFG
DIG vs baseline	0.009	116	7.48	50	48	-6	Frontal pole
	<0.001	193	6.75	50	-72	6	LOC
	<0.001	220	6.10	-8	50	-12	ACG/ paracingulate gyrus
DIG > CFF	0.003	134	5.15	-2	48	0	ACG paracingulate gyrus
CFF > DIG	0.008	114	6.19	40	36	30	MFG
	0.030	8	5.81	-40	36	24	MFG
Right FFG seed							
TFF vs baseline	<0.001	274	7.21	52	-66	-18	ITG/FFG
CFF vs baseline	<0.001	215	6.88	46	-60	-18	ITG/FFG
LET vs baseline	0.009	121	6.08	-46	-66	20	AG
	0.040	89	5.45	58	-60	12	STG
DIG vs baseline	0.009	123	7.74	38	-70	-12	ITG/FFG

Listed are MNI coordinates (x, y, z) of cluster maxima at p(CDT)<0.001, FWEc<0.05. TFF= trained false font, CFF=control false font, LET = letter, DIG = digit; MTG=middle temporal gyrus, ITG= inferior temporal gyrus, FFG= fusiform gyrus, STG= superior temporal gyrus, ACG= anterior cingulate gyrus, MFG = middle frontal gyrus, AG= angular gyrus, LOC= lateral occipital cortex, l=left, r=right

2.4 Discussion

Understanding how the functional specialization and the preferential response of distinct patches of the cortex is initialized during development and learning is crucial because such knowledge not only

allows characterizing normal developmental and learning-related plastic processes in the brain but more importantly allows detecting alterations that may either impede learning and predict poor learning outcomes or specifically facilitate learning. On the example of the well-known functional specialization of the left vOT/N1 to print in literates, this study aimed to clarify which processes drive neural specialization and to quantify the visual processing of characters of varying expertise, learning stage and familiarity levels in prereading children in the vOT and its electrophysiological correlate N1.

Our approach included, first, a well-controlled artificial character-speech sound learning procedure to characterize the emergence of preferential vOT responses to previously unknown characters and, second, the examination of the individually varying accumulated expertise of prevalent, culturally meaningful types of characters within the first years of a child's life. Learning to associate artificial letters to speech sounds was reflected in preferential activation for trained compared with novel characters in the visual N1 ERP and in the vOT cortex BOLD response. This result clearly demonstrates the initialization of specialized print processing after short GPC training and critically extends previous knowledge about the development of specialization to print in children (Brem et al., 2010) and adults (Dehaene et al., 2010). The well-controlled setting of the short artificial GPC training allowed for concluding that predominantly phonological association processes trigger the initial specialization for novel characters in the vOT. In addition, the ease of learning as quantified by the learning duration revealed that the faster children learned new associations, the stronger was the corresponding specialization of the vOT to single characters, confirming expertise dependent activation (Price & Devlin, 2011) emerging in the prereading brain. The preferential activation to trained characters in the vOT is likely to result from building up novel feedback circles to higher order cognitive areas in the prereading brain, which in turn, provide predictions about the content of the visual input (Price & Devlin, 2011). This conclusion is also substantiated by the emergent functional connectivity of lvOT to the left inferior parietal lobe, a brain structure considered crucial for reading (Turkeltaub et al., 2003; van der Mark et al., 2011). Our results thus point to a parallel development of feedback circuits and preferential functional activation to specific stimulus categories during learning and thus critically

extend previous findings on the mechanisms of functional specialization during development in the cortex (Saygin et al., 2016).

Changes in the vOT activity (Hashimoto & Sakai, 2004; Song et al., 2010) and stronger N1 activation have been reported when adults learn print-like stimuli (Maurer et al., 2010; Pegado et al., 2014) and with increasing literacy (Pegado et al., 2014). Similarly, preferential activation to words in prereaders has been shown by training real GPC over several weeks even though the children's reading skills were still rudimental after training (Brem et al., 2010). Such training effects suggest that learning grapheme - phoneme correspondences is the key factor for initializing specialization and preferential activation to print in the vOT but potential confounds introduced through implicit lexical processing when examining words rather than single letters in prereaders (Brem et al., 2010) or through established reading networks when testing adults (Hashimoto & Sakai, 2004; Maurer et al., 2010) could not be completely excluded in previous studies.

Here, we directly and exclusively manipulated the level of phonological associations of single characters in a group of prereading children through targeted training to mimic the process of letter-speech sound learning at school and show 1) that this learning and the corresponding cortical reorganization processes drive the emergence of functional specialization to the building blocks of words and 2) that the functional specialization to characters depends on learning skills. As grapheme-phoneme learning is considered the core principle of acquiring alphabetic languages (Blomert, 2011), learning performance in such model training and the corresponding level of neural specialization in prereaders might index success of reading acquisition later on. Knowledge about different learning courses regarding functional specialization is highly relevant and could critically improve early identification of children with poor reading outcomes across languages.

In addition to the experimental manipulation of expertise through phonological association training, we also compared character types naturally varying in their level of expertise (LET, DIG vs. NFF) regarding phonological, semantic and/or magnitude associations which are built up and refined over

the course of a child's development. In general, ROI analyses over bilateral vOT revealed a pronounced preference to LET. More specifically, the activation pattern over the left vOT ROIs nicely followed the learning stage related predictions made by the interactive account of vOT function: Character types building up new feedback circuits that allow associations to phonological codes such as newly learned artificial (TFF) or real letters (LET) yielded an enhanced activation as compared to NFF most probably as a result of imprecise top-down predictions. The left hemispheric BOLD response for explicitly learned DIG showed a significant difference neither to NFF nor to LET/TFF which can be explained with the more established feedback circuits and more precise phonological predictions. In addition, the training effect in the left hemisphere indicates that learning rapidly facilitates the transition to a goal-driven feedback loop. The pronounced activation to LET over the right vOT might be explained by immature hemispheric specialization in children (Ossowski & Behrmann, 2015) or alternatively index a different processing strategy in children with poor reading outcomes (Brem et al., 2013).

In addition to the vOT, we identified two cortical areas preferentially responding to LET. First, the activation pattern in the right superior temporal gyrus (STG) was mainly driven by enhanced activation to LET compared with NFF. The STG has shown anatomical alterations in relation to reading skills such as reductions in grey matter volume in dyslexic children (Richlan et al., 2013) or in at-risk children at prereading age (Black et al., 2012; Raschle et al., 2011), and increased grey matter volume in subjects who learned to read in adulthood (Carreiras et al., 2009). Whether or not the enhanced activation for LET in the present data reflects some compensatory processing of language information in children at heightened risk for dyslexia needs to be clarified. However, this region has been associated with the processing of speech and phonology and, especially the left STG has been implicated in graphophonological decoding (Jobard, Crivello, & Tzourio-Mazoyer, 2003). Given the reduced hemispheric specialization in young children (Ossowski & Behrmann, 2015), increased activation in the right hemisphere could also indicate early letter speech-sound integration as shown in previous studies (Blau et al., 2010; van Atteveldt, Formisano, Goebel, & Blomert, 2004). Second, LET showed stronger activation in the left middle frontal gyrus (MFG) of the dorsolateral prefrontal cortex as compared with

DIG, which could index increased attentional resources and/or enhanced control functions implicated in processing characters with less expertise. Such resources and corresponding activation may diminish with development from the younger to the older reader with increasing practice and automatization in print processing (B. A. Shaywitz et al., 2001; B. A. Shaywitz et al., 2007).

In contrast to the fMRI vOT data, the N1 ERP showed the most pronounced activation for DIG. N1 amplitude modulations have strongly been associated with the level of expertise to specific visual categories (Rossion, Gauthier, Goffaux, Tarr, & Crommelinck, 2002; Tanaka & Curran, 2001) including print (Brem et al., 2005; Maurer, Brem, et al., 2005). Single digits, the corresponding number names and initial associations to magnitudes are already explicitly introduced and trained in kindergarten and explain the relatively high level of expertise and correspondingly high electrophysiological response to this character type. The discrepancy in the N1 ERP and vOT BOLD signal regarding preferential response to either digits or letters may be explained by a differential weighting of the impact of various aspects of expertise and learning stage on the measured signals. The BOLD activation in the vOT may predominantly reflect integration of the visual input and of emerging phonological predictions. The activation in the N1 interval, known to scale with expertise (Brem et al., 2005; Rossion et al., 2002), assumingly reflects general, temporally co-occurring expertise effects, summed over multiple domains including visual familiarity and associations to phonological, semantic and/or magnitude representations (Brem et al., 2010; Maurer, Brem, et al., 2005; Park et al., 2014) and account for the pronounced activation to DIG and the somewhat weaker effects for TFF.

Taken together, the simultaneous EEG/fMRI data revealed a preferential N1 response for characters with explicitly learned associations, suggesting expertise dependent specialization relying on feedback information from phonological (TFF) or phonological and semantic/magnitude (DIG) information (Dehaene & Cohen, 2007). In contrast, fMRI activation in the vOT seems more inclined to reflect different learning stages, showing that LET and TFF (low and medium phonological association expertise respectively) are building new feedback circuits which might already be well established for DIG (Price & Devlin, 2011).

2.5 Conclusion

For the first time, we have demonstrated a significant modulation of visual character processing in the prereading brain after short GPC training (<30min), mimicking the first step in reading acquisition. This emerging functional specialization was reflected in a more pronounced activation for trained compared with novel false-fonts irrespective of imaging modality, and a strong relationship between the ease of learning and activation in the left vOT. Moreover, we show distinct expertise dependent activation differences for the visual N1 and for vOT BOLD responses. Our data suggest that the N1 ERP is sensitive to overall expertise associated with the visual input whereas fMRI activity in the left vOT rather quantifies the feedback integration from phonological areas in the different stages of learning. In summary, our results demonstrate that learning enhances preferential activation for printed characters in distinct cortical locations and within a well-defined temporal window in prereading children. These novel insights into learning-dependent beginning specialization of the vOT to print not only facilitate improving the identification of prereaders at risk for reading difficulties and hence, allowing for early, targeted intervention, but also pinpoint the parallel development of functional circuits and cortical specialization in the developing brain during learning.

2.6 Experimental design

2.6.1 Participants

A group of 31 native German speaking, prereading kindergarten children completed four parts of an audiovisual target detection task in a simultaneous EEG/fMRI session. 18 (8f, mean: 6.7+-.36y; Table 2.1) children with appropriate EEG and fMRI data quality were included in the main analysis. Five children with appropriate EEG quality in all four parts and six children with appropriate fMRI data quality for at least TFF and NFF were added in supplemental analyses to verify the results of the core group (Table S2.1 & Figure S2.1 & Figure S2.3).

Children's risk for developmental dyslexia varied and was estimated based on parents reading history assessed with the Adult Reading History Questionnaire (ARHQ; Lefly & Pennington, 2000). To control

for individual risk, the higher parental ARHQ value was included as a covariate variable in statistical models (behavioral, ERP and fMRI analyses). Subjects' intelligence scores (IQ) were within or above the normal range, as estimated with the block design test of the Wechsler Intelligence Scale for Children (HAWIK-IV; Petermann & Petermann, 2007). All children had normal or corrected to normal visual acuity and no diagnosis of attention-deficit/hyperactivity disorder or other neurological or cognitive impairments. The parents gave written informed consent and the children gave oral consent. The local ethics committee of the Canton of Zurich and neighboring Cantons in Switzerland approved the study. All participants received vouchers and presents as compensation.

2.6.2 Behavioral assessment

Prereading status was tested with a short list of twenty simple one- or two-syllable words of common first grade textbooks. Letter and number knowledge was assessed by asking the children to pronounce all 26 upper and lower case letters of the Latin alphabet and to name twenty-one numbers including all single digits from one to nine respectively.

2.6.3 Artificial GPC training

1-5 days (mean: 2.3d) prior the simultaneous EEG/fMRI session, all participants trained the correspondences between six false-font characters and familiar speech-sounds with an adapted version of the computer-based phonics training "GraphoGame" (Karipidis et al., 2017; Lyytinen et al., 2009; Lyytinen, Ronimus, Alanko, Poikkeus, & Taanila, 2007). To simulate reading acquisition, children learned to associate one of two sets of false-font characters with previously well-known speech sounds (Figure 2.1a). The children were assigned to train one of two false-font character sets using an adaptive randomization approach. During the training, the other set of false-font characters was passively presented in the background to control for effects of visual familiarity. Both sets of false-font characters were created based on six lower case letters of the Latin alphabet (Swiss School font: b, d, m, t, u, z) used in the audiovisual target detection task.

The visual stimuli during the training were presented on a laptop positioned in front of the child. The sounds spoken by a female voice were presented over headphones. The children had to choose the correct FF grapheme corresponding to the heard phoneme. The numbers of visual distractors (1-3) was adaptive and changed according to the accuracy rate of the previous trial. The training consisted of 131 trials divided into nine training levels and one test level. Struggling children completed supporting levels to train specifically correspondences with a high error rate. The training lasted until each child was able to match the six speech sounds to their corresponding characters or until each supporting level was maximally processed three times. In the test level, participants' performance on all correspondences was tested by displaying each FF character five times.

Training duration and accuracy was calculated for the complete training session. Training duration varied between children in that faster learners needed less time to learn successfully the associations in the GPC training. To account for the varying number of distractors, the accuracy was calculated using a weighting factor defined as the number of presented items proportional to the maximum possible number of presented items (Karipidis et al., 2017). On the day of the neuroimaging session, all subjects repeated the learned associations and completed a performance test.

2.6.4 Audiovisual target detection task

Participants performed an implicit audiovisual target detection task, which was divided into four parts of 375s each to maintain the attention of the young children (see Karipidis et al., 2017). A pediatric protocol was used and the task was embedded in a story. Each part of the task included a different type of characters: real letters (LET), two different sets of FF characters of which one was trained prior to the EEG-fMRI session (TFF) whereas the other was not trained (NFF), and digits (DIG; Figure 2.1a). All stimuli were presented in unimodal visual and auditory, and audiovisual congruent and incongruent conditions using Presentation® software (Version 16.4, www.neurobs.com). Every part consisted of 16 blocks (4 blocks/condition) presented four times whereby unimodal and bimodal blocks (15 items/block) alternated pseudorandomly separated by fixation periods of 6 or 12 s. Six targets (pictures and/or sounds of an animal, object) requiring a button press were presented in addition to a total of

54 stimuli per condition to maintain children's attention. The stimuli within each block were presented pseudorandomly for 613ms with an interstimulus interval of 331/695ms (Figure 2.1b). Here, we focus on the unimodal visual condition, (for analyses of audiovisual conditions see Karipidis et al., 2017). Visual information was presented using video goggles (VisuaStimDigital, Resonance Technology, Northride, CA). Characters were presented in black in the middle of a grey background (mean visual angles horizontally/vertically LET: 2.8°/4.8°; TFF: 2.9°/4.8°; NFF: 2.7°/4.8°; DIG: 3°/6.7°). In-scanner target detection accuracy (ACC) was high (>89%) and reasonable reaction times (RT) were recorded in all four parts and for all character types (Table S2.4). Performance did not significantly differ between the four parts (ACC: [F(3,15)=1.5, p=0.227]; RT: [F(3,15)=0.9, p=0.466]). Responses of two participants were not logged due to technical problems and therefore not included in this analysis.

2.6.5 EEG and fMRI acquisition

Using an MR-compatible 128-channel EEG system (Net Amps 400, 128-channel EGI HydroCelGeodesic Sensor Net) simultaneous EEG-fMRI recordings were performed on a Philips Achieva 3 Tesla scanner (Philips Medical Systems, Best, The Netherlands). Continuous EEG at a sampling rate of 1 kHz (DC-filter) was recorded with 128 scalp and two electrocardiogram (ECG) electrodes. To reduce gradient residuals during simultaneous EEG-fMRI recordings, the scanner clock and the EEG system were synchronized (Mandelkow et al., 2006). Electrode impedances were kept below 50 kΩ. The recording reference was located at Cz, the ground electrode posterior to Cz. Potential electrode vibration artifacts were minimized by covering the electrodes with a bandage retainer net.

A 32-elements receive head coil was used to acquire 189 volumes for each part of the task using a T2*-weighted whole-brain gradient echo-planar image sequence (EPI) with the following parameters: SofTone factor: 3, slices/volume: 31, repetition time (TR): 1.98s, echo time (TE): 30ms, slice thickness: 3.5mm, slice gap: 0.5mm, flip angle: 80°, field of view (FOV): 24x24cm^2, in plane resolution: 3x3mm^2, sensitivity-encoding reduction factor: 2.2. Specific emphasis was given on reducing scanner noise and improving auditory stimulation by using sound-absorbing over-ear headphones, a sound-absorbing mat in the MR-bore and a SofTone sequence. A custom-made head pad for the EEG net was used, to

reduce head movement and to ensure comfort. Additionally, a field map scan to perform B0 correction was recorded. T1-weigthed images were recorded with a 3D MP-RAGE sequence (slices: 176, TR/TE: 6.8/3.2s, voxel size: 1x1x1mm3, flip angle: 9°, FOV: 27x25.4cm2).

2.6.6 EEG analyses

Analyses were conducted using VisionAnalyzer 2.1 (BrainProducts GmbH, Munich, Germany). Channels with an overall poor data quality were topographically interpolated (range: 0-5 channels, mean: 1.57 channels SD: +-.06). Due to continuous artifacts on the cheek electrodes, we excluded four electrodes from further processing and analyses (E43, E48, E119, E120). In addition, each data set was visually inspected and periods with major artifacts were manually excluded. After MR artefact removal using the average template subtraction method (Allen et al., 2000) and ballistocardiogram correction using sliding average template subtraction, the data was filtered (0.1-30Hz and 50Hz Notch) and down sampled (500 Hz). Independent component analysis (ICA; Jung et al., 2000)) was applied to exclude blinks, eye movements, and residual ballistocardiogram artifacts. After artifact corrections, the data was rereferenced to the average reference (Lehmann & Skrandies, 1980). Trials with remaining artifacts exceeding +-200µV or identified by visual inspection were excluded. The data was segmented from -102ms to 498ms after visual presentation and averaged character type-wise. Core group grand averages included a mean of 41 epochs per character type (means: LET=48, TFF=45, NFF=45, DIG=40; range: 19 – 54 epochs). Using the GFP maxima of the mean ERPs over all four character types, the interval of the N1 was defined as ±30ms (194-254ms) around the N1 GFP peak. The mean amplitude values within these intervals were further analyzed.

2.6.7 Electrodes of interest analyses

To examine print specific activations over the posterior scalp, the mean amplitudes over a left (LOT), middle (MO), and right (ROT) electrode cluster were extracted (Figure 2.2a). These left, middle and right electrode clusters comprised of the following electrodes (LOT: E65, E68, E69, E70, E73; MO: E81, E82, E75, E74; ROT: E83, E88, E89, E90, E94). Statistical analyses for GFP and LOT/MO/ROT amplitudes were performed using LMM, including repeated measurements within each subject (SAS 9.4, SAS

Institute, Cary NC). In LMM fixed and random effects explain differences between subjects and the variability within subjects respectively. To investigate the different processing of the four character types the random intercept model with fixed factors electrode cluster (LOT, MO, ROT) and character type (LET, TFF, NFF, DIG) and the interaction of these factors was calculated, including the specific random intercept for each subject. Studentized conditional residuals were computed to identify and exclude potential outliers. To correct for variance inhomogeneity, an outlier cutoff of three standard deviations from the mean was used (Roth, Roesch-Ely, Bender, Weisbrod, & Kaiser, 2007). In addition, QQ-plots were inspected to ensure the assumption of normality and homoscedasticity of predicted versus conditional residual plots. For trends of specific interest and significant interactions, post-hoc t-tests were performed. Uncorrected p-values of post-hoc comparisons surviving Tukey-Kramer correction for multiple comparisons are specifically marked with asterisks within the text ($^{(*)}$=p_{corr}<0.1, *=p_{corr}<0.05, **=p_{corr}<0.01, ***=p_{corr}<0.001). Correlational analysis was performed to determine relations between stimulus types, using SPSS Version 22.0.0.0. For normally distributed data Pearson and for non-normally distributed data Spearman correlation was used.

2.6.8 fMRI analyses

Data was preprocessed and analyzed using SPM12 on MATLAB R2015b. After field map correction, images were spatially realigned and unwarped, slice time corrected, coregistered, segmented, and normalized using the deformations derived from the segmentation and a pediatric brain template created with the Template-O-Matic toolbox (Wilke, Holland, Altaye, & Gaser, 2008). After resampling (3x3x3mm^3), the data was smoothed with an isotropic 6mm full width at half maximum Gaussian kernel. Volumes with more than 1.5mm scan-to-scan movement were repaired by linear interpolation using the ArtRepair toolbox (Mazaika, Glovera, & Reiss, 2011). Due to technical problems and excessive movement, files of two children had to be adjusted in length.

Including six predictors (auditory, visual, congruent, incongruent, target, and response) and six movement parameters for each participant and each part of the experiment (LET, TFF, NFF, DIG), a random-effect GLM) was calculated. We report results of 2nd-level random effect analyses, one-sample

t-tests to characterize the general activation for each character type and second level t-tests based on first level contrasts to determine differences between visual character types of the experiment.

2.6.9 Region of interest analyses

We performed ROI analyses of the whole vOT and in distinct regions along the vOT. First, we created a functional mask (left: lvOT, right: rvOT) that included the sum of all bilateral occipitotemporal areas activated by any of the four visual character types (LET OR TFF OR NFF OR DIG logical operation at $p_{uncorr.}$<0.001), using MarsBaR (Brett, Anton, Valabregue, & Poline, 2002). Second, on an anterior to posterior axis, four 9x9x9mm cubes were created to cover the left vOT from the letter from area (Thesen et al., 2012) to the visual word form area (Brem et al., 2009; Vinckier et al., 2007). To derive the corresponding ROIs in the right hemisphere, R1-R4 were flipped: R1 (x=+/-42, y=-44, z=-22), R2 (x=+/-48, y=-56, z=-20), R3 (x=+/-52, y=-68, z=-18), R4 (x=+/-48, y=-80, z=-16; Figure 2.4c). Beta values of the four bilateral ROIs were extracted and an LMM with fixed factors ROI (R1, R2, R3, R4), hemisphere, and character type was computed, including a specific random intercept for each subject. To compute LMMs and correlations, the same procedure as for the EEG analyses was used.

2.6.10 Connectivity analyses

Seed to voxel functional connectivity analysis was performed using weighted GLM as implemented in the CONN toolbox (Whitfield-Gabrieli and Nieto-Castanon, 2012). The normalized anatomical image of each participant was segmented into white matter (WM), gray matter (GM) and cerebrospinal fluid (CSF) masks. Preprocessed functional data was band-pass filtered from 0.009 to 0.08 Hz and influences of motion, WM and CSF were regressed out using the CompCor strategy (Behzadi et al., 2007). To examine functional connectivity associated with GPC training and character type differences we defined a seed region (seed FFG, see Figure 2.4d) within the anatomical left fusiform gyrus (FFG; Talairach Daemon (TD) database (Lancaster et al., 2000); WFU Pickatlas, version 2.4 (Maldjian et al., 2003)) that showed functional activation to either TFF or NFF (logical operation: FFG AND TFF OR NFF). The seed was defined using MarsBaR (Brett et al., 2002) and for functional activation we applied

cluster-level FWE_{corr} $p<0.05$ on a cluster-defining threshold (CDT) of $p<0.001$. This left FFG seed was flipped to the right to also examine functional activation of the right hemispheric homologue.

For seed-voxel analyses, the residual time course for each seed was extracted and used to generate first-level correlation maps by computing Pearson's correlation coefficients to the time course of all other voxels. To perform second level GLM analyses, the first-level correlation coefficients were converted to normally distributed z-scores using the Fisher transformation. The individual familial risk score was entered as a between-subject covariate of no interest. In addition, we created a grey matter mask using the tissue probability mask of grey matter of the pediatric brain template. All voxels with a probability > 0.5 were defined as grey matter. Within the grey matter mask, a cluster-based FWE-corr threshold of $p < 0.05$ was applied on a voxel-wise uncorrected threshold of $p < 0.001$. In analogy to whole-brain correlational fMRI analysis for TFF, we examined the correlation of FFG seed-to-voxel connectivity with training duration (Figure 2.4d). Furthermore, one-sample and paired t-tests were computed on regression coefficients to yield functional connectivity maps for each character type (TFF, NFF, LET, DIG; see Supplemental Information Figure S2.4 and Table 2.3) against baseline and their differences (training effect, character type differences).

2.7 Acknowledgements

We thank A. Baur, D. Dornbierer, A. Roth, and M. Schneebeli for their assistance during recruitment, investigation, and data analyses and D. Brandeis for his valuable inputs on the text. We are grateful to U. Richardson and I. Kapanen (University of Jyväskylä, Finland) for their support in implementing the artificial GPC training. We thank all the participating children with their families.

2.8 Author contributions

Conceptualization, G.P., I.I.K., and S.B.; Methodology, G.P., I.I.K., M.R., and S.B.; Project Administration, G.P. and I.I.K.; Investigation, G.P., I.I.K., C.B., M.R., and S.B.; Resources, P.S., S.W., and S.B.; Writing-Original Draft, G.P., I.I.K., and S.B., Writing-Review and Editing, G.P., I.I.K., C.B., M.R., C.H., P.S., S.W., and S.B.; Funding Acquisition, S.B.

2.9 Supplemental Information

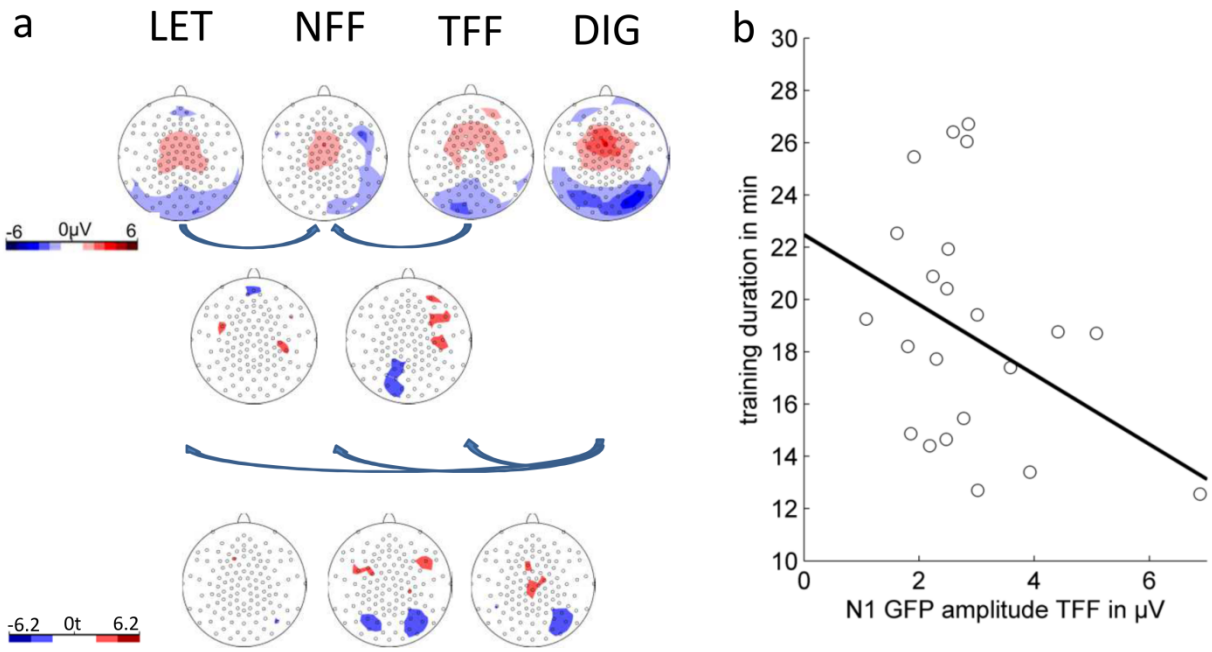

Figure S2.1. Verification of EEG analyses with an enlarged group of 23 subjects. The EEG analyses of the core group were repeated with an enlarged group of 23 children (Supplementary Table 2.1), to verify the results. The N1 amplitude analyses of this enlarged group substantiate the results of the main text in showing the same expertise and training effects. Left: N1 potential field maps of the grand averages (first row, in µV) for each character type and the statistical t-maps (rows 2-4), illustrating the differences between character types. The LMM for the electrode clusters with fixed factor character type (LET, TFF, NFF, DIG) and cluster (LOT, MO, ROT) revealed a significant character type effect [$F(3,239)=5.69$, $p=0.0009$]. This difference was driven by an enhanced negativity of DIG as compared to all other character types (DIG<LET: $t=-2.06$, $p=0.0404$, DIG<TFF: $t=-1.86$, $p=0.0634$, DIG<NFF: $t=-3.77$, $p=0.0002$*). In addition, the N1 negativity to TFF was significantly stronger than to NFF ($t=-3.26$, $p=0.0013$*) and also LET was significantly more negative than NFF ($t=-2.20$, $p=0.0288$). The LMM for GFP with fixed factor character type (LET, TFF, NFF, DIG) showed a significant character type effect [$F(3,63)=4.91$, $p=0.0040$]. Post-hoc tests revealed a significantly enhanced GFP to DIG as compared to all other character types (DIG>LET: $t=2.93$, $p=0.0047$*, DIG>TFF: $t=3.81$, $p>0.0003$*, DIG>NFF: $t=2.72$, $p=0.0085$). Right: The GFP for the N1 TFF correlated marginally with training measures (training duration: Pearson $r = -0.40$, $p = 0.073$).

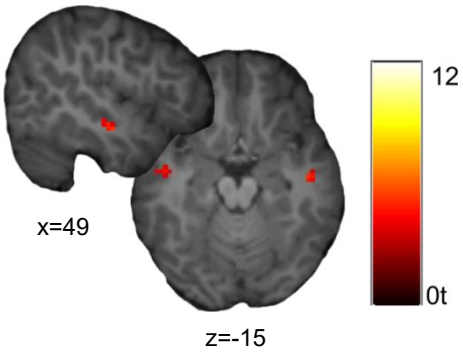

Figure S2.2. fMRI whole brain analysis of the core group (n=18): Training effect. The whole brain analysis of the contrast TFF vs NFF showed a bilateral middle temporal gyrus (MTG) activation (MNI x=49/-56, y=-12/-6, z=-15/-18, Supplementary Table 2.3) which was more pronounced for trained as compared to untrained, novel characters. Given that this activation did not survive the a priori defined cluster correction for multiple comparisons, this marginal effect shall be interpreted with care. Activation in the MTG has been related to integration of speech sounds and print in the process of reading acquisition and the bilateral activation could be explained by a diminished lateralization in language processing in young children (activation on axial and sagittal slices shown for $p<0.001$ (uncorrected) cluster size left MTG k=20, right MTG k=17).

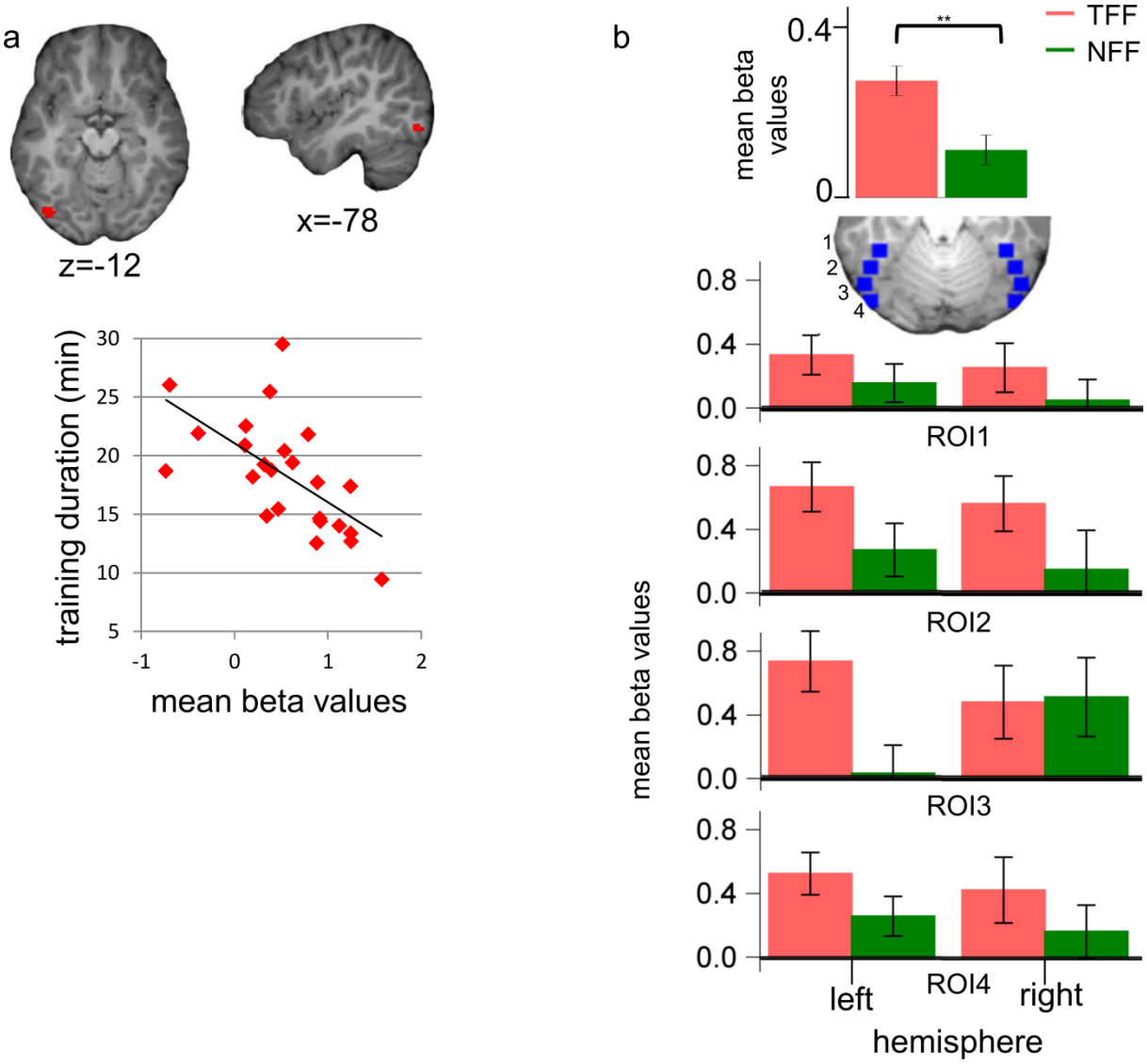

Figure S2.3. Verification of fMRI training effect in an enlarged group of 24 subjects. To verify the training effect, fMRI data of an enlarged group, including 24 children (Supplementary Table 2.1), was analysed. This enlarged fMRI group consisted of data sets meeting data quality criteria for TFF and NFF. Therefore, ROI analyses only included the TFF and NFF parts of the experiment. These analyses confirmed the results of the core group. (a) Correlation of BOLD responses to TFF in the left vOT ROI with children's training duration in the GPC training. Faster learning was correlated with significantly higher activation in the left vOT (small volume corrected $p(FWE_{corr})<0.05$). Below, the negative correlation of the significant vOT cluster activation is plotted against training duration for illustration purposes. (b) ROI analyses in the vOT. Top: The LMM with fixed factors ROI (R1, R2, R3, R4), hemisphere (l, r), and character type (TFF, NFF) showed significant main effects of ROI [F(3, 337)=3.92, p=0.0090] and character type [F(3,337)=15.33, p=0.0001] and a marginal non-significant interaction effect of ROI and hemisphere [F(3,337)=2.08, p=0.1021]. Post-hoc comparisons regarding the ROIs along the vOT pooled over both hemispheres revealed a significantly decreased overall activation for ROI 1 compared with ROI 3 (t=-3.38, p=0.0008*). Comparing character types across ROIs and hemispheres revealed stronger activation for TFF than NFF (t=3.91, p=0.0001**). Bottom: For illustration purposes, beta values of ROIs within each hemisphere are shown separately. Error bars denote standard error.

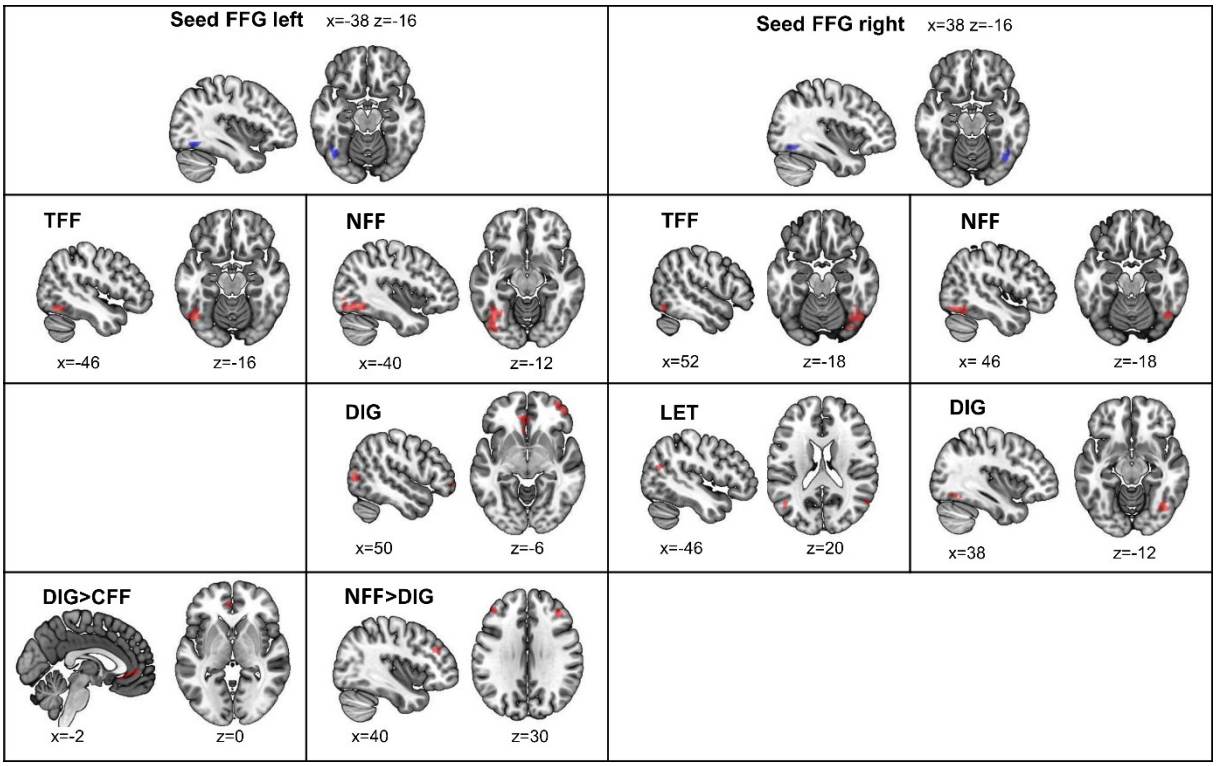

Figure S2.4. Functional connectivity results with left and right FFG seeds

Table S2.1. Characteristics and performance on behavioral measures for 23 (enlarged EEG-group) and 24 (enlarged fMRI-group) subjects included in supplemental analyses

Enlarged groups for supportive analyses	EEG-group	fMRI-group
N	23	24
Sex (male/female)	13/10	13/11
Age (y)	6.8 ±.36	6.8±.3
Handedness (right/left)	20/3	21/3
IQ estimation (nonverbal)[1)]	105 ±14	107±10
Familial risk for dyslexia[2)]	.53±.17	.52±.14
FF training set (1/2)	12/11	12/12
GPC Training duration (min)[4)]	18±4	18±4
GPC Trainings accuracy (weighted in %)[4)]	83±13	81±8
Letter speech-sound knowledge (52 upper and lower case)[3)]	16.7±10.4	17.5±8.2
Number knowledge (21 one- to three-digit numbers) [3)]	15.3±4.1	14.8±3.6

[1)] Block design test of the Wechsler Intelligence Scale for Children (HAWIK-IV)
[2)] Highest parental adult reading history questionnaire value (ARHQ)
[3)] Number of correctly named items
[4)] GPC: artificial grapheme-phoneme training

Table S2.2. Activations for each character type vs baseline in the core group (n=18)

cluster	cluster size	peak voxel	MNI coordinates			Hemisphere	Brain region
$p(FWE_{corr})$	k	T	x	y	z		
LET vs baseline							
0.00001	149	11.57	-41	24	39	l	MFG
		6.15	-53	30	30	l	Pars triangularis
		5.49	-44	15	48	l	MFG
0.00000	981	10.31	49	-75	-6	r	IOG
		8.71	40	-66	0	r	MOG
		8.67	25	-90	3	r	MOG
0.00000	704	9.39	-41	-69	-15	l	FG
		9.24	-32	-96	-3	l	MOG
		8.93	-41	-84	-9	l	IOG
0.01141	52	7.50	-44	45	-6	l	OFC
0.00000	296	6.74	49	33	30	r	MFG
		6.20	13	21	54	r	SFG
		5.85	40	15	48	r	MFG
0.00000	176	6.03	22	60	-9	r	OFC
		5.71	37	48	12	r	MFG
		5.70	46	48	-6	r	OFC
0.00010	107	6.01	-41	57	12	l	MFG
		5.26	-44	48	24	l	MFG
0.03826	40	4.65	-32	-60	54	l	SPG
TFF vs baseline							
0.00001	168	6.86	-47	-69	0	l	MOG
		4.97	-47	-60	-15	l	IOG
		4.80	-41	-69	-12	l	IOG
0.00000	471	5.93	43	-63	-12	r	ITG
		5.72	43	-60	-3	r	MTG
		5.57	52	-66	-3	r	ITG
NFF vs baseline							
0.00000	190	7.06	-38	-66	-15	l	FG
		6.68	-44	-72	-3	l	IOG
		4.89	-41	-84	-9	l	IOG
0.00000	449	7.03	43	-72	-6	r	ITG
		6.74	46	-60	-3	r	MTG
		5.33	25	-102	0	r	Calcarine sulcus
0.02993	44	4.88	-32	-93	-3	l	MOG
		3.93	-23	-93	-12	l	IOG
DIG vs baseline							
0.00124	114	6.62	25	-87	6	r	MOG
		5.11	40	-66	0	r	MOG
		4.65	52	-84	3	r	MOG

Listed are the MNI coordinates (x, y, z) of cluster maxima for p<0.001, k=40 corresponding to a cluster-wise error corrected threshold ($p(FWE_{corr})$<0.05). LET= letter, TFF= trained false-font, NFF=untrained, novel false-font, DIG= digit, MFG=middle frontal gyrus, MOG=middle occipital gyrus, IOG=inferior occipital gyrus, FG=fusiform gyrus, OFC=orbitofrontal cortex, ITG=inferior temporal gyrus, MTG=middle temporal gyrus, SFG=superior frontal gyrus, SPG=superior parietal gyrus, l=left, r=right.

Table S2.3. Main activation peaks of the second level t-tests for the contrast TFF vs. NFF

cluster	cluster size	peak voxel	MNI coordinates			Hemisphere	Brain region
$p(FWE_{corr})$	equivk	T	x	y	z		
TFF>NFF							
0.58486	17	5.32	49	-12	-15	r	MTG
0.46249	20	4.98	-56	-6	-18	l	MTG

Listed are MNI coordinates (x, y, z) of cluster maxima at an uncorrected p<0.001, k>15. TFF= trained false-font, NFF=untrained, novel false-font, MTG=middle temporal gyrus, l=left, r=right

Table S2.4. In-scanner performance in the audiovisual target detection experiment for the core group (n=18)

Measure	Mean ± SD	Range
In-scanner accuracy LET (%)	97±7.3	71-100
In-scanner reaction time LET (ms)	711±133.5	571-1005
In-scanner accuracy TFF (%)	92±11.2	60-100
In-scanner reaction time TFF (ms)	755±166.9	579-1118
In-scanner accuracy NFF (%)	89±12.7%	54-100
In-scanner reaction time NFF (ms)	719±132.2	533-905
In-scanner accuracy DIG (%)	90±13.4%	66-100
In-scanner reaction time DIG (ms)	761±188.6	512-1147

3 Study B: Initial reading skills modulate print-sensitive cortical processing after half a year of reading instruction: A pediatric simultaneous EEG-fMRI study

Georgette Pleisch[1,2], Iliana I. Karipidis[1,2], Alexandra Brem[1], Martina Röthlisberger[1], Alexander Roth[1], Daniel Brandeis[1,2,4,5], Susanne Walitza[1,2,5], Silvia Brem[1,2,3]

[1]Department of Child and Adolescent Psychiatry and Psychotherapy, Psychiatric Hospital, University of Zurich, Switzerland

[2]Neuroscience Center Zurich, University of Zurich and ETH Zurich, Zurich, Switzerland

[3]MR-Center of the University Hospital for Psychiatry and the Department of Child and Adolescent Psychiatry and Psychotherapy, University of Zurich, Switzerland

[4]Department of Child and Adolescent Psychiatry and Psychotherapy, Central Institute of Mental Health, Medical Faculty Mannheim/Heidelberg University, Mannheim, Germany.

[5]Center for Integrative Human Physiology Zurich, University of Zurich, Switzerland.

A similar version of this article has been published as:

Pleisch, G., Karipidis, I.I., Brem, A., Röthlisberger, M., Roth, A., Brandeis, D., Walitza, S., Brem, S., 2019b. Simultaneous EEG and fMRI reveals stronger sensitivity to orthographic strings in the left occipito-temporal cortex of typical versus poor beginning readers. Dev Cogn Neurosci, 100717.

3.1 Abstract

The level of reading skills in adults and children is mirrored in the strength of preferential neural activation of print relative to a visual control condition in the brain. Such print-sensitive activation is usually found in both, a characteristic ERP over the left occipitotemporal scalp around 150-250 ms and in the hemodynamic response of left vOT brain regions of literates. Intensive training of letter-speech sound correspondences initializes coarse print sensitivity when prereading children and illiterate

adults start formal reading instruction. Here, we examined two levels of print sensitivity in a sample of beginning readers at varying familial risk for developmental dyslexia after half a year of formal reading instruction at school. ERPs of processing words, nonwords and false-font strings were recorded during fMRI. Reading fluency was assessed with standardized reading scores and print-sensitive activation was compared between children with normal or poor reading development. Coarse print sensitivity was only detected in differential N1 ERP amplitude measures but not in the left vOT BOLD signal. Additionally, neither measure showed robust group differences for coarse or fine print-sensitive processing at this age. However, by emphasizing on the BOLD activation directly related to the N1, using single-trial ERP-informed fMRI analysis, we found a stronger modulation of left vOT activation by the N1 amplitude for normal readers than for poor readers. This finding confirms that the left vOT function is attuning to print processing from the start of reading acquisition but subtle group differences at this early stage may only be detectable when exploiting the advantages of different neuroimaging methods.

3.2 Introduction

Reading remains one of the most important cultural inventions in today's life and is crucial for a child's academic and personal development (Mugnaini, Lassi, La Malfa, & Albertini, 2009; Poskiparta, Niemi, Lepola, Ahtola, & Laine, 2003; Snowling, 2013). 3-10% of the children, however, do not master the challenges of fluent reading and are diagnosed with developmental dyslexia, a developmental reading disorder (Snowling, 2013). Familial risk increases the prevalence of dyslexia to 30-65% (Pennington & Lefly, 2001) in children of affected families. A better understanding of the neural variations in the underlying functional language network at an early stage of children's formal reading instruction may help to identify children with poor reading development at an early age and would allow for providing preventive support.

Developmental dyslexia has been associated with neurobiological deficits in efficiently processing print (Boros et al., 2016; Jobard et al., 2003; Norton et al., 2015; Ozernov-Palchik & Gaab, 2016; S. E. Shaywitz & Shaywitz, 2008). Neuroimaging studies consistently point to the left vOT cortex as a key

structure for fluent and efficient reading (Cohen et al., 2000; Cohen et al., 2002; Glezer et al., 2009; Price, Moore, & Frackowiak, 1996; Saygin et al., 2016), which is thereby often referred to as VWFS (Cohen et al., 2002; Vinckier et al., 2007). In the anterior part of the VWFS, a specific patch in the left mid fusiform gyrus, the so-called VWFA (Cohen et al., 2000; Cohen et al., 2002), shows preferential activation to print (Baker et al., 2007; Cohen et al., 2003; Vinckier et al., 2007) or even word forms (Glezer et al., 2009; Glezer & Riesenhuber, 2013), while a specific LFA is located somewhat more posterior (Tagamets, Novick, Chalmers, & Friedman, 2000; Thesen et al., 2012). Because reading is a relative new cultural invention, it has been suggested that the VWFA has adopted a special function in the orthographic recognition of written words (Cohen et al., 2000; Glezer & Riesenhuber, 2013) within the last few thousand years (Dehaene & Cohen, 2007) and is progressively specialized to process written words during reading acquisition.

The involvement of this region in visual orthographic print processing can be assessed by studying print-sensitive activation or the level of neural tuning to print. Coarse neural tuning is reflected by a preferential response to print (words, nonwords, letter strings) as compared to well matched visual control stimuli such as symbol strings or false-font strings (Baker et al., 2007; Dehaene-Lambertz & Gliga, 2004; Dehaene et al., 2001; R. Gaillard et al., 2006; C. Liu et al., 2008; Turkeltaub et al., 2003; Vinckier et al., 2007), while fine levels of neural tuning (Centanni et al., 2017; Glezer et al., 2009) are indexed by differential activation to real words compared with other orthographic strings (e.g. pseudowords, nonwords; Baker et al., 2007; Eberhard-Moscicka et al., 2015; Glezer et al., 2009; Zhao et al., 2014). Print-sensitive processing in the VWFA is a ubiquitous phenomenon, seen across different languages and writing systems (Cao et al., 2011; Hu et al., 2010; Paulesu et al., 2001). Print sensitivity in the VWFA either develops with the start of formal reading instruction (Ben-Shachar et al., 2011; Brem et al., 2013; Maurer et al., 2007; Saygin et al., 2016), or when illiterate adults (Dehaene et al., 2010) or children (Brem et al., 2010; James, 2010) receive intensive reading training. The process of developing functional specialization in this region builds on preexisting connections between the VWFS and higher order language areas as shown for prereading children (Saygin et al., 2016) and the cortical

plasticity of this region might be genetically modulated (Skeide et al., 2016) and preconstrain reading outcome.

While coarse print-sensitive activation shows an early maturation upon reading instruction in childhood (Brem et al., 2010; Eberhard-Moscicka et al., 2015; James, 2010; Maurer et al., 2007), full specialization and word selective responses (fine tuning) shows a more protracted development (Centanni et al., 2017; Kronschnabel, Schmid, Maurer, & Brandeis, 2013; but see Zhao et al., 2014).

Along with the development of the direct route in reading (Coltheart, Rastle, Perry, Langdon, & Ziegler, 2001), neural preference was assumed to arise for real words compared to pseudowords in the left vOT, however, this fine-tuned print-sensitive activation was not found in several studies (Binder, Medler, Westbury, Liebenthal, & Buchanan, 2006; Devlin et al., 2006; Kronbichler et al., 2004), which might be caused by the broad examination of the left vOT (Glezer et al., 2009). To overcome this problem, individual examinations of the left vOT revealed the expected preference for real words (Centanni et al., 2017; Glezer et al., 2009; Glezer & Riesenhuber, 2013).

The strength of the print-sensitive response has been associated with the expertise level of reading skills (Ben-Shachar et al., 2011; Dehaene et al., 2005; Zhao et al., 2014). Attenuated functional activation and diminished functional connectivity (B. A. Shaywitz et al., 2002; van der Mark et al., 2011) of this region during reading tasks (for meta-analyses see Maisog, Einbinder, Flowers, Turkeltaub, and Eden; 2008; Richlan et al.; 2009; Richlan, Kronbichler, and Wimmer; 2011) suggest a failure in orthographic processing, severely affecting the reading process. Print sensitivity is reduced in dyslexic children (Boros et al., 2016; Hoeft et al., 2007; Richlan et al., 2011; van der Mark et al., 2009), adolescents (Kronschnabel et al., 2013), and adults (Brambati et al., 2006; Paulesu et al., 2001; Richlan et al., 2009; Richlan et al., 2011). In correspondence, structural neuroimaging studies reported a reduction of grey matter volume in the left vOT of dyslexic readers (Kronbichler et al., 2008; Richlan et al., 2013).

The electrophysiological correlate of the left vOT activation is the visual N1 ERP with its characteristic negativity over the left occipitotemporal scalp after 150-250ms (N1, N170; Bentin et al., 1999; Brem et al., 2005; Maurer, Brem, et al., 2005; Pegado et al., 2014). Intracranial evidence (Nobre et al., 1994) together with EEG-source localization (Brem et al., 2009; Maurer, Brem, et al., 2005) and magnetoencephalography studies (MEG, Tarkiainen, Liljeström, Seppä, and Salmelin, 2003) provide substantial support for the generation of the visual N1 in the left vOT.

Coarse print-sensitive activation in the N1 develops when children learn to read (Cao et al., 2011; Eberhard-Moscicka et al., 2015; Maurer et al., 2006; Zhao et al., 2014) and shows an inverted U-shaped development with maximal differentiation in beginning readers (Maurer et al 2006). In accordance with BOLD activation in the VWFS, the tuning of the print-sensitive N1 is likewise initialized when children train the correspondences of letters and speech sounds (Brem et al., 2010; Eberhard-Moscicka et al., 2015; Zhao et al., 2014). Regarding the development of fine-tuned print-sensitive activation, the evidence is inconsistent. Although, high reading ability has been reported to enhance fine-tuned activation in young readers (Zhao et al., 2014), for young readers in general, fine-tuned activation was not evident (Eberhard-Moscicka et al., 2015).

Even though an atypical print-sensitive ERP response can already be seen in preschool children with poor reading outcomes (Maurer et al 2007, Brem et al 2013), the attenuation of print-sensitive processing in poor and dyslexic subjects is typically seen in literates: Stronger N1 print sensitivity mostly over left occipitotemporal areas in normal readers than dyslexic readers has been shown in ERP and MEG studies in adults (Helenius et al., 1999; Mahé, Bonnefond, & Doignon-Camus, 2013; Mahé et al., 2012), pre-adolescents (Araújo et al., 2012), and younger children (Brem et al., 2013; Hasko et al., 2013; Maurer et al., 2011), but were not evident in third (Fraga González et al., 2014) or fifth graders (Maurer et al., 2011). Fraga González et al. (2014) reported an even stronger N1 print sensitivity for dyslexic third grade children as compared to peers with normal reading abilities. These results may be explained with a developmental delay in the establishment of print-sensitive processing for dyslexic children (Brem et al., 2013; Fraga González et al., 2014; Maurer et al., 2011), even though some studies

reported attenuated print-sensitive N1 responses also in older children and adults (Araújo et al., 2015; Maurer et al., 2011).

In summary, print sensitivity in the visual N1 and the left vOT nicely reflects the level of reading experience and proficiency. Nevertheless, it is largely unknown in what pace this visual specialization develops within the first months of formal reading instruction, especially for beginning readers at familial risk for dyslexia. Previous cross-sectional and/or longitudinal studies most often focused on school children from the end of grade one onwards (Brem et al., 2013; Eberhard-Moscicka et al., 2015; Maurer et al., 2007; Zhao et al., 2014) rather than on children within the first half of the school year. Moreover, studies combining neuroimaging methods with high temporal (ERP) and high spatial (fMRI) resolution to gain more detailed insights about the development of print sensitivity and to directly measure the mutual relation of print-sensitive activation in N1 and left vOT are completely lacking in such children.

We hypothesize that the initial phase of intensive learning in the first months of formal tuition induces cortical specialization in the form of coarse tuning to print that is reflected by differential neural responses to print vs non-linguistic stimuli in the visual N1 and left vOT. We assumed that fine neural tuning as reflected by N1/left vOT differences in contrasting words and nonwords is not yet present in young children at familial risk for dyslexia with limited reading experience (Zhao et al., 2014). However, based on the findings of alterations in coarse print sensitivity in children with poor reading outcomes at preschool age (Brem et al., 2010; Maurer et al., 2007), we expected to find differences between normal and poor readers after half a year of reading. In particular, we assumed more pronounced coarse neural tuning to print for normal readers than poor readers, which should be evident in both ERP and fMRI measures.

To test these hypotheses, we examined 38 children at risk for developmental dyslexia and varying reading fluency in the middle of first grade. Eighteen children performed below the 16th percentile in a standardized reading fluency test and were classified as poor beginning readers. Twenty children

scored above the 16th percentile and formed the group of normal beginning readers. The children performed a visual one-back task with three types of stimuli (words, nonwords, false-font strings) during simultaneous EEG-fMRI recordings to assess both, measures of coarse and fine-tuning for print.

3.3 Methods

3.3.1 Participants

Healthy, German-speaking first-grade children at varying familial risk for developmental dyslexia were included in the study. The larger part this sample was recruited at kindergarten age for a longitudinal study from the greater area of the city of Zurich. Additional children were recruited in the middle of first grade (n=8) to enlarge the group for the present analyses. Children's familial risk for developmental dyslexia varied and was estimated based on parents reading history assessed with the ARHQ (risk: score > 0.3 Lefly and Pennington, 2000). The cut-off was applied to the higher value of both parents (for 15 children the risk came from the mother). For two children, ARHQ data of only one parent was available and used to determine their risk scores. In addition, two children had siblings with formal diagnosis of dyslexia and one child was delayed in its language development.

Behavioral assessments were performed with 49 children, including IQ (Culture Fair Intelligence Test, CFT 1-R; Weiss and Osterland, 1997), Hamburg Wechsler Intelligenztest für Kinder, HAWIK-IV;Petermann and Petermann, 2007), reading fluency (Salzburger Lese- und Rechtschreibtest, SLRT-II locally standardized in an additional sample of first grade children after half a year of reading instruction; Moll and Landerl, 2010), non-word repetition test (Mottier Silben, Wild and Fleck, 2013), phonological awareness and rapid automatized naming (Test für phonologische Bewusstheit und Bennengeschwindigkeit, TEPHOBE; Mayer, 2011). Out of the 49 children, 43 children took part in the neuroimaging session in the middle of first grade (school months 5-7). Five participants had to be excluded from further analyses because neuroimaging data could not be analyzed due to excessive motion (N=3), or had to be excluded because they fell asleep during scanning (N=2). The remaining 38 children (22f, aged 7.34y±0.3) with average IQ (102±9.7; Table 3.1) are included in the final analyses. The IQ assessment took place 7.3±0.5 month (range: 6.61-9.83m) after the simultaneous EEG-fMRI

session. One child, with whom the CFT 1-R score could not be conducted, was

Table 3.1
Group description of normal readers compared to poor readers.

	Normal readers		**Poor readers**		**Test statistics**
		range		**range**	
sex (female/male)	10/10		12/6		
handedness (left/right)	3/17		0/18		
familial risk for dyslexia	0.48±0.17	0.26-0.75	0.52±0.13		t(36)=-0.74, p=0.461
IQ estimate	102±8	85-120	103±11	84-123	t(36)=-0.40, p=0.685
age in years	7.3±0.3	6.9-7.7	7.4±0.4	6.8-8.21	t(36)=-0.10, p=0.921
Reading related skills					
word reading fluency[b]	48.3±23.2	11-99	6.3±5.0	0.5-13.5	t(21)=7.89, p=0.000
pseudoword reading fluency[b]	38.1±26	6-99	5.4±6.6	0.5-17	t(22)=5.43, p=0.000
phonological awareness[a]	23.8±3.6	13-28	22.2±3.4	17-28	t(36)=1.39, p=0.173
RAN objects[a]	0.7±0.1	0.52-1.04	0.6±0.1	0.35-0.78	t(36)=3.00, p=0.005
RAN letters[a]	1.2±0.3	0.79-1.79	0.8±0.3	0.39-1.22	t(36)=4.17, p=0.000
RAN numbers[a]	1.1±0.3	0.72-1.56	0.8±0.3	0.53-1.28	t(36)=2.98, p=0.005
non-word repetition[b]	38.3±21.1	4-77	29.4±21.5	1-75	t(36)=1.29, p=0.206
In-scanner task performance					
accuracy words	63.3±29.0	16.6-100	53.7±27.7	16.6-100	t(36)=1.05, p=0.303
reaction time words	897.5±219.8	424-1226	937.3±286.4	514-1506	t(35)=-0.48, p=0.638
accuracy nonwords	60.0±32.6	16.6-100	52.8±33.5	0-100	t(36)=0.67, p=0.505
reaction time nonwords	1063.9±331.4	698-1799	1047.5±253.3	593-16.31	t(32)=0.16, p=0.876
accuracy false-font strings	69.2±24.3	16.6-100	62.0±24.8	0-83.3	t(36)=0.89, p=0.377
reaction time false-font strings	883.1±241.1	548-1175	1048.8±285.6	668-1558	t(35)=-1.92, p=0.064

Note: Values are mean ±standard deviation. [a]Raw values, [b]Percentile scores based on age-matched norms.

classified as adequate intelligent based on the results of the HAWIK-IV (subtest: block design test) conducted in kindergarten (IQ: 95). All children had normal or corrected to normal visual acuity and no other neurological or cognitive impairments. One child was diagnosed with attention-

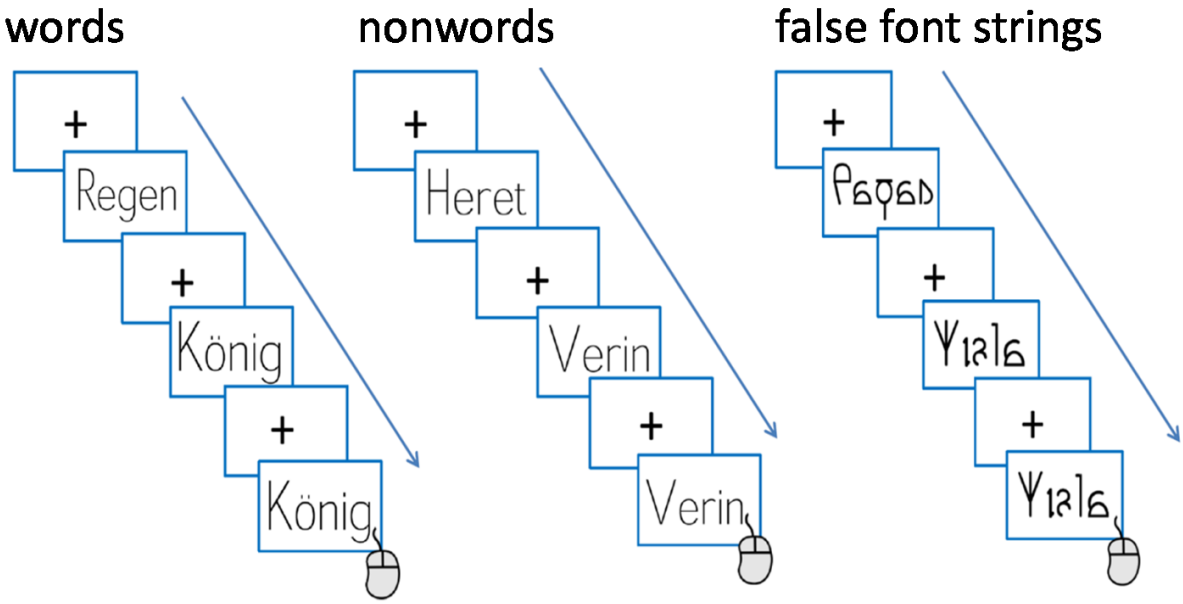

Figure 3.1. Visual one-back task with three conditions: blocks of words, nonwords and false-font strings were pseudorandomly presented to the children. The children decided whether a presented item is the same as the item presented in the previous trial via button press.

deficit/hyperactivity disorder; the medication was discontinued for 48 hours before the behavioral and the neuroimaging session. To verify the main findings, the core analyses have been repeated without the data of this child.

Based on standardized reading fluency scores, 18 children scoring below the 16 percentile in the mean of word and pseudoword (SLRT-II) reading were defined as poor readers (Table 3.1), the remaining 20 as normal readers. The behavioral testing took place 6±5.4d (range: 1-24d) before the imaging session, there was no difference between the two reading groups ($t(36)=-0.931$, $p=0.358$). The parents gave written informed consent and the children gave oral consent. The local ethics committee of the Canton of Zurich and neighboring Cantons in Switzerland approved the study. All participants received vouchers and presents as compensation.

3.3.2 Behavioral data: acquisition

During scanning, the children performed a visual one-back task with three conditions. In a block design real one- or two-syllable words, matched nonwords and false-font strings were presented (Figure 3.1). Participants were instructed to attend to the stimuli and to indicate immediate repetitions by a button press, the accuracy and reaction time were analysed to verify children's alertness. Each false-font character was derived from an alphabetical letter. The one- or two-syllable words were concrete nouns that consisted of 3-5 letters, with the initial letter capitalized according to German orthography. The words were extracted from the German Celex database (Baayen, Piepenbrock, & van H, 1993) and their Coltheart score (Coltheart, Davelaar, Jonasson, & Besner, 1977) ranged from 1 to 13 (mean: 5.6±3.3). Pronounceable character strings with a low Coltheart neighborhood score of 0.04±0.1 served as nonword stimuli. Additionally, words and nonwords were matched for bigram frequencies ($t(53)=1,279$, $p=0.206$). The visual stimuli were presented using video goggles (VisuaStimDigital, Resonance Technology, Northride, CA). Characters were presented in black in the middle of a grey background (mean visual angles horizontally/vertically words: 4.3°/2.0°; nonwords: 4.2°/1.9°; false-font string: 4.2°/1.9°). Responses and reaction times were recorded with Presentation (http://www.neurobs.com).

The experiment comprised of 180 trials (60 per condition) and included 18 targets (6 per condition). The trials were structured in 18 blocks of either words, nonwords, or false-font string. The blocks were presented in a fixed order, which was pseudo-randomized between participants. Within each block, the stimuli were presented in a fix order including one target. The trials started with a fixation cross (jitter: 1250-1550 ms) followed by the stimulus presentation for 660 ms. Resting periods of 6300 ms or 10900 ms were inserted between blocks. Before scanning, the children familiarized with the experiment by performing a similar task with more target stimuli out-side the scanner.

3.3.3 Behavioral data: Task performance analysis

The behavioral responses in the task were analyzed for differences in accuracy and reaction time in the two reading groups. Group differences were statistically tested with unpaired t-tests.

3.3.4 fMRI data: Acquisition

The experiment was carried out in a Philips Achieva 3 Tesla scanner (Philips Medical Systems, Best, The Netherlands) whole body magnetic resonance scanner using a 32-elements receive head coil to acquire 254 volumes. A T2*-weighted whole-brain gradient EPI sequence was applied to 31 slices (thickness 3.5mm /gap 0.5mm) with a repetition time (TR)=1.98s, echo time (TE)=30ms, flip angle of 80°, FOV= 24x24cm^2, in plane resolution=3x3mm^2, SENSE factor 2.2. To reduce scanner noise a SofTone factor of 3 was used. In order to correct for geometric distortion in EPI caused by magnetic field inhomogeneity, a field map scan to perform B0 correction was obtained before each dataset. A T1-weigthed 3-dimensional magnetization-prepared rapid-acquisition echo (3D MP-RAGE) pulse sequence with 176 slices, TR=6.8, TE=3.2ms, FOV= 27x25.4cm^2 voxel size= 1x1x1mm^3, and flip angle= 9° was used for the normalization procedure.

3.3.5 fMRI data: Preprocessing and second-level analyses

Functional images were preprocessed using SPM12 on MATLAB R2015b. A field map correction was applied. Spatial realignment to the first acquired image and unwarping was applied to correct for movements between scans and for distortions caused by magnetic field homogeneities and interpolation artifacts. Slice time correction was performed using a cubic spline interpolation algorithm to correct time differences between slices recorded within the same scan in the time series of individual slices and to resample them afterwards. Functional images of each participant were co-registered to the corresponding T1-weighted structural image. The deformations derived from the segmentation procedure and a pediatric brain template created with the Template-O-Matic toolbox (Wilke et al., 2008) were used for the subsequent normalization. After resampling (3x3x3 mm^3), a 6 mm full width half-maximum Gaussian kernel was applied to smooth the data. Volumes with more than 1.5 mm scan-to-scan movement were repaired by linear interpolation using the ArtRepair toolbox (Mazaika et al., 2011). Less than 10% (8.7%) of the scans per subject were interpolated.

A random-effect general linear model was calculated with five predictors (words, nonwords, false-font strings, targets, and responses) for each participant and condition. Six realignment parameters were

included as regressors into the model to control for head motion. First-level analyses on subject level included the contrast of each condition against baseline and the comparisons between the three conditions. Second-level random effect analyses were performed using one-sample t-tests and two-sample t-tests to characterize visual activation in each group separately and to determine condition differences between normal and poor readers, respectively. Significant differences are reported using a cluster-based FWE_{corr} threshold of $p<0.05$ (on a CDT of $p<0.001$).

3.3.6 fMRI data: Region-of-interest analysis in left vOT cortex

A region-of-interest (ROI) was used to clarify group and condition effects of our a-priori hypothesis in more detail. The borders of the ROI in the VWFS (Figure. 3.2) was defined by the intercept (logical operation OR) of 1), the combined functional activation mask of words, nonwords, and false-font string (logical operation AND) at $p<0.001$, $k=40$ (MarsBar Brett et al., 2002), 2) the anatomical mask of the left fusiform gyrus (aal) and 3) a 7 mm literature-based spherical ROI at (-44, -57, -15, MNI coordinates) described in a recent meta-analysis of reading related activations (Vandermosten, Hoeft, & Norton, 2016). The extracted betavalues were entered in a LMM with a fixed factor (condition), and a specific random intercept for each subject. In LMM fixed and random effects explain differences between subjects and the variability within subjects respectively. Studentized conditional residuals were computed to identify and exclude potential outliers. To correct for variance inhomogeneity, an outlier cutoff of three standard deviations from the mean was used (Roth et al., 2007). In addition, QQ-plots were inspected to ensure the assumption of normality and homoscedasticity of predicted versus conditional residual plots. Within-group differences between conditions and between-group differences were calculated post hoc using paired t-tests. The p-values of these post hoc analyses are Tukey-Kramer corrected.

3.3.7 EEG data: Acquisition

EEG was continuously recorded with an MR-compatible 128-channel EEG system (Net Amps 400, 128-channel EGI HydroCelGeodesic Sensor Net) and two ECG electrodes. Impedances were kept below 50kΩ and the data was sampled at 1kHz. Reference electrode was placed at Cz and the ground

electrode posterior to Cz. The EEG system was synchronized to the scanner clock to minimize gradient residuals occurring during simultaneous EEG-fMRI recordings (Mandelkow et al., 2006). A bandage retainer net covered the electrode net to reduce potential electrode vibration artifacts.

3.3.8 EEG data: Analysis

EEG data processing was performed with VisionAnalyzer 2.1 (BrainProducts GmbH, Munich, Germany). Four electrodes with poor data quality on the cheeks (E43, E48, E119, E120) were excluded from further processing. Preprocessing contained the following steps: Topographic interpolation of channels with poor data quality (range: 0-6 channels, mean: 2±1.9 channels), visual inspection and manual exclusion of periods with major artifacts (total duration mean), average template scanner artifact detection and removal (Allen et al., 2000), sliding average template ballistocardiogram correction, filtering (0.1-30Hz and 50Hz Notch), downsampling to 500 Hz, independent component analysis (Jung et al., 2000) to exclude blinks, eye movements, and residual ballistocardiogram artifacts, rereferencing to the average reference (Lehmann & Skrandies, 1980), automatic artifact removal of artefacts exceeding ±200mV, epoching from -50 ms to 550 ms after stimulus presentation, averaging condition-wise.

ERP were calculated based on 44.5 epochs per condition (mean words: 44.3, nonwords: 44.7, false-font string: 44.5; range: 21-54 epochs). Data of one child with poor ERP data quality (less than 33% acceptable epochs) was not included in the final sample of 38 children. The N1 interval was defined as ±30ms (184-244 ms) around the global field power peak (214 ms) in the grand average overall conditions and participants. A literature-based electrode cluster (Eberhard-Moscicka et al., 2015) was used for N1 amplitude analyses and included 13 left occipitotemporal electrodes (LOT; E50, E57, E58, E59, E63, E64, E65, E66, E68, E69, E70, E73, E74). Mean N1 amplitude values of this cluster were extracted for each condition and used for further analysis. Statistical analyses were performed using LMM and the same procedure was applied as in the fMRI ROI analysis.

3.3.9 Simultaneous EEG-fMRI data: EEG-informed fMRI analysis

In order to investigate the mutual influential mechanisms of the N1 ERP and the left vOT BOLD response, N1 mean amplitude values were extracted trial-wise and z-transformed. In the course of this transformation the values were multiplied by -1 to consider the reversed polarity of the N1 mean values (negative) and the vOT beta values (positive). ERP amplitudes of the left vOT electrode cluster were introduced as parametric modulator in the fMRI model. In addition, a regressor of no interest was added to model trials with insufficient EEG quality. The beta values of the parametric modulation in the described left vOT ROI were extracted and entered in a LMM to test for the interaction of the fixed factors condition and reading group.

3.4 Results

3.4.1 Behavioral data

The behavioral analysis of the reaction time and accuracy did not differ between the two reading groups (accuracy: $p>0.139$, reaction time: $p>0.253$).

3.4.2 Whole brain differences between conditions and groups

The functional brain imaging data showed that both groups activated the occipitotemporal cortex including the left vOT (Figure S3.1) during visual processing in all conditions. In addition, print-sensitive activation was shown in the left hemisphere including the left inferior frontal, and superior and middle temporal regions (word/nonword>false-font string). False-font strings showed more pronounced activation in the bilateral vOT and inferior parietal cortex as compared to words/nonwords (false-font string>word/nonword, Table 3.2). These effects were evident in the whole sample and in both the poor and normal reading group (Figure S3.1). No significant differences were observed for processing words and nonwords. Two-sample t-tests revealed no significant differences between the two groups in any condition or condition difference at the chosen, cluster-level corrected threshold of $p<0.05$ (Figure S3.2).

3.4.3 ROI analyses in the left vOT

The LMM of the left vOT ROI revealed a significant main effect of condition [F(2,70)=9.86, p=0.0002] and an interaction of condition x reading group [F(2,70)=3.66, p=0.0308]. Post hoc t-tests showed stronger BOLD activation for false-font strings than for words (t(70)=-4.26, p_{corr}=0.0009) or for nonwords (t(70)=-4.30, p_{corr}=0.0008) in poor readers, while normal readers showed neither coarse nor

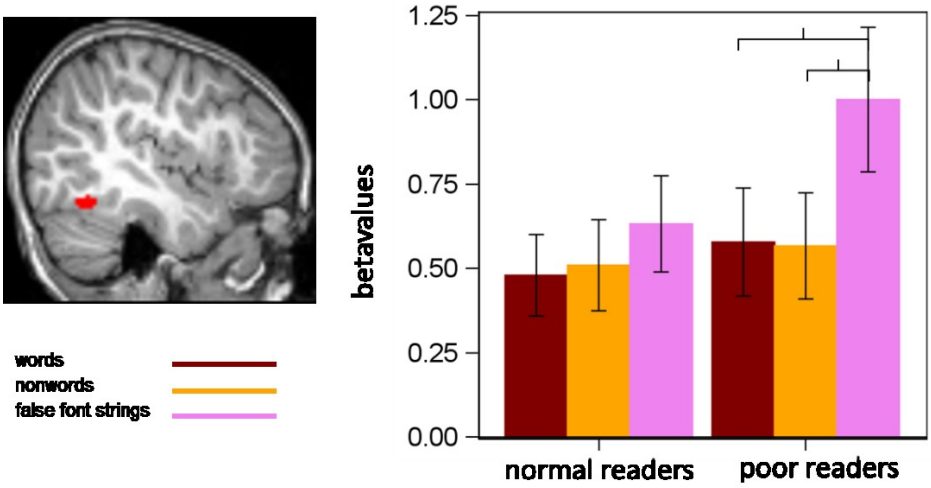

Figure 3.2. ROI analysis: The ROI was defined as the overlapping cluster of functional activation over all three conditions, anatomical atlas of the left fusiform gyrus and a 7 mm literature based left vOT sphere. The extracted betavalues revealed stronger activation for false-font strings than for words or nonwords in poor-reading children. Error bars show standard error of the mean.

fine neural tuning differences (all p>0.2, Figure 3.2). Inspection of individual beta values within this ROI revealed that only 31.6% of the children (normal, n=9; poor, n=3) showed higher beta values for words or nonwords (normal: Δβ W> FF=-0.18+-0.48; Δβ NW> FF =-0.15+-0.61; poor: Δβ W> FF=-0.48+-0.53; Δβ NW> FF =-0.49+-0.58) as compared to false-font strings whereas the other children showed equal (n=2) or lower beta values for words/non words.

3.4.4 ERP N1 amplitude analyses

ERP data showed a pronounced occipitotemporal negativity in the potential field maps after 200ms (N1) for words and nonwords while the N1 for false-font strings was less pronounced (Figure S3.3). Analysis of the GFP confirmed the overall difference in the N1 strength by showing a significant main effect condition [F(2,72)=6.22, p=0.0032]. Post hoc t-tests revealed a stronger N1 GFP for words

(t(72)=-3.45, p_{corr}=0.0027)) compared to false-font strings but no difference between words and nonwords.

The amplitude analysis of the left occipitotemporal electrode cluster revealed a main effect of condition [F(2,72)=10.66, p<0.0001]. Inspection of individual mean N1 amplitudes revealed that 79% of the children yielded coarse print sensitivity (word or nonword more negative than false-font: normal

Table 3.2
MNI coordinates and anatomical brain regions for fMRI activation maxima of the three conditions against baseline and the condition differences (CDT p<0.001, k≥44, FWE-corr p<0.05).

p(FWE-corr)	k	T	MNI coordinates x y z			Hemisphere	Brain region
words							
0.00000	900	10.64	-41	-87	-9	l	inferior occipital gyrus
0.00000	926	8.98	40	-87	-9	r	inferior occipital gyrus
0.00019	138	8.66	31	21	6	r	insula
0.00000	617	7.57	10	9	51	r	superior motor area
0.00168	100	7.14	-29	27	3	l	insula
0.00069	115	5.78	43	33	33	r	middle frontal
0.00012	147	5.60	28	-57	45	r	angular gyrus
0.00377	87	5.38	-29	-54	48	l	inferior parietal
0.00001	196	5.27	-44	0	30	l	precentral
nonwords							
0.00000	1100	8.85	-26	-93	-3	l	inferior occipital
0.00000	291	6.24	-5	6	57	l	superior motor area
0.00005	149	5.99	28	-69	39	r	superior occipital
0.00000	209	5.83	-44	0	27	l	precentral
0.00369	81	5.35	43	33	36	r	middle frontal
0.00000	223	5.25	-26	-72	30	l	middle occipital
0.04349	48	4.65	34	21	6	r	insula
false-font strings							
0.00000	1294	11.28	43	-69	-6	r	inferior temporal
0.00000	1252	10.77	-41	-69	-12	l	inferior occipital gyrus
0.00000	364	6.27	31	-66	54	r	superior parietal
0.00006	157	5.24	-26	-72	30	l	middle occipital
0.00145	101	5.09	-11	15	45	l	superior frontal
words>false-font strings							
0.00000	190	6.70	-53	-6	48	l	postcentral
0.00003	149	6.65	-59	-39	6	l	mid temporal
0.00000	239	5.83	-5	3	63	l	supp motor area
0.01837	55	4.72	-50	15	-3	l	inferior frontal gyrus
nonwords>false-font strings							
0.00000	254	6.15	-56	3	21	l	precentral
0.02304	57	4.76	-65	-27	3	l	mid temporal
false-font strings>words							
0.00000	668	8.16	43	-60	-12	r	inferior temporal
0.00000	346	6.15	-50	-66	-3	l	mid temporal
0.00032	110	5.42	52	-27	42	r	postcentral
0.04708	44	4.44	37	-75	45	r	angular

0.01997	54	4.44	19	-78	57	r	superior parietal
false-font strings>nonwords							
0.00000	809	8.60	40	-60	-9	r	temporal inferior
0.00000	222	6.61	-53	-69	-3	l	occipital inferior
0.00209	91	5.75	61	-24	45	r	supra marginal
0.01704	61	5.00	-41	-27	48	l	postcentral
0.03133	53	4.92	-29	-39	-18	l	Fusiform
0.04287	49	4.76	25	-78	57	r	superior parietal
words>nonwords							
no suprathreshold clusters							
nonwords>words							
no suprathreshold clusters							

Note: l = left hemisphere, r = right hemisphere, MNI = Montreal Neurological Institute, k = cluster size

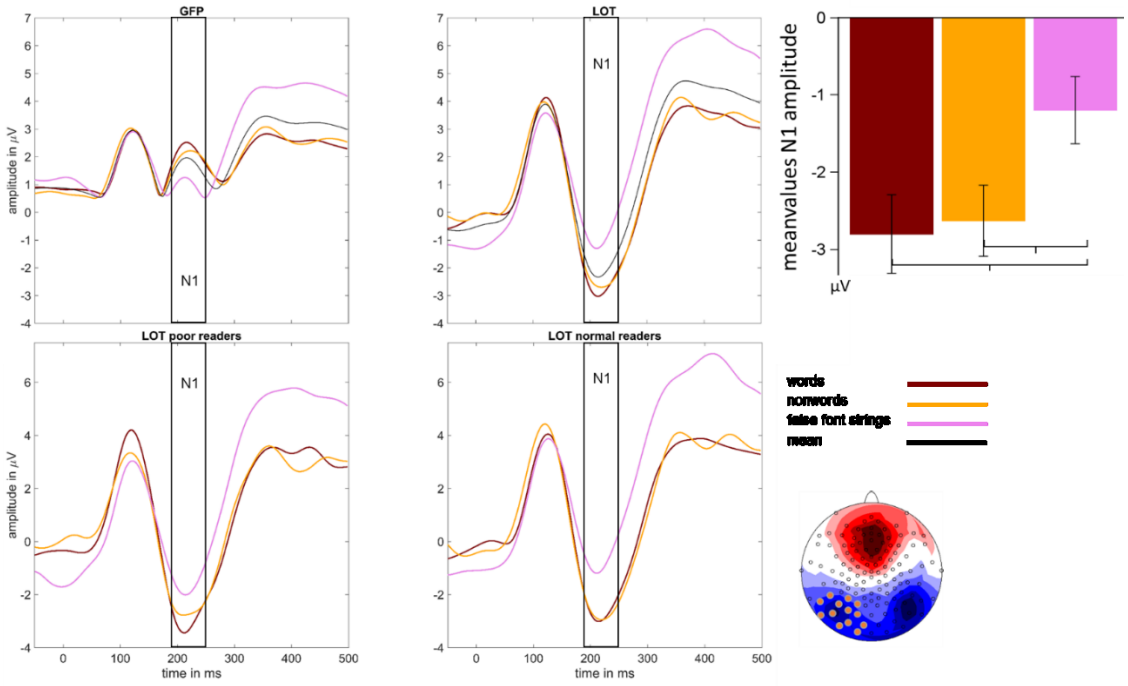

Figure 3.3. EEG analysis: Depicted are the GFP of the three conditions and the mean GFP waveform. The N1 interval (184-244 ms) is defined as the mean GFP peak (214 ms) ± 30 ms. Mean amplitude values were calculated for LOT electrodes of interest depicted on the topographic map of the mean N1 amplitude. ERP waveform for the LOT cluster for the whole group for the three conditions and the mean and for the two reading groups for the three conditions. The bars on the right display the print sensitivity effect for the whole groupe after half a year of formal reading instruction. Error bars show standard error of the mean.

readers: 85%, ΔN1μV W>FF= -1.85+-2.41, ΔN1μV NW>FF= -1.87+-2.05; poor readers: 72.2%, ΔN1μV W>FF= -1.34+-2.88, ΔN1μV NW>FF= -.95+-2.09) while only 53% of all children showed some fine tuning in the N1 to words as compared to nonwords (normal: 45%, ΔN1μV W>NW= 0.019+-1.93; poor 61.1%, ΔN1μV W>NW= -0.038+-2.51).

Post hoc t-tests confirmed the expected pronounced coarse print sensitivity (words>false-font string: (t(72)=-4.22, p_{corr}=0.0002); and nonwords>false-font string: (t(72)=-3.73, p_{corr}=0.0011) effects but did not provide evidence for fine neural tuning to words (words vs nonwords). Differences between poor and normal readers were not significant [F(2,72)=.074, p=0.4792, Figure S3.4].

3.4.5 N1 ERP informed fMRI analysis in the left vOT ROI

Mean amplitudes of the left electrode cluster were extracted trial-wise for each condition separately and entered in the first-level model of the fMRI analyses to perform the parametric modulation. The

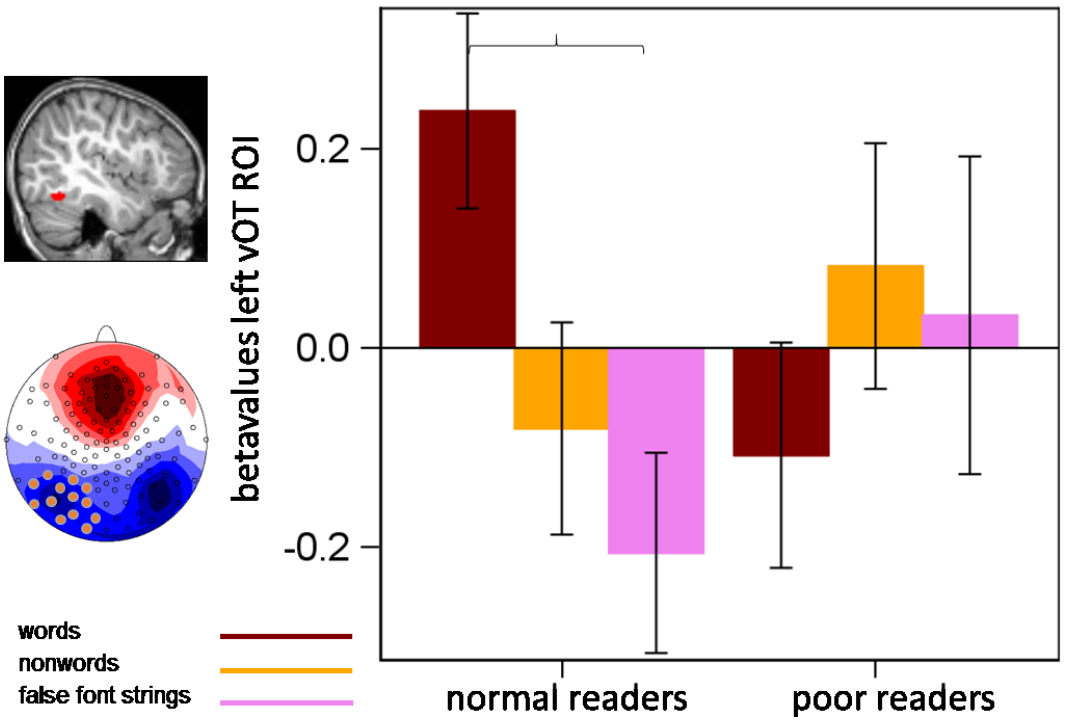

Figure 3.4. EEG informed fMRI: The single-trial-wise extracted N1 ERP meanvalues modulated the hemodynamic response in the left vOT ROI stronger for words than for false-font strings in normal readers. Error bars show standard error of the mean.

left vOT ROI analyses of the N1 amplitude ERP informed parametric modulation showed a significant condition x reading group interaction [F(2,72)=4.23, p<0.0183]. Normal readers show stronger beta-values for words than for false-font strings (t(72)=2.97, p_{corr}=0.0453) while poor readers showed no differences between conditions (all p>0.2, Figure 3.4). Inspection of individual N1 amplitude modulated betavalue differences showed that 63.2% of all children had a stronger BOLD response to

words than false-font strings, whereby this difference was present in 80% of normal (ΔN1β W>FF=0.44+-0.62) and 44.4% of the poor (ΔN1β W>FF= -0.13+-0.7) readers.

3.5 Discussion

This study addressed the questions of whether coarse and fine levels of print sensitivity are evident in the amplitude of the visual N1 ERP and the BOLD signal of the left vOT after half a year of formal reading instruction and whether activation differences between normal and poor beginning readers are present at this early learning stage. In addition, we aimed to clarify the relation between N1 amplitudes over the left occipitotemporal scalp and the BOLD signal within the left vOT.

3.5.1 Print sensitivity in the left occipitotemporal cortex and the visual N1

On a whole brain level, print-sensitive BOLD responses were detected in brain areas of the left hemisphere and included the inferior frontal, superior and middle temporal regions, which are part of the classic reading network (Perfetti et al., 2007; Price, 2012; Raschle et al., 2012; Richlan et al., 2011; Ziegler & Goswami, 2005). Neither on whole brain level, nor in a predefined VWFA ROI did we find coarse or fine levels of print-sensitive activation in our group of beginning readers. Only 32% of the children showed some print-sensitive processing in the VWFA ROI. In contrast to the results of the BOLD signal, print-sensitive N1 amplitudes were detected in almost 80% of the children and thereby confirmed previous ERP findings at the end of first grade (Eberhard-Moscicka et al., 2015; Zhao et al., 2014). Moreover, our data show that coarse print sensitivity is already evident after half a year of formal reading instruction in the ERP and demonstrate that formal reading training rapidly induces neural tuning to print (Brem et al., 2010; Maurer et al., 2007).

By comparing groups of normal and poor beginning readers, we aimed to clarify on whether the VWFA and N1 print sensitivity are modulated by reading skills. After half a year of reading instruction, neither the N1 ERP nor the whole-brain activation patterns showed significant differences between the two reading groups. This finding indicates that the difference between normal and poor readers on the behavioral level is not yet paralleled by typical alterations in lvOT activation on the neural level at such an early learning stage and thus contrasts to findings in more experienced readers (Araújo et al., 2012;

Hasko et al., 2013; Maurer et al., 2011). Interestingly however, analyses of the VWFA ROI yielded differential activation patterns for normal and poor readers. The higher activation in the left vOT to false-font strings than to words and nonwords in poor readers fits the selectionistic view of categorical development (Cantlon et al., 2011) stating that emerging specialization of the left vOT to print is based on a reduction of the activation for irrelevant rather than an increase of activation for relevant information with development and learning (Cantlon et al., 2011). Such a reduction of activation for non-preferred information is assumed to result from selective pruning and thus strengthens the specific neural response of a preferred category (Cantlon et al., 2011). Hence, the stronger activation for false-font strings in poor readers indicates that they have not yet reached a more advanced level of specialization for print, which is comparable to normal readers. This is also reflected by exploring the individual BOLD responses within this area, which show that roughly 45% of the normal but only 17% of the poor readers show higher BOLD signals to words as compared to non-linguistic stimuli within the VWFA. The absence of the expected attenuation in the ERP and BOLD print sensitivity measures may also be explained by the focus on children at a varying risk for developmental dyslexia. It has been shown previously, that children at risk for or children with poor reading outcomes at preschool age show microstructural alterations (Raschle et al., 2011), altered functional BOLD signals in tasks requiring phonological processing (Black et al., 2012; Raschle, Stering, Meissner, & Gaab, 2013), and altered N1 ERPs (Bach, Richardson, Brandeis, Martin, & Brem, 2013; Brem et al., 2013; Maurer et al., 2007) as compared to peers. Such children may thus develop print-sensitive processing later than children without risk for developmental dyslexia may. Longitudinal studies comparing the development of the left vOT in children with and without risk would be important to track different developmental trajectories of establishing print sensitivity.

To clarify further the role and level of specialization of the vOT in this initial learning stage, we used our simultaneous EEG-fMRI approach to infer about the variation in the VWFA BOLD signal directly related to the variation in the N1 amplitude within the first 250 ms of information processing. It is well-known that fMRI responses reflect a rather stationary signal accumulating activation of the same

region within seconds and that the same brain region can repeatedly be activated during the time course of visual information processing (Dale et al., 2000; Lin, Belliveau, Dale, & Hämäläinen, 2006; A. K. Liu, Dale, & Belliveau, 2002). The role of the VWFA area in implicit and rapid processing of information (within the first few hundred milliseconds and more specifically around the time of maximal N1 activity) may thus be superimposed by the stationary characteristics of the BOLD signal. The parametric modulation of the BOLD signal in the VWFA with the N1 amplitude thus help to disentangle the BOLD signal of a specific brain structure dominating a specific temporal interval of interest. In line with the assumption of neural generators of the N1 in the left vOT, the amplitude of the visual print-sensitive N1 activation modulated the left vOT BOLD response. More importantly, coarse sensitivity to print in the left vOT as revealed by the single trial N1-ERP informed fMRI analysis was more pronounced in the group of normal readers. 80% of the beginners with age appropriate reading skills showed a positive BOLD contrast for words vs. false-font strings as compared to less than half of the poor readers. This method thus allows concluding that initial specialization in the form of coarse print-sensitive processing is already evident in the VWFA BOLD of (mainly) normal readers and most likely reflects activation in the N1 time range.

Our results are in accordance with previous studies (Brem et al., 2010; Dehaene et al., 2010; Eberhard-Moscicka et al., 2015; Maurer et al., 2007; Skeide et al., 2017) showing that the left vOT starts to adapt to functions of reading with the start of reading training or formal reading instruction (B. A. Shaywitz et al., 2002). Training, practice and the resulting increase in expertise is accompanied by important changes in neural networks that can be measured with neuroimaging techniques. It remains to be further clarified whether the reduced neural specialization found in poor readers is a persistent impairment (Mahé et al., 2012) or rather a developmental delay and will eventually adapt to the level of normal readers with more practice (Araújo, Faísca, Bramão, Petersson, & Reis, 2014; Fraga González et al., 2014; Maurer et al., 2011).

3.5.2 Fine neural tuning in the left vOT

Our experimental paradigm did not only allow us to explore the level of coarse print sensitivity in our children but also to look at a more elaborate level of fine tuning to word forms by comparing the processing of words and nonwords. While in general a relatively late development of fine-tuning within the left vOT is assumed (Centanni et al., 2017; Kronschnabel et al., 2013), a few studies reported some word sensitive responses in the first years of schooling already (Zhao et al., 2014). Our results support a delayed maturation of word sensitive responses after establishment of coarse print tuning, given that neither ERP amplitudes, topographies nor BOLD signal differences showed any differential activation between words and nonwords in our first grade children.

3.5.3 Conclusion

In conclusion, we were able to show, that children at varying risk for developmental dyslexia exhibit a coarse print-sensitive response in the N1 ERP but not yet in the BOLD response of the VWFA after only half a year of tuition, while no signs for fine neural tuning was observed in any of the analyses. Nevertheless, neural differences between normal and poor readers are not yet as prominent as in more experienced readers. Only a refined analyses combining ERP and fMRI measures through single trial ERP informed BOLD analyses within the VWFA was sensitive to trace the beginning alterations in the functional specialization to print between groups, by revealing that the left vOT cortex is significantly more sensitive to print in normal readers than in poor readers. Hence, we could directly show that the implicit and automatic print processing stage seems impaired in poor beginning readers. This study thus not only provides support for the importance of establishing cortical sensitivity to print during reading acquisition. Moreover, we show that a combination of neuroimaging methods may be more sensitive to capture small but important functional impairments of neural networks in the developing brain. Our findings of functional impairments in a brain structure known to be critical for efficient and fluent reading from the very beginning of reading instruction therefore call for early identification and supportive training for children at risk for developmental dyslexia.

3.6 Acknowledgements

We thank T. Aegerter, F. Aepli, F. Mergen-Felten, L. Götze, M. Hartmann, M. Schneebeli, S. Suter, and Margot Raith for their assistance during recruitment, investigation, and data analyses. We are grateful to P. Stämpfli for the technical support of MRI recordings. This study was supported by the Swiss National Science Foundation (grant: 32003B_141201), the Hartmann Müller Foundation (grant: 1912) and the Olga Mayenfisch Foundation. Finally, we thank all the participating children with their families.

3.7 Author contributions

Conceptualization, G.P., I.I.K., and S.B.; Methodology, G.P., I.I.K., M.R., and S.B.; Project Administration, G.P. and I.I.K.; Investigation, G.P., I.I.K., A.B., M.R., and S.B.; Analyses: G.P., I.I.K., A.R., Resources, D.B., S.W., and S.B.; Writing-Original Draft, G.P., I.I.K., and S.B., Writing-Review and Editing, G.P., I.I.K., A.B., M.R., D.B., A.R., S.W., and S.B.; Funding Acquisition, S.B.

3.8 Supplementary materials

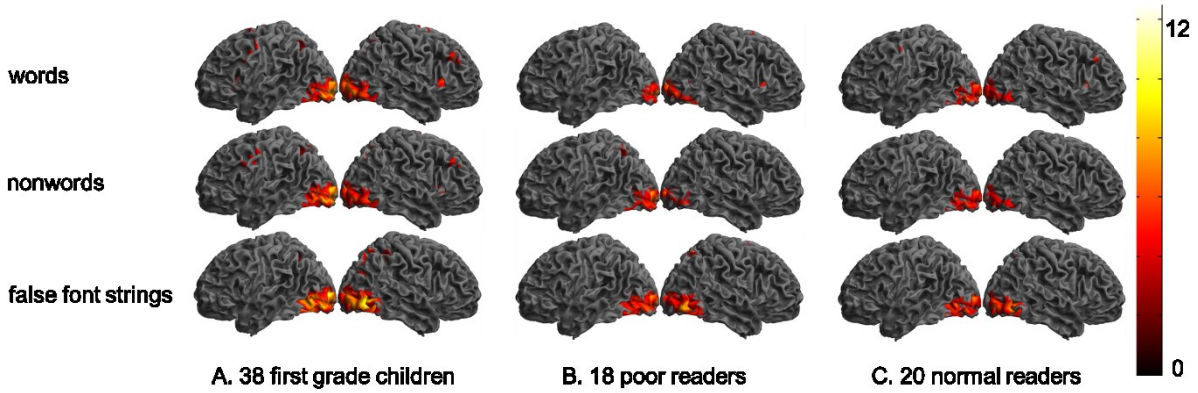

Figure S3.1: Brain activity elicited by words > baseline, nonwords > baseline and false-font strings > baseline for the whole group of first grade children (A) and for each reading group separately (B&C; cluster-level FWE corrected $p<0.05$ on a voxel-wise uncorrected level of $p<0.001$, $k>48$, $t>4.65$). Significant clusters for the whole group (A) are listed in Table 3.2.

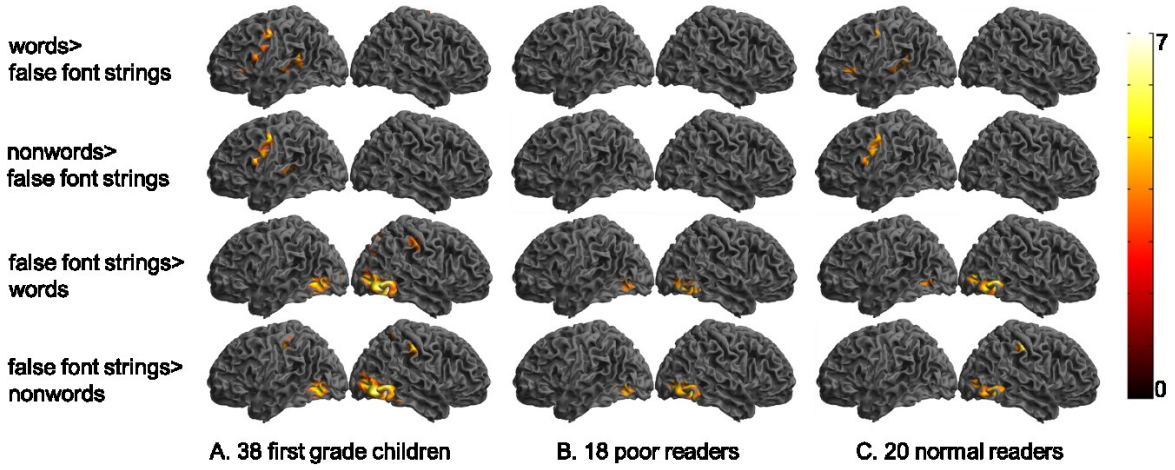

Figure S3.2: Significant condition contrasts for the whole group of first grade children (A) and for each reading group separately (B&C; cluster-level FWE corrected $p<0.05$ on a voxel-wise uncorrected level of $p<0.001$, $k>43$, $t>4.44$). Significant clusters for the whole group (A) are listed in Table 3.2.

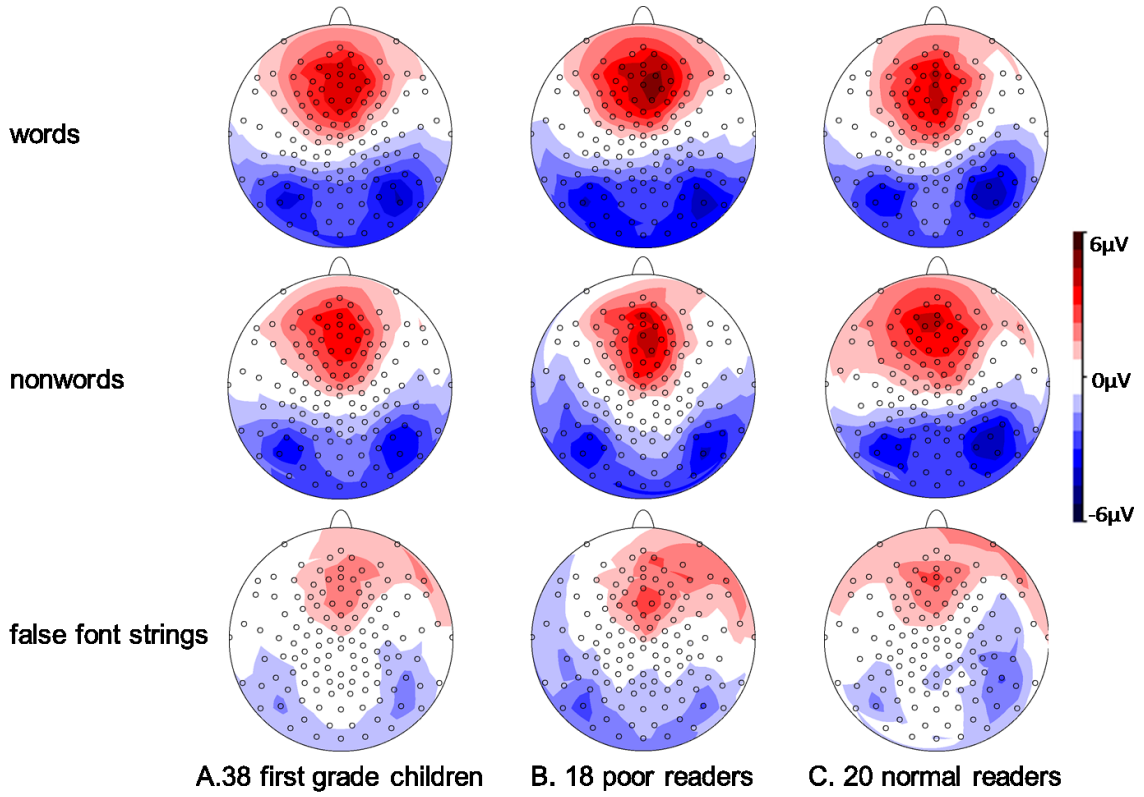

Figure S3.3: Mean amplitude values for the interval (184-244 ms) depicted on topographical maps for the three conditions for the whole group of first grade children and for each reading group separately (B&C).

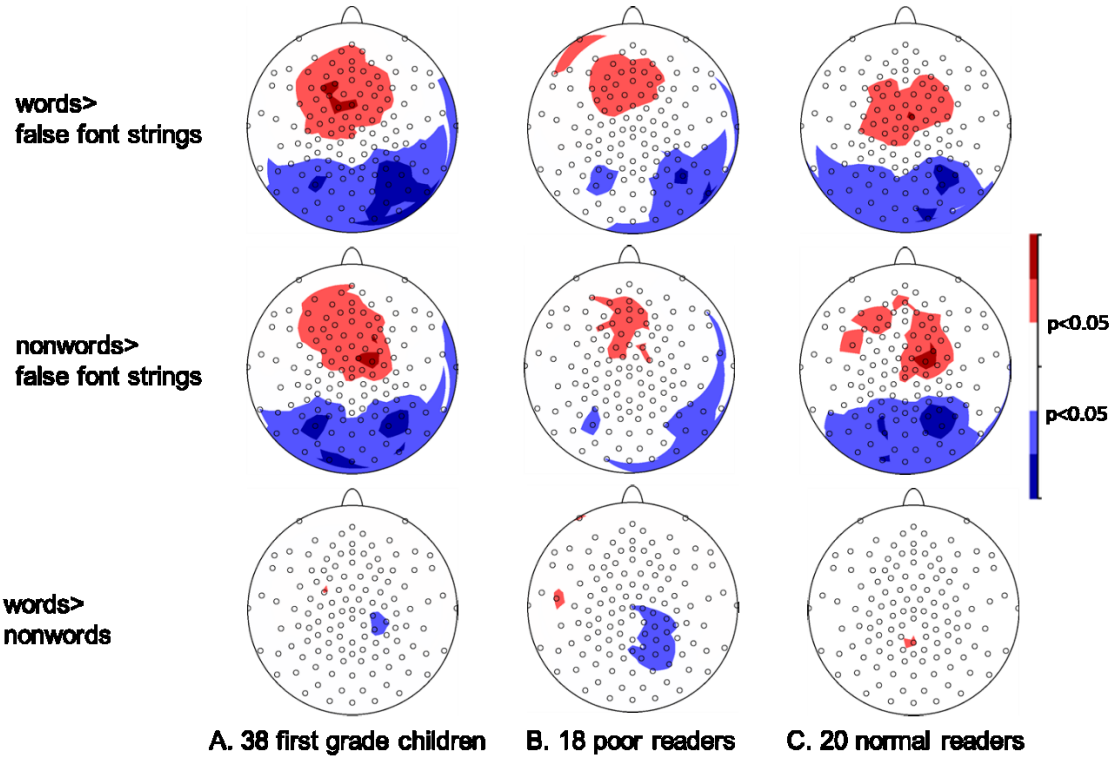

Figure S3.4: Statistical maps (t-maps) for amplitude differences between the three conditions for the whole group of first grade children (A) and for each reading group separately (B&C).

4 General Discussion

This thesis focuses on investigating the neural development of visual print sensitivity in children at familial risk for developmental dyslexia shortly before and shortly after the beginning of reading acquisition. We demonstrated rapid specialization to single characters in occipitotemporal brain regions, following a short training in prereading children that mimicked initial reading acquisition (Study A). The training performance and the level of expertise modulated neural activation, and this reflected functional specialization in the vOT and in the print-sensitive N1 ERP. Learning phonological associations enhanced the connectivity between visual and higher-order language areas and thus drove this functional specialization. In addition, visual processing was shown to depend on training performance. The same children were tested again after half a year of formal reading instruction at school to investigate how they processed words, nonwords, and false-font strings (Study B). In addition, we were interested in the divergent development of normal and poor readers. We found that print-sensitive activation was evident in the N1 and in brain areas of the reading network. Interestingly, ROI analysis in the left vOT showed a stronger activation for false-font strings than for words in poor readers. In addition, we performed a single-trial EEG-informed fMRI analysis and found a stronger modulation of the N1 in the left vOT for normal readers than for poor readers.

4.1 Manipulating the level of visual specialization for print

In study A, we used ERPs and fMRI to measure neural responses to letters, digits, and to trained and novel false-font characters in the vOT cortex of 18 six-year-old children just prior to formal reading instruction. Before scanning, the children trained to associate false-font characters with speech sounds. This training modulated both the ERP and BOLD signals, and induced increased functional connectivity (for BOLD) between the vOT and inferior parietal regions. These findings demonstrate fast learning-related changes and important functional reorganization processes, including the establishment of novel functional connections in the child brain.

4.1.1 The selection of the stimuli

To manipulate the level of expertise in prereading children, four distinct character conditions were chosen. Digits from one to six were chosen as a type of characters that is already well known by all the children in the sample. Even though digits are written symbols comparable to the letters of the alphabet, single digits are not associated with single sounds, but with words. In addition, as phonological associations of single digits are bound to a word, these associations result in meaning. Thus, the semantic impact of single digits is higher than that of single letters, which do not have a meaning per se. In addition to the semantic content, digits are also associated with mathematical magnitude (Kucian, von Aster, Loenneker, Dietrich, & Martin, 2008). These differences may have a considerable impact on the intensity and the locus of the neural activation. Potentially, this could imply that the use of digits as a control condition might have compromised the conclusion of study A. Nonetheless, because the print-sensitive N1 is an early ERP component assigned to sensory processing, digits were chosen to investigate print-sensitive activation for a culturally learned character type requiring a high level of expertise even in prereading children.

Moreover, print sensitivity was also measured by presenting real letters to the prereaders. It was expected that some of the kindergarten children would be experienced in recognizing and processing single letters of the alphabet and that some children might not have such experience, depending on their literacy environment. Thus, letter knowledge was tested in the behavioral session and we found that on average the children were able to name the sounds of 29% of the letters. This finding confirmed the assumption that real letters in prereading children are not a suitable character type for which to assume no knowledge or expertise. To test the impact of letter knowledge on neural print processing directly, individual letter knowledge was correlated with the ERP and fMRI data. This analysis revealed no significant effect, so it is unlikely that the variability in letter knowledge influenced this experimental condition. Therefore, real letters seem suitable as a character type requiring a varying level of expertise.

During reading acquisition at school, culturally defined letters, some of which are not yet familiar to the children, are associated with speech sounds, which the children already use in their spoken language. To investigate this learning process, we developed an artificial script. The level of expertise was manipulated by using artificial characters that were either explicitly trained or novel to all the participating children independently of their previous experience. The children learned the associations of six false-font characters with six well-known speech sounds of the German language. This training aimed to mimic the way in which letters are taught at school and thus the learning processes that occur when children begin reading. Learning an artificial script might have interfered with real letter-speech sound associations that the children already knew before the training. Importantly, the training was especially designed to avoid confusion with already known letter-speech sound correspondences; this was achieved by introducing speech sounds that, based on findings in previous studies of our lab were less likely to have preexisting associations to letters in preschool children. Additionally, children were clearly informed that they were learning letters of a secret made-up language.

The other set of false-font characters was novel to all the children. The children did not learn phonological associations for these characters. However, to rule out any effects of visual familiarity, the novel characters were presented in the background throughout the computerized training. This approach ensured that the learned false-font characters and the novel false-font characters were presented visually for a similar amount of time.

To sum up, the stimuli were chosen to investigate different levels of expertise. Trained artificial letters reflect immediate learning, while the novel artificial letters reflect no learning. Kindergarten children are already experts in identifying digits, but most children at that age do not know real letters. Therefore, the stimuli required different levels of expertise and were suitable to investigate visual print processing in EEG and fMRI.

4.1.2 Print sensitivity in prereading children

Despite the careful selection of the visual characters presented to distinguish between different levels of visual expertise in prereading children, the results did not show a clear pattern. We expected that print sensitivity would be reflected in a stronger N1 and a stronger activation in the left VWFS for trained false-font characters than novel false-font characters. The N1 was indeed stronger for trained characters than for novel characters, but the stronger activation for trained false-font characters in the left VWFS was not statistically significant in comparison to novel false-font characters, despite the fact that the expected pattern was evident in a ROI close to the VWFA. The print sensitivity found in the EEG confirmed previous findings regarding the training of print stimuli (Brem et al., 2010; Maurer et al., 2007). The lack of significance in the fMRI result makes the interpretation difficult, although the results of the ROI analyses point in the same direction as previous findings (Brem et al., 2009; Vinckier et al., 2007), suggesting a hierarchical processing of print stimuli in the left vOT. In addition, the finding indicates that a specialized pattern in the left vOT is responsible for single-letter processing. Such a LFA was proposed by Thesen et al. (2012).

The reason for the present inconsistent finding might be the relatively small size of the sample. It seems that a sample of 18 subjects was sufficient to show training effects in EEG but might be too low to substantiate subtle effects in fMRI. To test this assumption we performed additional analyses including 23 subjects in the enlarged EEG sample and 24 subjects in the enlarged fMRI sample. The additional analyses confirmed the training effect only in a stronger N1 for trained false-font characters than for novel false-font characters, but not in the left vOT.

However, a correlational analysis with the main sample (n=18) revealed a strong relation between activation in the left vOT and the training duration. The faster the children learned the artificial letters, the stronger was the neural response to the trained stimuli in left vOT. This clarifies that the training-induced print sensitivity in the left vOT significantly dependet on training duration and therefore the ability to learn the artificial letters. This finding also suggests that slow learners at risk for

developmental dyslexia may eventually become poor readers and therefore, may show a diminished visual specialization for trained stimuli as early as kindergarten.

In sum, the artificial-letter training led to an increase in visual expertise as shown in the print sensitivity found in the N1 ERP. In addition, the findings of the fMRI analyses point to a specialization in the left vOT, which was confirmed by the fact that the faster children learned the associations the stronger were the print-sensitive activations in the left vOT.

The next level of expertise examined was activation for real letters. Here, we expected that constant exposure in everyday life and the slightly varying learning stages within the group of children would mean that, some expertise might already be reflected in the N1 and in the vOT BOLD response, but not to the same extent as for explicitly trained characters. The comparison of the N1 between real letters and the novel false-font characters revealed no print sensitivity for real letters. This finding confirmed the assumption that only explicit training and not mere visual familiarity leads to print-sensitive activation. However, the fMRI data showed a stronger print-sensitive activation in the left and the right vOT for real letters than for novel false-font characters. The print-sensitive activation found for real letters in the vOT of prereaders seems to contradict to the finding in the EEG data, in which no print sensitivity was found for real letters.

This contradiction might be explained by the genetic factors that influence visual processing. This assumption is supported by the fact that the activation for letters was stronger than for novel false-font characters in the right hemisphere. Given that the sample consisted of children at familial risk for developmental dyslexia, the right-hemispheric activation for real letters might reflect compensatory mechanisms that have been described for dyslexic readers (Bach et al., 2010). In particular, poor readers have been reported to show no clear left lateralized language processing as is expected in normal readers (Brem et al., 2009; W. D. Gaillard et al., 2003; Holland et al., 2007; Wood et al., 2004). The identification of specific gene variants for dyslexia (Carrion-Castillo et al., 2013) has led to the conclusion that neurons designated for the left vOT migrate in dyslexic people to unspecific areas of

the brain (Galaburda et al., 1985). Hence, language-related processes, for example phoneme discrimination, that normally take place in the left vOT are impaired (Centanni et al., 2014). Such impairements might be compensated by a stronger engagement of the right hemisphere when processing visually familiar real letters. Importantly, children at familial risk might eventually undergo a shift from more bilateral to left-lateralized language processing later in their development (Maurer et al., 2011; Ossowski & Behrmann, 2015).

In sum, the results for the processing of real letters, showed the expected ambiguous activation for print sensitivity in EEG and in fMRI. The preferential processing of real letters in the right hemisphere might have been caused by underlying genetic or maturational effects. Future research is needed to uncover the exact role of the right hemisphere when children develop visual specialization for print and how this development is related to familial and genetic risks for developmental dyslexia.

The last level in the manipulation of visual expertise involved presenting single digits. We expected that well-known digits would reflect a higher expertise level than the other character types in both EEG and fMRI data. The activation for digits in the EEG showed the strongest N1 activation of all the other character types, which might reflect the high level of visual expertise (Rossion et al., 2002; Tanaka & Curran, 2001). However, expertise in the print-sensitive N1 has been shown to be characterized by lower activation in adults than in children (Maurer et al., 2006). Assuming such a decrease in activation with increasing expertise, processing might become more focal and therefore, the overall elicited neural activation would be reduced. In contrast, children in the phase of extensive learning activate less specific areas and hence, the overall neural activation is stronger than the focal activation in adult experts. However, the present results regarding visual processing of digtis are not in accordance with this assumption. Hence, prereading children might not yet have reached the assumed full expertise in processing digits.

The results of visual prossesing in fMRI were unexpected, as digits elicited activations in the left and in the right hemisphere comparable to those elicited by trained false-font characters, novel false-font characters, and real letters. It could be argued that this finding is in line with the inverted U-shaped

model of expertise (Price & Devlin, 2011), with reduced activation reflecting expertise. However, the difference from the immediate learning stage of the trained false-font characters was not significant, which indicates that both trained false-font characters and well-known digits are reflected in similar activations in the vOT. Overall, the divergent results of processing digits in EEG and fMRI were partly unexpected.

4.1.3 The interactive account model

Expertise in langauge processing has been previously explained in the interactive account model by Price and Devlin (2011). This model suggests three stages of learning that follow an inverted U-shaped course. The authors define learning as the coupling of sensory information with representations stored in higher cognitive areas. Stage 1 is characterized by no learning. This means that printed stimuli are processed without information from higher cognitive areas. Hence, no expectations are created and no errors occur in the prediction of subsequent processes. Therefore, stage 1 of learning is characterized by low activation. In stage 2, the actual learning occurs. Previous experiences have been stored in higher-order cognitive areas, and new sensory input leads to predicitions about subsequent processes. These predicitions may be correct, or they may lead to prediticition errors. Wrong predictions lead to wrong conclusions, and therefore, adjustments take place. Such loops enable learning and lead to strong neural activation, reflecting how energy consuming this refining process is. As practice and learning continues, in stage 3 a level of expertise is reached at which the prediction errors decrease, and thus, the neural activation declines (Price & Devlin, 2011).

The integration of the results of the Study A in this model is of high interest but bears some obstacles. The characters chosen follow the line of the model. Novel false-font characters imply no learning at stage 1, at stage 2, the trained false-font characters signal immediate learning. Digits represent stage 3, reflecting the high expertise of children for this stimulus category. Finally, real letters, which are not explicitly trained but of which children possess some implicit knowledge, are expected to range between stages 1 and 2.

The results of the ERP analysis partly followed the expected inverted U-shape, as novel false-font characters showed the lowest N1 activation, trained false-font characters a higher N1 activation and the strength of the N1 activation to real letters was found to be between these two conditions. However, the activation for digits did not show the expected decrease in activation, despite the high level of expertise. Instead, digits elicited the strongest activation of all the other character types. Thus, the children may not yet have reached the full level of expertise, despite the explicit teaching of numbers in kindergarten. This leads to the assumption that the N1 activation found for digits in the present data might not reflect visual print sensitivity at an expert level (stage 3), but probably reflects the stage of intensive learning (stage2).

The fMRI data pesented here are not easily integrated into the proposed interactive account model. The activation for real letters was the strongest, especially in the right hemisphere, although we expected the strongest activation for trained false-font characters. Nevertheless, novel false-font characters seemed to reflect stage 1 of learning, as the activation was the lowest, at least in the left hemisphere. Digits showed a low fMRI activation that may indicate expertise at stage 3. However, this conclusion should be drawn with caution, as a corresponding result was not found for the activation for digits in the EEG data. In conclusion, it is partly possible to integrate the present results into the interactive account model. However, whether the activation in EEG and fMRI reflect the same neural activity and how the information from the two modalities can be intergrated into the model remain open questions.

4.2 Neural print tuning in beginning readers

In study B, the same children as in study A were tested again after half a year of formal reading instruction at school. EEG and fMRI data were recorded simultaneously in 38 children while they processed real words, nonwords, and false-font strings. Before the scanning session, the children were tested in their reading fluency. Given that the sample consisted of children at familial risk for developmental dyslexia, we expected that approximately half of the sample would have low reading

fluency. Indeed, 18 of the children scored below the 16th percentile in the mean reading fluency score and were therefore classified as poor readers. The remaining 20 children scored above the 16th percentile and were classified as normal readers. We aimed to identify print-sensitive activation in beginning readers in a stronger N1 ERP and left vOT activation for words compared to false-font strings. In addition, we expected that normal readers would already show distinct print tuning while poor readers would not.

4.2.1 The role of initial reading skills

Usually, the distinction between German-speaking normal and poor readers is made based on reading fluency (Schulte-Korne, 2010), which can be measured by a 1-minute single word and pseudoword reading test (Landerl & Moll, 2014). Insufficient reading fluency, despite adequate schooling and normal intelligence leads to the diagnosis of developmental dyslexia.

Because developmental dyslexia has a neurobiological origin (Lyon, Shaywitz, & Shaywitz, 2003), dyslexic adult readers show weaker activations in reading-related brain regions (van der Mark09, Richlan09, Kronschnabel13). In addition, diminished neural activity to visually presented words has been shown to be evident in dyslexic school-children (Fraga González et al., 2014; Hasko et al., 2013; Maurer et al., 2007). However, it remains unclear, how early in the course of reading acquisition the neural differentiation between normal and poor readers begins. Study B aimed to shed light on this open question by investigating neural print tuning in beginning readers. We expected neural differences reflecting print sensitivity to be shown in stronger activations in the N1 and in the left vOT (Kronschnabel et al., 2013; Maurer et al., 2009; Richlan et al., 2009) for normal readers than for poor readers.

In the visual N1 ERP, print-sensitive activation did not differ between normal and poor readers. This effect seems to be similar to that reported by Coch (2015), namely that at an early learning stage the long-known reading shift is still absent on a neural level. The reading shift occurs when children finish the reading acquisition process and from then on actively use reading as a tool to enlarge their

knowledge (Chall & Jacobs, 1983). It has been suggested that this change takes place during fourth grade (Chall & Jacobs, 1983). Hence, it might be possible that neural differences in print sensitivity between normal and poor readers are still small in first grade.

In the fMRI, the ROI analysis of the left vOT revealed an interesting result. Poor readers showed a stronger activation for false-font strings than for words. Cantlon et al. (2011)'s model provides a possible explanation for this result. It proposes a reduction in activation for nonpreferred visual categories in the vOT. Pruning mechanisms reduce connections that are seldom used. The stronger activation in the vOT for false-font strings than for words indicate that the pruning may be protracted in poor readers.

Additionally, the impact of the experimental paradigm should be taken into account. During the visual one-back task, the children had to press a button whenever a stimulus was presented twice in a row. The accuracy rates of the children in this task revealed that several children (n=5) only reacted to less than six of the targets. After the data of these children were excluded, analyses revealed that the main results remain the same, except for that showing that poor readers show a stronger activation in the left vOT for false-font strings than for words. Although the task has been repeatedly used in studies with children (Eberhard-Moscicka et al., 2015; Maurer et al., 2011), it was shown to be challenging for such young children. In particular, the complex structure of the false-font strings might have led to the low accuracy rates.

4.2.2 Acquisition and analysis of simultaneous EEG-fMRI in children

Before discussing the analysis and results of simultaneous EEG-fMRI data, the challenges of acquiring concurrent EEG and fMRI in young children are briefly discussed. The most challenging factors of pediatric neuroimaging are the reduced attention span of children, higher movement rates, and motivational factors (Bookheimer, 2000). In a simultaneous setting, additional drawbacks such as signal loss and extensive pre-measurement preparation times arise (Huster et al., 2012). Despite these

challenges, simultaneous EEG-fMRI data were successfully acquired for this thesis in a state-of-the-art quality.

Meeting the high-quality requirements of multimodal neuroimaging enabled us to integrate the information gained by the two modalities. A single-trial EEG-informed fMRI analysis used amplitudes of the N1 ERP to perform a parametric modulation of the hemodynamic response. This analysis revealed a stronger print-sensitive modulation of the left vOT by the visual N1 for normal readers than for poor readers. This finding indicates that the differences expected between normal and poor readers are already emerging at the neural level during the initial reading acquisition, but only multimodal analysis could uncover these small differences in neural print tuning. Overall, half a year of formal reading instruction yielded clear differences at a neural level between normal readers and poor readers print sensitivity.

4.3 Limitations

Overall, the insights of the two studies enlarge the current knowledge regarding print sensitivity and highlight the effects of training and initial reading fluency. However, some limitations need to be mentioned. The main limitation of the study was that the sample consisted only of children at familial risk for developmental dyslexia. The comparison to an age-matched healthy control group would have enhanced the interpretation of the present results, as we cannot rule out that normal readers at risk use compensatory processes to achieve high reading fluency scores. Hence, future studies with similar aims also need to recruit and assess children not at familial risk for developmental dyslexia.

Moreover, simultaneous recordings of EEG and fMRI present challenges regarding data quality, especially when measuring young children. The demanding protocol was tiring for some children, especially in kindergarten. However, the protocol was divided into several parts to help retain children's attention and motivation. In addition, the children collected points for each task, and the points could be exchanged for presents.

Lying in the scanner while wearing an EEG electrode net may provoke some irritation to the scalp, and the pressure of the headphones used as protection against scanner noise may cause some disconfort. Such factors may lead to head movements that would affect data quality. Several precautions were taken to make the situation for the children as comfortable as possible. A custom-made head pad ensured that the pressure of the electrodes on the back of the head was cushioned. In addition, several breaks were introduced after each or every second task. Nevertheless, several data sets had to be excluded because of poor data quality either in EEG or fMRI or because some children fell asleep. In kindergarten, this resulted in only 18 complete data sets that met our stringent data quality standards. However, in first grade, half a year after the first recordings, the data quality was considerably better. The better data quality probably resulted from the fact that the children were already used to the scanning procedure and that they were older and could thus concentrate and lie still for a longer period.

4.4 Implications and impact of studying the development of neural print tuning

Despite these limitations, the findings of these studies enhance current knowledge regarding the early development of neurobiological mechanisms in visual print processing. In particular, the current state of knowledge was complemented by new insights into how training induces print-sensitive activation in reading-naïve children and into fine neural differences in coarse print tuning between normal and poor readers after half a year of reading instruction.

These novel findings form a well-studied foundation for future research questions regarding print tuning and reading acquisition in young children. This PhD thesis was part of a larger longitudinal study using state-of-the-art multimodal methodology that provides a novel framework in pediatric neuroimaging. Multimodal neuroimaging recordings and combined analyses will improve our understanding of normal and impaired reading acquisition and lead to more elaborate and scientifically supported diagnosis and interventions.

For children suffering from developmental dyslexia, it is crucial to start supporting training parallel to their formal reading instruction. However, developmental dyslexia is usually only diagnosed in second grade or later, so reading development is protracted from the very beginning. Therefore, affected children have a substantial drawback to catch up with their normal reading peers. Earlier diagnosis is thus urgently needed, and this may be advanced by new tools. Artificial letter training has the potential to meet this need, as it clearly discriminated between fast and slow learning. The predictive value of the training needs to be investigated further for it to become a simple, computer-based tool for school settings and clinical applications. Finally, the present thesis investigated the neural aspects underlying developmental dyslexia with the long-term aim of promoting the development of new interventions and teaching materials.

4.5 Conclusion

This thesis aimed to investigate the development of visual specialization for print with simultaneous EEG and fMRI recordings. Firstly, the impact of expertise on print processing was investigated in prereading children. An artificial-letter training initialized print-sensitive activation, and the neural print tuning depended on the ability to learn print specific material. Secondly, after half a year of formal reading instruction, differences between normal reading and poor-reading children were already evident in neural print tuning. This finding was particularly underpinned by the stronger print-specific modulation of the vOT by the N1 ERP in normal readers than in poor readers. These results show that expertise for visual print processing is developed with explicit training, and differences between normal and poor readers are already evident after half a year of formal reading instruction. These findings advance current knowledge about the neurobiological mechanisms involved in reading acquisition in children at familial risk and will have implications for the development of new teaching material and interventions to ensure an enjoyable start into the reading adventure for all first-grade children.

Abbreviations

ACC	accuracy
ARHQ	Adult Reading History Questionnaire
BOLD	blood-oxygen-level dependent response
CDT	cluster-defining threshold
CFT	Culture Fair Intelligence Test
CSF	cerebrospinal fluid
DIG	digits
ECG	electrocardiogram
EEG	electroencephalography
EPI	echo-planar image sequence
ERP	event related potential
FG	fusiform gyrus
fMRI	functional magnetic resonance imaging
FOV	field of view
FWE_{corr}	family-wise error corrected
GFP	global field power
GLM	general linear models
GM	grey matter
GPC	grapheme-phoneme correspondence
HAWIK	Hamburg Wechsler Intelligenztest für Kinder
ICA	Independent component analysis
IOG	inferior occipital gyrus
IQ	intelligence quotient
ITG	inferior temporal gyrus
LET	Letters
LFA	letter form area
LFP	local field potentials
LMM	linear mixed models
LOT	left occipitotemporal
MEG	magnetoencephalography studies
MFG	middle frontal gyrus
MNI	Montreal Neurological Institute
MO	middle occipital
MOG	middle occipital gyrus
MTG	middle temporal gyrus
NFF	novel false-fonts
OFC	orbitofrontal cortex
RAN	Rapid naming
ROT	right occipitotemporal
RT	reaction time
SFG	superior frontal gyrus
SLRT	Salzburger Lese- und Rechtschreibtest
SPG	superior parietal gyrus
STG	superior temporal gyrus

TE	echo time
TEPHOBE	Test für phonologische Bewusstheit und Bennengeschwindigkeit
TFF	trained false-fonts
TR	repetition time
vOT	ventral occipitotemporal
VWFA	visual word form area
VWFS	visual word form system
WM	white matter
3D MP-RAGE	3-dimensional magnetization-prepared rapid-acquisition echo

References

Abboud, S., Maidenbaum, S., Dehaene, S., & Amedi, A. (2015). A number-form area in the blind. *Nature communications, 6*.

Allen, P. J., Josephs, O., & Turner, R. (2000). A method for removing imaging artifact from continuous EEG recorded during functional MRI. *NeuroImage, 12*(2), 230-239.

Araújo, S., Bramão, I., Faísca, L., Petersson, K. M., & Reis, A. (2012). Electrophysiological correlates of impaired reading in dyslexic pre-adolescent children. *Brain and Cognition, 79*(2), 79-88.

Araújo, S., Faísca, L., Bramão, I., Petersson, K. M., & Reis, A. (2014). Lexical and Phonological Processes in Dyslexic Readers: Evidence from a Visual Lexical Decision Task. *Dyslexia, 20*(1), 38-53.

Araújo, S., Faísca, L., Bramão, I., Reis, A., & Petersson, K. M. (2015). Lexical and sublexical orthographic processing: An ERP study with skilled and dyslexic adult readers. *Brain and Language, 141*, 16-27.

Baayen, R. H., Piepenbrock, R., & van H, R. (1993). *The CELEX lexical data base on [CD-ROM]*. Linguistic Data Consortium, University of Pennsylvania.

Bach, S., Brandeis, D., Hofstetter, C., Martin, E., Richardson, U., & Brem, S. (2010). Early emergence of deviant frontal fMRI activity for phonological processes in poor beginning readers. *NeuroImage, 53*(2), 682-693.

Bach, S., Richardson, U., Brandeis, D., Martin, E., & Brem, S. (2013). Print-specific multimodal brain activation in kindergarten improves prediction of reading skills in second grade. *NeuroImage, 82*, 605-615.

Baker, C. I., Liu, J., Wald, L. L., Kwong, K. K., Benner, T., & Kanwisher, N. (2007). Visual word processing and experiential origins of functional selectivity in human extrastriate cortex. *Proceedings of the National Academy of Sciences, 104*(21), 9087-9092.

Behzadi, Y., Restom, K., Liau, J., & Liu, T. T. (2007). A component based noise correction method (CompCor) for BOLD and perfusion based fMRI. *NeuroImage, 37*(1), 90-101.

Ben-Shachar, M., Dougherty, R. F., Deutsch, G. K., & Wandell, B. A. (2011). The development of cortical sensitivity to visual word forms. *Journal of Cognitive Neuroscience, 23*(9), 2387-2399.

Bentin, S., Mouchetant-Rostaing, Y., Giard, M.-H., Echallier, J.-F., & Pernier, J. (1999). ERP manifestations of processing printed words at different psycholinguistic levels: time course and scalp distribution. *Cognitive Neuroscience, Journal of, 11*(3), 235-260.

Berger, H. (1929). Über das elektrenkephalogramm des menschen. *European Archives of Psychiatry and Clinical Neuroscience, 87*(1), 527-570.

Binder, J. R., Medler, D. A., Westbury, C. F., Liebenthal, E., & Buchanan, L. (2006). Tuning of the human left fusiform gyrus to sublexical orthographic structure. *NeuroImage, 33*(2), 739-748.

Black, J. M., Tanaka, H., Stanley, L., Nagamine, M., Zakerani, N., Thurston, A., . . . Glover, G. H. (2012). Maternal history of reading difficulty is associated with reduced language-related gray matter in beginning readers. *NeuroImage, 59*(3), 3021-3032.

Blau, V., Reithler, J., van Atteveldt, N., Seitz, J., Gerretsen, P., Goebel, R., & Blomert, L. (2010). Deviant processing of letters and speech sounds as proximate cause of reading failure: a functional magnetic resonance imaging study of dyslexic children. *Brain, 133*, 868-879.

Bledowski, C., Kadosh, K. C., Wibral, M., Rahm, B., Bittner, R. A., Hoechstetter, K., . . . Linden, D. E. (2006). Mental chronometry of working memory retrieval: a combined functional magnetic resonance imaging and event-related potentials approach. *Journal of Neuroscience, 26*(3), 821-829.

Blomert, L. (2011). The neural signature of orthographic-phonological binding in successful and failing reading development. *NeuroImage, 57*(3), 695-703.

Bookheimer, S. Y. (2000). Methodological issues in pediatric neuroimaging. *Mental retardation and developmental disabilities research reviews, 6*(3), 161-165.

Booth, J. R., Burman, D. D., Santen, F. W. V., Harasaki, Y., Gitelman, D. R., Parrish, T. B., & Mesulam, M. M. (2001). The development of specialized brain systems in reading and oral-language. *Child Neuropsychology, 7*(3), 119-141.

Boros, M., Anton, J.-L., Pech-Georgel, C., Grainger, J., Szwed, M., & Ziegler, J. C. (2016). Orthographic processing deficits in developmental dyslexia: Beyond the ventral visual stream. *NeuroImage, 128*, 316-327.

Brambati, S. M., Termine, C., Ruffino, M., Danna, M., Lanzi, G., Stella, G., . . . Perani, D. (2006). Neuropsychological deficits and neural dysfunction in familial dyslexia. *Brain Research, 1113*(1), 174-185.

Braun, M., Hutzler, F., Ziegler, J. C., Dambacher, M., & Jacobs, A. M. (2009). Pseudohomophone effects provide evidence of early lexico-phonological processing in visual word recognition. *Human Brain Mapping, 30*(7), 1977-1989.

Brem, S., Bach, S., Kucian, K., Guttorm, T. K., Martin, E., Lyytinen, H., . . . Richardson, U. (2010). Brain sensitivity to print emerges when children learn letter–speech sound correspondences. *Proceedings of the National Academy of Sciences, 107*(17), 7939-7944.

Brem, S., Bach, S., Kujala, J. V., Maurer, U., Lyytinen, H., Richardson, U., & Brandeis, D. (2013). An Electrophysiological Study of Print Processing in Kindergarten: The Contribution of the Visual N1 as a Predictor of Reading Outcome. *Developmental Neuropsychology, 38*(8), 567-594.

Brem, S., Bucher, K., Halder, P., Summers, P., Dietrich, T., Martin, E., & Brandeis, D. (2006). Evidence for developmental changes in the visual word processing network beyond adolescence. *NeuroImage, 29*(3), 822-837.

Brem, S., Halder, P., Bucher, K., Summers, P., Martin, E., & Brandeis, D. (2009). Tuning of the visual word processing system: Distinct developmental ERP and fMRI effects. *Human Brain Mapping, 30*(6), 1833-1844.

Brem, S., Hunkeler, E., Mächler, M., Kronschnabel, J., Karipidis, I. I., Pleisch, G., & Brandeis, D. (2017). Increasing expertise to a novel script modulates the visual N1 ERP in healthy adults. *International Journal of Behavioral Development*, 1-9.

Brem, S., Lang-Dullenkopf, A., Maurer, U., Halder, P., Bucher, K., & Brandeis, D. (2005). Neurophysiological signs of rapidly emerging visual expertise for symbol strings. *Neuroreport, 16*(1), 45-48.

Brett, M., Anton, J.-L., Valabregue, R., & Poline, J.-B. (2002). Region of interest analysis using the MarsBar toolbox for SPM 99. *NeuroImage, 16*(2), 497.

Brunswick, N., McCrory, E., Price, C., Frith, C., & Frith, U. (1999). Explicit and implicit processing of words and pseudowords by adult developmental dyslexics. *Brain, 122*(10), 1901-1917.

Cantlon, J. F., Pinel, P., Dehaene, S., & Pelphrey, K. A. (2011). Cortical representations of symbols, objects, and faces are pruned back during early childhood. *Cerebral Cortex, 21*(1), 191-199.

Cao, F., Khalid, K., Lee, R., Brennan, C., Yang, Y., Li, K., . . . Booth, J. R. (2011). Development of brain networks involved in spoken word processing of Mandarin Chinese. *NeuroImage, 57*(3), 750-759.

Carreiras, M., Quiñones, I., Hernández-Cabrera, J. A., & Duñabeitia, J. A. (2014). Orthographic coding: brain activation for letters, symbols, and digits. *Cerebral Cortex, 25*(12), 4748-4760.

Carreiras, M., Seghier, M. L., Baquero, S., Estévez, A., Lozano, A., Devlin, J. T., & Price, C. J. (2009). An anatomical signature for literacy. *Nature, 461*(7266), 983-986.

Carrion-Castillo, A., Franke, B., & Fisher, S. E. (2013). Molecular genetics of dyslexia: an overview. *Dyslexia, 19*(4), 214-240.

Centanni, T. M., Chen, F., Booker, A. M., Engineer, C. T., Sloan, A. M., Rennaker, R. L., . . . Kilgard, M. P. (2014). Speech sound processing deficits and training-induced neural plasticity in rats with dyslexia gene knockdown. *PloS one, 9*(5), e98439.

Centanni, T. M., King, L. W., Eddy, M. D., Whitfield-Gabrieli, S., & Gabrieli, J. D. (2017). Development of sensitivity versus specificity for print in the visual word form area. *Brain and Language, 170*, 62-70.

Chall, J. S., & Jacobs, V. A. (1983). Writing and reading in the elementary grades: Developmental trends among low SES children. *Language arts, 60*(5), 617-626.

Clark, K. A., Helland, T., Specht, K., Narr, K. L., Manis, F. R., Toga, A. W., & Hugdahl, K. (2014). Neuroanatomical precursors of dyslexia identified from pre-reading through to age 11. *Brain, 137*(12), 3136-3141.

Coch, D. (2015). The N400 and the fourth grade shift. *Developmental science, 18*(2), 254-269.
Cohen, L., & Dehaene, S. (2004). Specialization within the ventral stream: the case for the visual word form area. *NeuroImage, 22*(1), 466-476.
Cohen, L., Dehaene, S., Naccache, L., Lehéricy, S., Dehaene-Lambertz, G., Hénaff, M.-A., & Michel, F. (2000). The visual word form area. *Brain, 123*(2), 291-307.
Cohen, L., Lehéricy, S., Chochon, F., Lemer, C., Rivaud, S., & Dehaene, S. (2002). Language-specific tuning of visual cortex? Functional properties of the Visual Word Form Area. *Brain, 125*(5), 1054-1069.
Cohen, L., Martinaud, O., Lemer, C., Lehericy, S., Samson, Y., Obadia, M., . . . Dehaene, S. (2003). Visual word recognition in the left and right hemispheres: anatomical and functional correlates of peripheral alexias. *Cerebral Cortex, 13*(12), 1313-1333.
Coltheart, M., Davelaar, E., Jonasson, T., & Besner, D. (1977). Access to the internal lexicon.
Coltheart, M., Rastle, K., Perry, C., Langdon, R., & Ziegler, J. (2001). DRC: a dual route cascaded model of visual word recognition and reading aloud. *Psychological Review, 108*(1), 204-256.
Dale, A. M., Liu, A. K., Fischl, B. R., Buckner, R. L., Belliveau, J. W., Lewine, J. D., & Halgren, E. (2000). Dynamic Statistical Parametric Mapping: Combining fMRI and MEG for High-Resolution Imaging of Cortical Activity. *Neuron, 26*(1), 55-67.
Damasio, A. R., & Damasio, H. (1983). The anatomic basis of pure alexia. *Neurology, 33*(12), 1573-1573.
Dawson, G. D. (1951). A summation technique for detecting small signals in a large irregular background. *The Journal of physiology, 115*(1), 2-3.
Debener, S., Ullsperger, M., Siegel, M., Fiehler, K., von Cramon, D. Y., & Engel, A. K. (2005). Trial-by-trial coupling of concurrent electroencephalogram and functional magnetic resonance imaging identifies the dynamics of performance monitoring. *Journal of Neuroscience, 25*(50), 11730-11737.
Dehaene-Lambertz, G., & Gliga, T. (2004). Common neural basis for phoneme processing in infants and adults. *Journal of Cognitive Neuroscience, 16*(8), 1375-1387.
Dehaene, S., & Cohen, L. (2007). Cultural recycling of cortical maps. *Neuron, 56*(2), 384-398.
Dehaene, S., & Cohen, L. (2011). The unique role of the visual word form area in reading. *Trends Cognitive Science, 15*(6), 254-262.
Dehaene, S., Cohen, L., Sigman, M., & Vinckier, F. (2005). The neural code for written words: a proposal. *Trends Cognitive Science, 9*(7), 335-341.
Dehaene, S., Naccache, L., Cohen, L., Bihan, D. L., Mangin, J.-F., Poline, J.-B., & Rivière, D. (2001). Cerebral mechanisms of word masking and unconscious repetition priming. *Nature Neuroscience, 4*, 752-758.
Dehaene, S., Pegado, F., Braga, L. W., Ventura, P., Nunes Filho, G., Jobert, A., . . . Cohen, L. (2010). How learning to read changes the cortical networks for vision and language. *Science, 330*(6009), 1359-1364.
Devlin, J. T., Jamison, H. L., Gonnerman, L. M., & Matthews, P. M. (2006). The role of the posterior fusiform gyrus in reading. *Journal of Cognitive Neuroscience, 18*(6), 911-922.
Eberhard-Moscicka, A. K., Jost, L. B., Raith, M., & Maurer, U. (2015). Neurocognitive mechanisms of learning to read: print tuning in beginning readers related to word-reading fluency and semantics but not phonology. *Developmental science, 18*(1), 106-118.
Ehri, L. C. (2005). *Development of sight word reading: Phases and findings*.
Eichele, T., Specht, K., Moosmann, M., Jongsma, M. L., Quiroga, R. Q., Nordby, H., & Hugdahl, K. (2005). Assessing the spatiotemporal evolution of neuronal activation with single-trial event-related potentials and functional MRI. *Proceedings of the National Academy of Sciences, 102*(49), 17798-17803.
Eklund, A., Nichols, T. E., & Knutsson, H. (2016). Cluster failure: Why fMRI inferences for spatial extent have inflated false-positive rates. *Proceedings of the National Academy of Sciences, 113*(28), 7900-7905.
Epstein, R., & Kanwisher, N. (1998). A cortical representation of the local visual environment. *Nature, 392*(6676), 598.

Foundas, A. L., Daniels, S. K., & Vasterling, J. J. (1998). Anomia: case studies with lesion localization. *Neurocase, 4*(1), 35-43.

Fraga González, G., Žarić, G., Tijms, J., Bonte, M., Blomert, L., & van der Molen, M. W. (2014). Brain-potential analysis of visual word recognition in dyslexics and typically reading children. *Frontiers Human Neuroscience, 8*, 1-14.

Fraga González, G., Žarić, G., Tijms, J., Bonte, M., Blomert, L., & van der Molen, M. W. (2015). A randomized controlled trial on the beneficial effects of training letter-speech sound integration on reading fluency in children with dyslexia. *PloS one, 10*(12), e0143914.

Friston, K. (2010). The free-energy principle: a unified brain theory? *Nature Reviews Neuroscience, 11*(2), 127-138.

Gaillard, R., Naccache, L., Pinel, P., Clémenceau, S., Volle, E., Hasboun, D., . . . Adam, C. (2006). Direct intracranial, FMRI, and lesion evidence for the causal role of left inferotemporal cortex in reading. *Neuron, 50*(2), 191-204.

Gaillard, W. D., Sachs, B. C., Whitnah, J. R., Ahmad, Z., Balsamo, L. M., Petrella, J. R., . . . Xu, B. (2003). Developmental aspects of language processing: fMRI of verbal fluency in children and adults. *Human Brain Mapping, 18*(3), 176-185.

Galaburda, A. M., Sherman, G. F., Rosen, G. D., Aboitiz, F., & Geschwind, N. (1985). Developmental dyslexia: four consecutive patients with cortical anomalies. *Annals of Neurology, 18*(2), 222-233.

Galuschka, K., Ise, E., Krick, K., & Schulte-Körne, G. (2014). Effectiveness of treatment approaches for children and adolescents with reading disabilities: a meta-analysis of randomized controlled trials. *PloS one, 9*(2), e89900.

Gauthier, I., Tarr, M. J., Moylan, J., Skudlarski, P., Gore, J. C., & Anderson, A. W. (2000). The fusiform "face area" is part of a network that processes faces at the individual level. *Journal of Cognitive Neuroscience, 12*(3), 495-504.

Glezer, L. S., Jiang, X., & Riesenhuber, M. (2009). Evidence for highly selective neuronal tuning to whole words in the "visual word form area". *Neuron, 62*(2), 199-204.

Glezer, L. S., Kim, J., Rule, J., Jiang, X., & Riesenhuber, M. (2015). Adding Words to the Brain's Visual Dictionary: Novel Word Learning Selectively Sharpens Orthographic Representations in the VWFA. *The Journal of Neuroscience, 35*(12), 4965-4972.

Glezer, L. S., & Riesenhuber, M. (2013). Individual variability in location impacts orthographic selectivity in the "visual word form area". *Journal of Neuroscience, 33*(27), 11221-11226.

Gooch, D., Hulme, C., Nash, H. M., & Snowling, M. J. (2014). Comorbidities in preschool children at family risk of dyslexia. *Journal of Child Psychology and Psychiatry, 55*(3), 237-246.

Hannagan, T., Amedi, A., Cohen, L., Dehaene-Lambertz, G., & Dehaene, S. (2015). Origins of the specialization for letters and numbers in ventral occipitotemporal cortex. *Trends Cognitive Science, 19*(7), 374-382.

Hashimoto, R., & Sakai, K. L. (2004). Learning letters in adulthood: direct visualization of cortical plasticity for forming a new link between orthography and phonology. *Neuron, 42*(2), 311-322.

Hasko, S., Groth, K., Bruder, J., Bartling, J., & Schulte-Korne, G. (2013). The time course of reading processes in children with and without dyslexia: an ERP study. *Frontiers Human Neuroscience, 7*, 570.

Hasson, U., Harel, M., Levy, I., & Malach, R. (2003). Large-scale mirror-symmetry organization of human occipito-temporal object areas. *Neuron, 37*(6), 1027-1041.

Hauser, T. U., Hunt, L. T., Iannaccone, R., Walitza, S., Brandeis, D., Brem, S., & Dolan, R. J. (2015). Temporally dissociable contributions of human medial prefrontal subregions to reward-guided learning. *Journal of Neuroscience, 35*(32), 11209-11220.

Hauser, T. U., Iannaccone, R., Ball, J., Mathys, C., Brandeis, D., Walitza, S., & Brem, S. (2014). Role of the medial prefrontal cortex in impaired decision making in juvenile attention-deficit/hyperactivity disorder. *JAMA psychiatry, 71*(10), 1165-1173.

Helenius, P., Tarkiainen, A., Cornelissen, P., Hansen, P., & Salmelin, R. (1999). Dissociation of normal feature analysis and deficient processing of letter-strings in dyslexic adults. *Cerebral Cortex, 9*(5), 476-483.

Hoeft, F., Ueno, T., Reiss, A. L., Meyler, A., Whitfield-Gabrieli, S., Glover, G. H., . . . Gabrieli, J. D. E. (2007). Prediction of children's reading skills using behavioral, functional, and structural neuroimaging measures. *Behavioral Neuroscience, 121*(3), 602-613.

Holland, S. K., Vannest, J., Mecoli, M., Jacola, L. M., Tillema, J.-M., Karunanayaka, P. R., . . . Byars, A. W. (2007). Functional MRI of language lateralization during development in children. *International journal of audiology, 46*(9), 533-551.

Houdé, O., Rossi, S., Lubin, A., & Joliot, M. (2010). Mapping numerical processing, reading, and executive functions in the developing brain: an fMRI meta-analysis of 52 studies including 842 children. *Developmental science, 13*(6), 876-885.

Hu, W., Lee, H. L., Zhang, Q., Liu, T., Geng, L. B., Seghier, M. L., . . . Yang, Y. M. (2010). Developmental dyslexia in Chinese and English populations: dissociating the effect of dyslexia from language differences. *Brain, 133*(6), 1694-1706.

Huettel, S. A., Song, A., & McCarthy, G. (2009). *Functional Magnetic Resonance Imaging* Massachusetts: Sinauer: ISBN 978-0-87893-286-3.

Huster, R. J., Debener, S., Eichele, T., & Herrmann, C. S. (2012). Methods for simultaneous EEG-fMRI: an introductory review. *Journal of Neuroscience, 32*(18), 6053-6060.

Iannaccone, R., Hauser, T. U., Staempfli, P., Walitza, S., Brandeis, D., & Brem, S. (2015). Conflict monitoring and error processing: new insights from simultaneous EEG–fMRI. *NeuroImage, 105*, 395-407.

James, K. H. (2010). Sensori-motor experience leads to changes in visual processing in the developing brain. *Developmental science, 13*(2), 279-288.

Jobard, G., Crivello, F., & Tzourio-Mazoyer, N. (2003). Evaluation of the dual route theory of reading: a metanalysis of 35 neuroimaging studies. *NeuroImage, 20*(2), 693-712.

Johnson, M. H. (2011). Interactive specialization: a domain-general framework for human functional brain development? *Dev Cogn Neurosci, 1*(1), 7-21.

Jung, T.-P., Makeig, S., Westerfield, M., Townsend, J., Courchesne, E., & Sejnowski, T. J. (2000). Removal of eye activity artifacts from visual event-related potentials in normal and clinical subjects. *Clinical Neurophysiology, 111*(10), 1745-1758.

Kanwisher, N., McDermott, J., & Chun, M. M. (1997). The fusiform face area: a module in human extrastriate cortex specialized for face perception. *Journal of Neuroscience, 17*(11), 4302-4311.

Kanwisher, N., & Yovel, G. (2006). The fusiform face area: a cortical region specialized for the perception of faces. *Philosophical Transactions of the Royal Society of London B: Biological Sciences, 361*(1476), 2109-2128.

Karipidis, I. I., Pleisch, G., Röthlisberger, M., Hofstetter, C., Dornbierer, D., Stämpfli, P., & Brem, S. (2017). Neural initialization of audiovisual integration in prereaders at varying risk for developmental dyslexia. *Human Brain Mapping, 38*(2), 1038-1055.

Kast, M., Bezzola, L., Jancke, L., & Meyer, M. (2011). Multi- and unisensory decoding of words and nonwords result in differential brain responses in dyslexic and nondyslexic adults. *Brain and Language, 119*(3), 136-148.

Kourtzi, Z., & Kanwisher, N. (2001). Representation of perceived object shape by the human lateral occipital complex. *Science, 293*(5534), 1506-1509.

Kronbichler, M., Hutzler, F., Wimmer, H., Mair, A., Staffen, W., & Ladurner, G. (2004). The visual word form area and the frequency with which words are encountered: evidence from a parametric fMRI study. *NeuroImage, 21*(3), 946-953.

Kronbichler, M., Wimmer, H., Staffen, W., Hutzler, F., Mair, A., & Ladurner, G. (2008). Developmental dyslexia: gray matter abnormalities in the occipitotemporal cortex. *Human Brain Mapping, 29*(5), 613-625.

Kronschnabel, J., Schmid, R., Maurer, U., & Brandeis, D. (2013). Visual print tuning deficits in dyslexic adolescents under minimized phonological demands. *NeuroImage, 74*, 58-69.

Kucian, K., von Aster, M., Loenneker, T., Dietrich, T., & Martin, E. (2008). Development of neural networks for exact and approximate calculation: A FMRI study. *Developmental Neuropsychology, 33*(4), 447-473.

Landerl, K., & Moll, K. (2014). *Dissoziationen zwischen Störungen des Lesens und Störungen des Rechtschreibens*. Oldenburg: ISB-Verlag.

Lefly, D. L., & Pennington, B. F. (2000). Reliability and validity of the adult reading history questionnaire. *Journal of Learning Disabilities, 33*(3), 286-296.

Lehmann, D., & Skrandies, W. (1980). Reference-free identification of components of checkerboard-evoked multichannel potential fields. *Electroencephalography and Clinical Neurophysiology, 48*(6), 609-621.

Lin, F.-H., Belliveau, J. W., Dale, A. M., & Hämäläinen, M. S. (2006). Distributed current estimates using cortical orientation constraints. *Human Brain Mapping, 27*(1), 1-13.

Liu, A. K., Dale, A. M., & Belliveau, J. W. (2002). Monte Carlo simulation studies of EEG and MEG localization accuracy. *Human Brain Mapping, 16*(1), 47-62.

Liu, C., Zhang, W.-T., Tang, Y.-Y., Mai, X.-Q., Chen, H.-C., Tardif, T., & Luo, Y.-J. (2008). The visual word form area: evidence from an fMRI study of implicit processing of Chinese characters. *NeuroImage, 40*(3), 1350-1361.

Logothetis, N. K., Pauls, J., Augath, M., Trinath, T., & Oeltermann, A. (2001). Neurophysiological investigation of the basis of the fMRI signal. *Nature, 412*(6843), 150-157.

Luck, S. J. (2014). *An introduction to the event-related potential technique*: MIT press.

Lyon, G. R., Shaywitz, S. E., & Shaywitz, B. A. (2003). A definition of dyslexia. *Annals of dyslexia, 53*(1), 1-14.

Lyytinen, H., Erskine, J., Kujala, J., Ojanen, E., & Richardson, U. (2009). In search of a science-based application: A learning tool for reading acquisition. *Scandinavian Journal of Psychology, 50*(6), 668-675.

Lyytinen, H., Ronimus, M., Alanko, A., Poikkeus, A.-M., & Taanila, M. (2007). Early identification of dyslexia and the use of computer game-based practice to support reading acquisition. *Nordic Psychology, 59*(2), 109-126.

Mahé, G., Bonnefond, A., & Doignon-Camus, N. (2013). Is the impaired N170 print tuning specific to developmental dyslexia? A matched reading-level study with poor readers and dyslexics. *Brain and Language, 127*(3), 539-544.

Mahé, G., Bonnefond, A., Gavens, N., Dufour, A., & Doignon-Camus, N. (2012). Impaired visual expertise for print in French adults with dyslexia as shown by N170 tuning. *Neuropsychologia, 50*(14), 3200-3206.

Maisog, J. M., Einbinder, E. R., Flowers, D. L., Turkeltaub, P. E., & Eden, G. F. (2008). A meta-analysis of functional neuroimaging studies of dyslexia. *Annals of the New York Academy of Sciences, 1145*, 237-259.

Malach, R., Levy, I., & Hasson, U. (2002). The topography of high-order human object areas. *Trends Cognitive Sciences, 6*(4), 176-184.

Mandelkow, H., Halder, P., Boesiger, P., & Brandeis, D. (2006). Synchronization facilitates removal of MRI artefacts from concurrent EEG recordings and increases usable bandwidth. *NeuroImage, 32*(3), 1120-1126.

Maurer, U., Blau, V. C., Yoncheva, Y. N., & McCandliss, B. D. (2010). Development of visual expertise for reading: rapid emergence of visual familiarity for an artificial script. *Developmental Neuropsychology, 35*(4), 404-422.

Maurer, U., Brandeis, D., & McCandliss, B. D. (2005). Fast, visual specialization for reading in English revealed by the topography of the N170 ERP response. *Behavioral Brain Function, 1*, 13.

Maurer, U., Brem, S., Bucher, K., & Brandeis, D. (2005). Emerging neurophysiological specialization for letter strings. *Journal of Cognitive Neuroscience, 17*(10), 1532-1552.

Maurer, U., Brem, S., Bucher, K., Kranz, F., Benz, R., Steinhausen, H. C., & Brandeis, D. (2007). Impaired tuning of a fast occipito-temporal response for print in dyslexic children learning to read. *Brain, 130*, 3200-3210.

Maurer, U., Brem, S., Kranz, F., Bucher, K., Benz, R., Halder, P., . . . Brandeis, D. (2006). Coarse neural tuning for print peaks when children learn to read. *NeuroImage, 33*(2), 749-758.

Maurer, U., Bucher, K., Brem, S., Benz, R., Kranz, F., Schulz, E., . . . Brandeis, D. (2009). Neurophysiology in preschool improves behavioral prediction of reading ability throughout primary school. *Biological Psychiatry, 66*(4), 341-348.

Maurer, U., Schulz, E., Brem, S., der Mark, S., Bucher, K., Martin, E., & Brandeis, D. (2011). The development of print tuning in children with dyslexia: evidence from longitudinal ERP data supported by fMRI. *NeuroImage, 57*(3), 714-722.

Mayer. (2011). *Test zur Erfassung der phonologischen Bewusstheit und der Benenngeschwindigkeit (TEPHOBE)*. München: Ernst Reinhardt Verlag.

Mazaika, P. K., Glovera, G. H., & Reiss, A. L. (2011). Rapid motions in pediatric and clinical populations. *Psychiatry, 65*(11), 1315-1323.

Moll, K., & Landerl, K. (2010). SLRT-II: Lese-und Rechtschreibtest. *Huber, Bern*.

Mugnaini, D., Lassi, S., La Malfa, G., & Albertini, G. (2009). Internalizing correlates of dyslexia. *World Journal of Pediatrics, 5*(4), 255-264.

Nobre, A. C., Allison, T., & McCarthy, G. (1994). Word recognition in the human inferior temporal lobe. *Nature, 372*(6503), 260-263.

Norton, E. S., Beach, S. D., & Gabrieli, J. D. (2015). Neurobiology of dyslexia. *Current Opinion in Neurobiology, 30*, 73-78.

Ogawa, S., Lee, T.-M., Kay, A. R., & Tank, D. W. (1990). Brain magnetic resonance imaging with contrast dependent on blood oxygenation. *Proceedings of the National Academy of Sciences, 87*(24), 9868-9872.

Ossowski, A., & Behrmann, M. (2015). Left hemisphere specialization for word reading potentially causes, rather than results from, a left lateralized bias for high spatial frequency visual information. *Cortex, 72*, 27-39.

Ozernov-Palchik, O., & Gaab, N. (2016). Tackling the 'dyslexia paradox': reading brain and behavior for early markers of developmental dyslexia. *Wiley Interdisciplinary Reviews: Cognitive Science, 7*(2), 156-176.

Pammer, K., Hansen, P. C., Kringelbach, M. L., Holliday, I., Barnes, G., Hillebrand, A., . . . Cornelissen, P. L. (2004). Visual word recognition: the first half second. *NeuroImage, 22*(4), 1819-1825.

Park, J., Chiang, C., Brannon, E. M., & Woldorff, M. G. (2014). Experience-dependent hemispheric specialization of letters and numbers is revealed in early visual processing. *Journal of Cognitive Neuroscience, 26*(10), 2239-2249.

Park, J., Hebrank, A., Polk, T. A., & Park, D. C. (2012). Neural dissociation of number from letter recognition and its relationship to parietal numerical processing. *Journal of Cognitive Neuroscience, 24*(1), 39-50.

Pascual-Marqui, R. D. (1999). Review of methods for solving the EEG inverse problem. *International journal of bioelectromagnetism, 1*(1), 75-86.

Paulesu, E., Démonet, J.-F., Fazio, F., McCrory, E., Chanoine, V., Brunswick, N., . . . Frith, C. D. (2001). Dyslexia: cultural diversity and biological unity. *Science, 291*(5511), 2165-2167.

Pegado, F., Comerlato, E., Ventura, F., Jobert, A., Nakamura, K., Buiatti, M., . . . Morais, J. (2014). Timing the impact of literacy on visual processing. *Proceedings of the National Academy of Sciences, 111*(49), E5233-E5242.

Pennington, B. F., & Lefly, D. L. (2001). Early reading development in children at family risk for dyslexia. *Child Development, 72*(3), 816-833.

Perfetti, C. A., Liu, Y., Fiez, J., Nelson, J., Bolger, D. J., & Tan, L.-H. (2007). Reading in two writing systems: Accommodation and assimilation of the brain's reading network. *Bilingualism: Language and Cognition, 10*(2), 131-146.

Petermann, F., & Petermann, U. (Eds.). (2007). *Hamburg-Wechsler-Intelligenztest für Kinder - IV: HAWIK-IV; Manual; Übersetzung und Adaption der WISC-IV von David Wechsler*. Bern; Göttingen [u.a.]: Huber.

Pflugshaupt, T., Gutbrod, K., Wurtz, P., von Wartburg, R., Nyffeler, T., de Haan, B., . . . Mueri, R. M. (2009). About the role of visual field defects in pure alexia. *Brain, 132*(7), 1907-1917.

Piaget, J. (1965). The stages of the intellectual development of the child. *Educational psychology in context: Readings for future teachers*, 98-106.

Poskiparta, E., Niemi, P., Lepola, J., Ahtola, A., & Laine, P. (2003). Motivational-emotional vulnerability and difficulties in learning to read and spell. *British Journal of Educational Psychology, 73*(2), 187-206.

Price, C. J. (2012). A review and synthesis of the first 20years of PET and fMRI studies of heard speech, spoken language and reading. *NeuroImage, 62*(2), 816-847.

Price, C. J., & Devlin, J. T. (2003). The myth of the visual word form area. *NeuroImage, 19*(3), 473-481.

Price, C. J., & Devlin, J. T. (2011). The interactive account of ventral occipitotemporal contributions to reading. *Trends Cognitive Science, 15*(6), 246-253.

Price, C. J., Moore, C., & Frackowiak, R. (1996). The effect of varying stimulus rate and duration on brain activity during reading. *NeuroImage, 3*(1), 40-52.

Raschle, N. M., Chang, M., & Gaab, N. (2011). Structural brain alterations associated with dyslexia predate reading onset. *NeuroImage, 57*(3), 742-749.

Raschle, N. M., Stering, P. L., Meissner, S. N., & Gaab, N. (2013). Altered Neuronal Response During Rapid Auditory Processing and Its Relation to Phonological Processing in Prereading Children at Familial Risk for Dyslexia. *Cerebral Cortex, 24*(9), 2489-2401.

Raschle, N. M., Zuk, J., & Gaab, N. (2012). Functional characteristics of developmental dyslexia in left-hemispheric posterior brain regions predate reading onset. *Proceedings of the National Academy of Sciences, 109*(6), 2156-2161.

Richlan, F., Kronbichler, M., & Wimmer, H. (2009). Functional abnormalities in the dyslexic brain: a quantitative meta-analysis of neuroimaging studies. *Human Brain Mapping, 30*(10), 3299-3308.

Richlan, F., Kronbichler, M., & Wimmer, H. (2011). Meta-analyzing brain dysfunctions in dyslexic children and adults. *NeuroImage, 56*(3), 1735-1742.

Richlan, F., Kronbichler, M., & Wimmer, H. (2013). Structural abnormalities in the dyslexic brain: a meta-analysis of voxel-based morphometry studies. *Human Brain Mapping, 34*(11), 3055-3065.

Rossion, B., Gauthier, I., Goffaux, V., Tarr, M. J., & Crommelinck, M. (2002). Expertise training with novel objects leads to left-lateralized facelike electrophysiological responses. *Psychological Science, 13*(3), 250-257.

Roth, A., Roesch-Ely, D., Bender, S., Weisbrod, M., & Kaiser, S. (2007). Increased event-related potential latency and amplitude variability in schizophrenia detected through wavelet-based single trial analysis. *International Journal of Psychophysiology, 66*(3), 244-254.

Saygin, Z. M., Osher, D. E., Norton, E. S., Youssoufian, D. A., Beach, S. D., Feather, J., . . . Kanwisher, N. (2016). Connectivity precedes function in the development of the visual word form area. *Nature Neuroscience, 19*(9), 1250-1255.

Schendan, H. E., Ganis, G., & Kutas, M. (1998). Neurophysiological evidence for visual perceptual categorization of words and faces within 150 ms. *Psychophysiology, 35*(3), 240-251.

Schulte-Korne, G. (2010). The prevention, diagnosis, and treatment of dyslexia. *Dtsch Arztebl Int, 107*(41), 718-726. doi:10.3238/arztebl.2010.0718

Shaywitz, B. A., Shaywitz, S. E., Pugh, K. R., Fulbright, R. K., Skudlarski, P., Mencl, W. E., . . . Klorman, R. (2001). The functional neural architecture of components of attention in language-processing tasks. *NeuroImage, 13*(4), 601-612.

Shaywitz, B. A., Shaywitz, S. E., Pugh, K. R., Mencl, W. E., Fulbright, R. K., Skudlarski, P., . . . Lyon, G. R. (2002). Disruption of posterior brain systems for reading in children with developmental dyslexia. *Biological Psychiatry, 52*(2), 101-110.

Shaywitz, B. A., Skudlarski, P., Holahan, J. M., Marchione, K. E., Constable, R. T., Fulbright, R. K., . . . Shaywitz, S. E. (2007). Age-related changes in reading systems of dyslexic children. *Annals of Neurology, 61*(4), 363-370.

Shaywitz, S. E., & Shaywitz, B. A. (2008). Paying attention to reading: the neurobiology of reading and dyslexia. *Development and Psychopathology, 20*(4), 1329-1349.

Shum, J., Hermes, D., Foster, B. L., Dastjerdi, M., Rangarajan, V., Winawer, J., . . . Parvizi, J. (2013). A brain area for visual numerals. *The Journal of Neuroscience, 33*(16), 6709-6715.

Sigman, M., Pan, H., Yang, Y., Stern, E., Silbersweig, D., & Gilbert, C. D. (2005). Top-down reorganization of activity in the visual pathway after learning a shape identification task. *Neuron, 46*(5), 823-835.

Skeide, M. A., Kraft, I., Müller, B., Schaadt, G., Neef, N. E., Brauer, J., . . . Friederici, A. D. (2016). NRSN1 associated grey matter volume of the visual word form area reveals dyslexia before school. *Brain, 139*(10), 2792-2803.

Skeide, M. A., Kumar, U., Mishra, R. K., Tripathi, V. N., Guleria, A., Singh, J. P., . . . Huettig, F. (2017). Learning to read alters cortico-subcortical cross-talk in the visual system of illiterates. *Science Advances, 3*(5), e1602612.

Snowling, M. J. (2013). Early identification and interventions for dyslexia: a contemporary view. *Journal of Research in Special Educational Needs, 13*(1), 7-14.

Song, Y., Hu, S., Li, X., Li, W., & Liu, J. (2010). The role of top-down task context in learning to perceive objects. *The Journal of Neuroscience, 30*(29), 9869-9876.

Srihasam, K., Mandeville, J. B., Morocz, I. A., Sullivan, K. J., & Livingstone, M. S. (2012). Behavioral and anatomical consequences of early versus late symbol training in macaques. *Neuron, 73*(3), 608-619.

Szwed, M., Ventura, P., Querido, L., Cohen, L., & Dehaene, S. (2012). Reading acquisition enhances an early visual process of contour integration. *Developmental science, 15*(1), 139-149.

Tagamets, M.-A., Novick, J. M., Chalmers, M. L., & Friedman, R. B. (2000). A parametric approach to orthographic processing in the brain: an fMRI study. *Journal of Cognitive Neuroscience, 12*(2), 281-297.

Tanaka, J., & Curran, T. (2001). A neural basis for expert object recognition. *Psychological Science, 12*(1), 43-47.

Tarkiainen, A., Helenius, P., Hansen, P. C., Cornelissen, P., & Salmelin, R. (1999). Dynamics of letter string perception in the human occipitotemporal cortex. *Brain, 122*(11), 2119-2132.

Tarkiainen, A., Liljeström, M., Seppä, M., & Salmelin, R. (2003). The 3D topography of MEG source localization accuracy: effects of conductor model and noise. *Clinical Neurophysiology, 114*(10), 1977-1992.

Thesen, T., McDonald, C. R., Carlson, C., Doyle, W., Cash, S., Sherfey, J., . . . Devinsky, O. (2012). Sequential then interactive processing of letters and words in the left fusiform gyrus. *Nature communications, 3*, 1-9.

Thorpe, S., Fize, D., & Marlot, C. (1996). Speed of processing in the human visual system. *Nature, 381*(6582), 520-522.

Turkeltaub, P. E., Gareau, L., Flowers, D. L., Zeffiro, T. A., & Eden, G. F. (2003). Development of neural mechanisms for reading. *Nature Neuroscience, 6*(7), 767-773.

Ullsperger, M., & Debener, S. (2010). *Simultaneous EEG and fMRI: recording, analysis, and application*: Oxford University Press.

van Atteveldt, N. M., Formisano, E., Goebel, R., & Blomert, L. (2004). Integration of letters and speech sounds in the human brain. *Neuron, 43*(2), 271-282.

van der Mark, S., Bucher, K., Maurer, U., Schulz, E., Brem, S., Buckelmuller, J., . . . Brandeis, D. (2009). Children with dyslexia lack multiple specializations along the visual word-form (VWF) system. *NeuroImage, 47*(4), 1940-1949.

van der Mark, S., Klaver, P., Bucher, K., Maurer, U., Schulz, E., Brem, S., . . . Brandeis, D. (2011). The left occipitotemporal system in reading: disruption of focal fMRI connectivity to left inferior frontal and inferior parietal language areas in children with dyslexia. *NeuroImage, 54*(3), 2426-2436.

Vandermosten, M., Hoeft, F., & Norton, E. S. (2016). Integrating MRI brain imaging studies of pre-reading children with current theories of developmental dyslexia: a review and quantitative meta-analysis. *Current opinion in behavioral sciences, 10*, 155-161.

Vinckier, F., Dehaene, S., Jobert, A., Dubus, J. P., Sigman, M., & Cohen, L. (2007). Hierarchical coding of letter strings in the ventral stream: dissecting the inner organization of the visual word-form system. *Neuron, 55*(1), 143-156. doi:10.1016/j.neuron.2007.05.031

Vogel, A. C., Petersen, S. E., & Schlaggar, B. L. (2014). The VWFA: it's not just for words anymore. *Frontiers Human Neuroscience, 8*(88).

Weiss, R. H., & Osterland, J. (1997). *CFT 1-R. Grundintelligenztest Skala 1 - Revision*. Göttingen: Hogrefe.
West, M., & Chew, H. E. (2014). *Reading in the mobile era: A study of mobile reading in developing countries* (R. Kraut Ed.). Paris, France: United Nations Educational, Scientific and Cultural Organization.
Whitfield-Gabrieli, S., & Nieto-Castanon, A. (2012). Conn: a functional connectivity toolbox for correlated and anticorrelated brain networks. *Brain connectivity, 2*(3), 125-141.
Wild, N., & Fleck, C. (2013). Neunormierung des Mottier-Tests für 5-bis 17-jährige Kinder mit Deutsch als Erst-oder als Zweitsprache. *Praxis Sprache, 3*, 152-158.
Wilke, M., Holland, S. K., Altaye, M., & Gaser, C. (2008). Template-O-Matic: a toolbox for creating customized pediatric templates. *NeuroImage, 41*(3), 903-913.
Wood, A. G., Harvey, A. S., Wellard, R. M., Abbott, D. F., Anderson, V., Kean, M., . . . Jackson, G. D. (2004). Language cortex activation in normal children. *Neurology, 63*(6), 1035-1044.
Xue, G., Chen, C., Jin, Z., & Dong, Q. (2006). Language experience shapes fusiform activation when processing a logographic artificial language: an fMRI training study. *NeuroImage, 31*(3), 1315-1326.
Yoncheva, Y. N., Blau, V. C., Maurer, U., & McCandliss, B. D. (2010). Attentional focus during learning impacts N170 ERP responses to an artificial script. *Developmental Neuropsychology, 35*(4), 423-445.
Yoncheva, Y. N., Wise, J., & McCandliss, B. (2015). Hemispheric specialization for visual words is shaped by attention to sublexical units during initial learning. *Brain and Language, 145*, 23-33.
Yovel, G., & Kanwisher, N. (2004). Face perception: domain specific, not process specific. *Neuron, 44*(5), 889-898.
Zhao, J., Kipp, K., Gaspar, C., Maurer, U., Weng, X., Mecklinger, A., & Li, S. (2014). Fine neural tuning for orthographic properties of words emerges early in children reading alphabetic script. *Journal of Cognitive Neuroscience, 26*(11), 2431-2442.
Ziegler, J. C., & Goswami, U. (2005). Reading acquisition, developmental dyslexia, and skilled reading across languages: a psycholinguistic grain size theory. *Psychological Bulletin, 131*(1), 3-29.

Acknowledgements

Finally, we reached the section in which I would like to express my gratitude for the support I received during my PhD. This thesis would not have been possible without the help and encouragement of many people.

First and foremost, I would like to thank my direct supervisor Prof. Silvia Brem for her constant academic and personal guidance through the course of the LEXI-project. I sincerely appreciate the confidence she placed in me since the beginning of the project.

I am grateful to Prof. Moritz Daum for his interest in our research and for his willingness to be the head of my thesis committee.

Many thanks go to Prof. Urs Maurer. He shared his fascination for EEG and promoted my interest in neuroimaging research.

I would like to thank Prof. Daniel Brandeis for his support and interesting suggestions whenever we discussed my data.

I thank Dr. Philipp Stämpfli for his help during the measurements in the MR centre and his willingness to be a assessor during my PhD defence.

I sincerely thank Prof. Dr. med. Dipl.-Psych. Susanne Walitza for her genuine interest in our research and her personal support during the project. I also want to thank her for providing the infrastructure at the Department of Child and Adolescent Psychiatry and Psychotherapy.

My special thanks go to Dr. des. Iliana Karipidis. Since the beginning of our LEXI-project, we have undergone the same pains and struggles, but also the same joys and funny moments. Thank you for your support and friendship; it was a pleasure working with you!

Our challenging project would not have been possible without the help of research assistants, students and interns forming the Lexi team. Thank you all for your high commitment! In addition, a thank-you

belongs to all the other present and former researchers and staff members at the Department of Child and Adolescent Psychiatry and Psychotherapy.

Finally, I cordially thank my family and my friends for their constant encouragement and their understanding during stressful times. Dominik thank you for your love and your encouragement when I was desperate.

This work would not have been possible without the Lexi-children. Many thanks go to the children and their families for participating continuously in our project.

Curriculum vitae

Georgette Pleisch

Date of Birth February 18, 1980

Education and Professional Experience

2013 – 2017	Ph.D. student at the Developmental Neuroimaging lab of the Department of Child and Adolescent Psychiatry and Psychotherapy, University Hospital of Psychiatry, Zurich
2006 – 2013	Bachelor and Master of Science in Psychology, Department of Cognitive Psychology and Cognitive Neurosciences, University of Zurich
2002 – 2013	Several full-time and part-time teaching positions in public schools
2000 – 2002	Teachers´ College in Chur, Degree: Lehrerpatent/ Schooling permission
1995 – 2000	Evangelische Mittelschule EMS in Schiers, Degree: Matura

Publications

Pleisch, G., Karipidis, I. I., Brauchli, C., Röthlisberger, M., Hofstetter, C., Stämpfli, P., & Brem, S. (2017). Emerging neural specialization of the ventral occipitotemporal cortex with literacy acquisition. (prepared for submission).

Pleisch, G., Karipidis, I. I., Brem, A., Röthlisberger, M., Roth, A., Brandeis, D.; Walitza, S., & Brem, S. (2017). Initial reading skills modulate print-sensitive cortical processing after half a year of reading instruction: A pediatric simultaneous EEG-fMRI study. (prepared for submission).

Brem, S., Hunkeler, E., Mächler, M., Kronschnabel, J., Karipidis, I. I., Pleisch, G., & Brandeis, D. (2017). Increasing expertise to a novel script modulates the visual N1 ERP in healthy adults. International Journal of Behavioral Development.

Karipidis, I. I., Pleisch, G., Röthlisberger, M., Hofstetter, C., Dornbierer, D., Stämpfli, P., & Brem, S. (2017). Neural initialization of audiovisual integration in prereaders at varying risk for developmental dyslexia. Human Brain Mapping, 38(2), 1038-1055.

Karipidis, I. I., Pleisch, G., Brandeis, D., Roth, A., Röthlisberger, M., Schneeberli, M., Walitza, S., & Brem, S. (2017). Simulating reading acquisition: a multimodal neuroimaging approach to predict reading fluency. (submitted)

Jost, L. B., Eberhard-Moscicka, A. K., Pleisch, G., Heusser, V., Brandeis, D., Zevin, J. D., & Maurer, U. (2015). Native and non-native speech sound processing and the neural mismatch responses: A longitudinal study on classroom-based foreign language learning. Neuropsychologia, 72, 94-104.